NUREG/CR-4018
UCID-20212

SSI Sensitivity Studies and Model Improvements for the US NRC Seismic Safety Margins Research Program

J. J. Johnson,* Q. R. Maslenikov,* and B. J. Benda*

Prepared for
U.S. Nuclear Regulatory Commission

*Structural Mechanics Associates, 2400 Old Crow Canyon Rd., San Ramon, CA

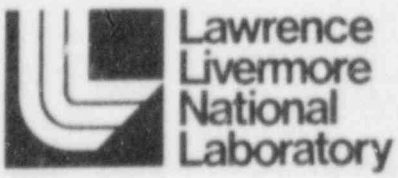

GPO Printed copy price: $5.50

NUREG/CR-4018
UCID-20212
RD

SSI Sensitivity Studies and Model Improvements for the US NRC Seismic Safety Margins Research Program

Manuscript Completed: January 1984
Date Published: November 1984

Prepared by
J. J. Johnson, O. R. Maslenikov, and B. J. Benda

Lawrence Livermore National Laboratory
7000 East Avenue
Livermore, CA 94550

Prepared for
Division of Engineering Technology
Office of Nuclear Regulatory Research
U.S. Nuclear Regulatory Commission
Washington, D.C. 20555
NRC FIN No. A0126

ABSTRACT

The Seismic Safety Margins Research Program (SSMRP) is a US NRC-funded program conducted by Lawrence Livermore National Laboratory. Its goal is to develop a complete fully coupled analysis procedure for estimating the risk of an earthquake-induced radioactive release from a commercial nuclear power plant. In Phase II of the SSMRP, the methodology was applied to the Zion nuclear power plant. Three topics in the SSI analysis of Zion were investigated and reported here -- flexible foundation modeling, structure-to-structure interaction, and basemat uplift. The results of these investigations were incorporated in the SSMRP seismic risk analysis.

TABLE OF CONTENTS

LIST OF FIGURES

LIST OF FIGURES (continued)

LIST OF FIGURES (continued)

LIST OF FIGURES (continued)

LIST OF TABLES

LIST OF TABLES (continued)

EXECUTIVE SUMMARY

The Seismic Safety Margins Research Program (SSMRP) is a U. S. Nuclear Regulatory Commission - funded multiyear research program conducted by Lawrence Livermore National Laboratory (LLNL). Its objective was to develop a complete, fully coupled analysis procedure (including methods and computer programs) for estimating the risk of earthquake-induced radioactive release from a commercial nuclear power plant. The analysis procedure is based on a state-of-the-art seismic and systems analysis process and explicitly includes the uncertainties inherent in such a process.

The SSMRP was developed and executed in two phases. The first phase concentrated on methodology development and demonstration calculations performed on the Zion nuclear power plant. The second phase, recently completed, incorporated additional models, improvements to existing models, and improvements to the probabilistic computational procedure. Phase II culminated in the performance of numerous seismic risk analyses of the Zion nuclear power plant. Also, in Phase II, sensitivity studies on a number of topics were performed. SSI sensitivity studies and model improvements in three areas are reported here: flexible foundation modeling, structure-to-structure interaction, and basemat uplift.

Flexible foundation modeling

In the SSMRP Phase II response calculations of the Zion nuclear power plant, structures on three separate foundations were analyzed with SMACS -- two containment buildings and the auxiliary-fuel handling-turbine building (AFT) complex. Modeling of the foundations of the containment buildings and AFT complex were necessary. For the response calculations, rigid foundations were assumed -- an obvious assumption for the

containment building but one which required further investigation for the AFT complex. This study investigated the effect on in-structure response of assuming the AFT complex foundation to behave rigidly by performing comparative analyses -- one assuming the AFT complex foundation to behave rigidly, the second assuming the AFT complex foundation to be composed of a series of rigid segments interconnected by structural elements.

The methodology to perform SSI analysis of structures whose foundations are assumed to behave flexibly is an extension of the substructure approach and originally developed by Profs. Luco and Wong. Important features of the methodology are modeling the structure by its fixed-base and pseudostatic modes and the explicit development and use of coupling stiffness matrices between structure and foundation degrees-of-freedom and foundation degrees-of-freedom themselves. Implementation and verification of the methodology was done as part of this study.

Analysis of the Zion AFT complex used the complete SSMRP structure model -- each half model contained 3888 structure degrees-of-freedom and 1482 foundation degrees-of-freedom. The foundation degrees-of-freedom were reduced to 66 for the total structure by imposing kinematic constraints corresponding to modeling the foundation as a series of 11 rigid segments.

A comparison of in-structure response at locations important to the Zion seismic risk analysis showed that modeling the AFT complex foundation as rigid was a good assumption. Some variability in response was seen, however, no clear conservative or unconservative bias was observed. In essence, the interconnecting walls and slabs of this structure serve to increase the effective stiffness of the foundation. Assessments of the effects of foundation flexibility must treat these

stiffening effects of structural elements to yield proper results.

Structure-to-structure interaction

During an earthquake, the vibration of one structure can affect the motion of an adjacent structure due to through-soil coupling. This phenomenon is denoted structure-to-structure interaction and is of potential significance at a nuclear power plant because of the small distances which separate adjacent structures and the massive structure-foundation systems involved. Two characteristics of the structures and foundations affect structure-to-structure interaction -- the relative size of the foundations and the relative mass of the structures. In both cases, the larger affects the smaller. For Zion, the AFT complex structure and foundation are significantly larger than the containment buildings and are predicted to affect them.

For Phase II of the SSMRP, structure-to-structure interaction was included in two ways -- it was modeled explicitly in the response calculations and sensitivity studies were performed based on seismic response and seismic risk to quantify its importance. As in the flexible foundation assessment, comparative claculations were made, i.e. with and without structure-to-structure interaction. In terms of seismic response, one finds structure response of the containment shell and internal structure to increase due to structure-to-structure interaction -- the greatest increase occurs in the vertical direction. This is due to the additional induced response due to rocking of the AFT complex. The AFT complex structure response is minimally affected, as one would expect. In terms of piping system response, location of the piping system plays a major role. Responses of piping systems residing within the containment or running between containment and the AFT complex

are significantly affected by structure-to-structure interaction. Responses, in general, increase -- in some instances, by a factor of 2 or greater. Hence, structure-to-structure interaction can have an important effect on seismic response.

An additional measure of sensitivity is seismic risk. Hence, seismic risk analyses were performed for the two cases -- with and without structure-to-structure interaction. The overall effect of structure-to-structure interaction was to increase core melt frequency per year by approximately 20% (3.57E-6 vs. 2.94E-6) and to increase the dose to the public by approximately 10% (9.63 vs. 8.7 man-rem/year). The basic reason for this increase is the increase in seismic responses of the containment building and piping systems therein.

Basemat uplift

When one considers the range of earthquakes for the seismic risk analysis, it is necessary to include consideration of phenomena which may not be of major consequence in the design process. One such consideration is soil-foundation separation or uplift. For the Zion containment building, as for other structures having a large height-to-diameter ratio, overturning moments due to its seismic response lead to a prediction of uplift. Uplift, per se, is not critical. The consequences of uplift are in general, of second order. However, the potential exists for large soil pressures to develop due to a redistribution of stress. Peak toe pressures may increase to the point of exceeding the soil bearing capacity causing failure. A further consequence of uplift itself and potential soil failure is increased relative displacements between adjacent structures which then causes failure of interconnecting pipes. This aspect was included in the SSMRP Phase II seismic risk analyses.

To estimate the excitation levels at which uplift and soil failure occur, a series of linear analyses was performed using SMACS for a range of earthquakes. A post-processing of SMACS's results determined overturning moments and peak toe pressures, including the effects of dead weight and buoyancy. These linearly calculated values were, then, approximately adjusted for nonlinear effects based on published studies. The result was an estimated median horizontal acceleration of the containment building foundation of 0.70g to cause soil failure.

1. INTRODUCTION

1.1 Background

The Seismic Safety Margins Research Program (SSMRP) is a U.S. Nuclear Regulatory Commission - funded multiyear program conducted by Lawrence Livermore National Laboratory (LLNL). Its objective was to develop a complete, fully coupled analysis procedure (including methods and computer programs) for estimating the risk of earthquake - induced radioactive release from a commercial nuclear power plant. The analysis procedure is based upon a state-of-the-art seismic and systems analysis process and explicitly includes the uncertainties inherent in such a process.

Seismic risk analysis can be considered in five steps: seismic hazard characterization (seismic hazard curve, frequency characteristics of the motion); seismic response of structures and components; structure and component failure descriptions; plant logic models (fault trees and event trees); and probabilistic failure and release calculations. For the SSMRP, the seismic responses of structures and components are calculated by the computer program SMACS [1]. SMACS links together seismic input, soil-structure interaction (SSI), structure response, and piping system /component response calculations. To execute SMACS, models of SSI, structures, piping systems, and components must be developed and input.

The SSMRP was developed and executed in two phases. The first phase concentrated on development of the overall seismic risk assessment methodology and demonstration calculations performed on the Zion nuclear power plant. The second phase, recently completed [2], incorporated additional models, improvements to existing models, and improvements to the probabilistic computational procedure. Phase II culminated in a

seismic risk analysis of the Zion nuclear power plant. Also, in Phase II, sensitivity studies on a number of topics were performed. The present report documents model improvements and sensitivity studies related to SSI which were performed in Phase II of the SSMRP.

1.2 Objective and Scope

Three aspects of SSI were more fully investigated in Phase II: flexible foundation modeling, structure-to-structure interaction, and basemat uplift. In all cases, the Zion nuclear power plant structures were the subjects of the sensitivity studies; however, the results have generic implications. This report is organized as follows.

Section 2 presents the flexible foundation sensitivity study. The methodology development and its application to the Zion auxiliary-fuel handling-turbine building (AFT) complex are reported.

Section 3 describes the structure-to-structure interaction sensitivity study and its incorporation into the SSMRP Phase II response calculations. The effect of structure-to-structure interaction on seismic responses and seismic risk are discussed.

Section 4 reports an investigation of uplift of the Zion containment building foundation and the consequences.

Section 5 contains conclusions and recommendations for future study.

2. FLEXIBLE FOUNDATION ASSESSMENT OF THE ZION AFT COMPLEX

2.1 Objectives and Scope

In the SSMRP, seismic responses are calculated by the computer program SMACS [1] which links together seismic input, soil-structure interaction (SSI), major structure response, and subsystem response. SSI and major structure response are calculated simultaneously by the substructure approach to SSI. The substructure approach divides the SSI problem into a series of simpler problems, typically three, solves each independently and superposes the results. The three steps are: determination of the foundation input motion; determination of the foundation impedances; and analysis of the coupled soil-structure system. The procedure is described in detail in Ref. 1 and expanded upon in subsequent sections here. Of importance to the present discussion, is that determination of the foundation input motion and foundation impedances is dependent on the stiffness of the structures' foundations (along with other parameters). The stiffness aspect is investigated here.

In the SSMRP Phase II response calculations of the Zion nuclear power plant [2], structures on three separate foundations were analyzed with SMACS -- two containment buildings (units 1 and 2) and the auxiliary - fuel handling - turbine building (AFT) complex. Figure 2.1 shows a layout of the Zion plant. Figure 2.2 shows a cross-section through the Zion containment building including a schematic representation of the site. Figure 2.3 shows two sections through the AFT complex. Modeling the foundations of the containment building and AFT complex were essential to the analysis process. Modeling the containment building foundation was straightforward -- it was modeled by a circular cylindrical foundation, embedded 36 ft. and 157 ft. in diameter. Modeling the complicated geometry and embedment of the AFT complex was considerably more

difficult. Reference 3 describes in detail the process and sensitivity studies performed to arrive at the model used in the SMACS response calculations. For the containment buildings and the AFT complex, rigid foundations were assumed. In the case of the containment building (Fig. 2.2), a rigid foundation is easily justifiable considering the thickness of the foundation and the stiffening effects of the containment shell and internal structure. However, modeling the AFT complex foundation as rigid required further investigation. Foundation modeling represents a source of modeling uncertainty.

To investigate the effect on in-structure response of assuming the AFT complex foundation to behave rigidly, comparative analyses were performed -- one assuming the AFT complex foundation to behave rigidly, the second assuming the AFT complex foundation to be composed of a series of rigid segments interconnected by structural elements. The results are presented here. Section 2.2 describes the methodology for flexible foundation analysis which is an extension of the substructure approach to SSI. Section 2.3 presents the basic elements of the analysis of the Zion AFT complex. Section 2.4 itemizes the analyses performed and presents the results. Finally, Sec. 2.5 states observations and conclusions.

2.2 Flexible Foundation Methodology

2.2.1 Background

The methodology to perform SSI analysis of structures whose foundations are assumed to behave flexibly is an extension of the substructure approach. Recall the elements of the substructure approach as applied to structures with assumed rigid foundations (Fig. 2.4).

Free-field ground motion. Specification of the free-field ground motion entails specifying the control point, the frequency characteristics of the control motion (typically, time histories or response spectra), and the spatial variation of the motion. In all SSMRP modeling to date, the control point has been specified on the free surface of soil or rock, the control motion has been acceleration time histories, and, in most cases, vertically incident plane waves have been assumed, which defines the spatial variation of motion once the soil properties are identified.

Foundation input motion. The foundation input motion differs from the free-field ground motion in all cases, except for surface foundations subjected to vertically incident waves. The motions differ for primarily two reasons. First, the free-field motion varies with soil depth. Second, the soil-foundation interface scatters waves because points on the foundation are constrained to move according to its geometry and stiffness. The foundation input motion $\{U^*\}$ is related to the free-field ground motion by means of a transformation defined by a scattering matrix $[S(\omega)]$, which is complex valued and frequency dependent:

$$\{U^*(\omega)\} = [S(\omega)]\{f(\omega)\} \tag{2.1}$$

The vector $\{f(\omega)\}$ is the complex Fourier transform of the free-field ground motion, which contains its complete description. A discussion of scattering matrices and their characteristics is contained in Refs. 1 and 3.

Foundation impedances. Foundation impedances $[K_s(\omega)]$ describe the force-displacement characteristics of the soil. They depend on the soil configuration and material behavior, the frequency of the excitation, and the geometry of the foundation. In general, for a linear elastic or viscoelastic material and a

uniform or horizontally stratified soil deposit, each element of the impedance matrix is complex-valued and frequency dependent. For a rigid foundation, the impedance matrix is a 6 x 6 which relates a resultant set of forces and moments to the six rigid-body degrees-of-freedom.

Structure model. The dynamic characteristics of the structures to be analyzed are described by their fixed-base eigensystem and modal damping factors. The structures' dynamic characteristics are then projected to a point on the foundation at which the total motion of the foundation, including SSI effects, is determined.

SSI analysis. The final step in the substructure approach is the actual SSI analysis. The results of the previous steps -- foundation input motion, foundation impedances, and structure model -- are combined to solve the equations of motion for the coupled soil-structure system. For a single rigid foundation, the SSI response computation requires solution of, at most, six simultaneous equations -- the response of the foundation. The formulation is in the frequency domain. Hence, one can write the equation of motion for the unknown harmonic foundation response $\{U\} \exp(i\omega t)$ for any frequency ω, about a reference point normally selected on the foundation

$$\left(-\omega^2\left([M_o] + [M_b(\omega)]\right) + [K_s(\omega)]\right)\{U\} = [K_s(\omega)]\{U^*\} \qquad (2.2)$$

Equation 2.2 separates the effects due to scattering from those caused by interaction between soil, structure, and foundation. The effects of scattering are included in the foundation input motion $\{U^*\}$. The interaction effects of the structure, foundation, and soil are represented in the term

$$\left(-\omega^2\left([M_o] + [M_b(\omega)]\right) + [K_s(\omega)]\right),$$

where $[M_o]$ is the mass matrix of the foundation, $[M_b(\omega)]$ is the

frequency-dependent equivalent mass matrix of the structure, and $[K_s(\omega)]$ is the impedance matrix of the foundation. The total motion $\{U\}$ of the foundation results from a combination of both types of effects.

The equivalent mass matrix of the structure, when multiplied by ω^2, represents the force-displacement relationship of the structure subjected to base excitations. All of the physical and dynamic characteristics of the structure pertinent to the solution are contained in it:

$$[M_b(\omega)] = [M_{bo}] + [\Gamma]^T[D(\omega)]\,[\Gamma] \qquad (2.3a)$$

The matrix $[M_{bo}]$ is the 6 x 6 mass matrix of the structure for rigid translations and rotations about the reference point:

$$[M_{bo}] = [\alpha]^T[M][\alpha] \quad , \qquad (2.3b)$$

where $[M]$ is the mass matrix of the structure and $[\alpha]$ defines the node point locations relative to the reference point. $[M_{bo}]$ is independent of frequency.

The second term on the right-hand side of Eq. 2.3a represents the dynamic behavior of the structure using its fixed-base modes. The matrix $[\Gamma]$ comprises the modal participation factors for base translations and rotations:

$$[\Gamma] = [\Phi]^T[M][\alpha] \quad , \qquad (2.3c)$$

where the columns of $[\Phi]$ are the mass normalized fixed-base mode shapes. Finally, the diagonal matrix $[D(\omega)]$ contains the dynamic amplification factors $D_j(\omega)$ for each fixed-base mode of the structure:

$$D_j(\omega) = \frac{(\omega/\omega_j)^2}{(1 - \omega^2/\omega_j^2) + 2i\beta_j(\omega/\omega_j)} \qquad (j = 1,nf) \qquad (2.3d)$$

where

ω_j = the frequency of the jth fixed-base mode,
β_j = the modal damping ratio of the jth fixed-base mode,
nf = the number of fixed-base modes included in the solution.

Note that the term $[M_b(\omega)]$ is complex-valued for damped structures. Once the equations of motion (eq. 2.2) are solved for the response $\{U\}$ of the foundation (three translations and three rotations), in-structure response may be obtained simply as

$$\{U_{STR}(\omega)\} = [\alpha]\{U(\omega)\} + [\Phi]^T[D(\omega)][\Gamma]\{U(\omega)\} \quad . \qquad (2.4)$$

The methodology to perform SSI analysis of structures whose foundations are assumed to behave flexibly required major modifications to two steps of the substructure approach -- structure model and SSI analysis. Those modifications are presented in the following sections.

2.2.2 Derivation of equations of motion

The equations of motion for an elastic damped structure partitioned into structure degrees-of-freedom 1 and foundation degrees-of-freedom 2 can be written as follows. The formulation is in the frequency domain, as before, and the unknown harmonic structure and foundation response are denoted $\{U_1\}$ exp ($i\omega t$) and $\{U_2\}$ exp ($i\omega t$) for any frequency ω .

$$\left(-\omega^2 \begin{bmatrix} M_1 & 0 \\ 0 & M_2 \end{bmatrix} + i\omega \begin{bmatrix} C_{11} & C_{12} \\ C_{21} & C_{22} \end{bmatrix} + \begin{bmatrix} K_{11} & K_{12} \\ K_{21} & K_{22} \end{bmatrix} \right) \begin{Bmatrix} U_1 \\ U_2 \end{Bmatrix} = \begin{Bmatrix} P_1 \\ P_2 \end{Bmatrix} \quad (2.5)$$

where

M_1 = mass matrix of the structure
M_2 = mass matrix of the foundation

C_{11} = viscous damping matrix of the structure
$C_{12} = C_{21}^T$ = coupling damping matrices
C_{22} = viscous damping matrix of the foundation
K_{11} = stiffness matrix of structure
$K_{12} = K_{21}^T$ = coupling stiffness matrices
K_{22} = stiffness matrix of the foundation
P_1 = nodal loads applied to the structure
P_2 = nodal loads applied to the foundation.

Assuming no external loads applied to the structure ($P = 0$), eq. 2.5 can be rewritten as:

$$\left(-\omega^2[M_1] + i\omega[C_{11}] + [K_{11}]\right)\{U_1\} = -\left(i\omega[C_{12}]+[K_{12}]\right)\{U_2\} \quad (2.6a)$$

$$\left(-\omega^2[M_2] + i\omega[C_{22}] + [K_{22}]\right)\{U_2\} = \{P_2\}-\left(i\omega[C_{21}]+[K_{21}]\right)\{U_1\} \quad (2.6b)$$

In-structure response

Let us concentrate first on the expression for in-structure response given the response on the foundation (eq. 2.6a). The general approach to solving eq. 2.6 is based on the pseudostatic mode method, i.e. assume the in-structure displacements U_1 to be composed of two parts -- a pseudostatic portion U_1^s and a dynamic portion U_1^d .

$$\{U_1\} = \{U_1^s\} + \{U_1^d\} \quad (2.7)$$

where $\{U_1^s\}$ is defined by

$$[K_{11}]\ \{U_1^s\} = -\ [K_{12}]\ \{U_2\} \quad (2.8a)$$

and

$$\{U_1^s\} = - [K_{11}]^{-1}[K_{12}]\{U_2\} = [P]\{U_2\} \tag{2.8b}$$

The pseudostatic portion U_1^s can be interpreted as the response induced in the structure due to foundation motions, excluding inertia effects, whereas the dynamic portion U_1^d can be viewed as a perturbation of the pseudostatic response due to inertia effects. The matrix $[P]$ is the pseudostatic modes.

Substituting eqs. 2.7 and 2.8 into eq. 2.6a leads to:

$$\begin{aligned}\left(-\omega^2[M_1] + i\omega[C_{11}] + [K_{11}]\right)\{U_1^d\} = &- \omega^2[M_1][K_{11}]^{-1}[K_{12}]\{U_2\} \\ &-i\omega\left([C_{12}]-[C_{11}][K_{11}]^{-1}[K_{12}]\right)\{U_2\}\end{aligned} \tag{2.9}$$

Equation 2.9 is written in terms of the structure degrees-of-freedom, the number of which is, in general, large. The pseudostatic mode method, however, efficiently uses an eigenfunction expansion of U_1^d . Assume U_1^d can be represented by an eigenfunction expansion which diagonalizes the mass, stiffness, and damping matrices ($[M_1]$, $[K_{11}]$, and $[C_{11}]$ respectively).

Consider the undamped free vibration problem

$$[M_1]\{\ddot{U}_1^d\} + [K_{11}]\ \{U_1^d\} = 0 \tag{2.10a}$$

and the linear coordinate transformation

$$\{U_1^d\} = [\phi]\ \{q\} \tag{2.10b}$$

where $\{q\}$ is of the form $\exp(i\omega t)$ and the columns of $[\phi]$ are the eigenvectors $\{\phi_j\}$. Substitution of eq. 2.10b into eq.

2.10a leads to the standard eigenvalue problem:

$$([K_{11}] - [\omega_j^2][M_1])[\Phi]\{q\} = 0 \tag{2.10c}$$

The resulting eigensystem is assumed to satisfy

$$\begin{aligned}
[\Phi]^T[M_1][\Phi] &= [I] \\
[\Phi]^T[C_{11}][\Phi] &= [2\beta_j\omega_j] \\
[\Phi]^T[K_{11}][\Phi] &= [\omega_j^2]
\end{aligned} \tag{2.10d}$$

where ω_j and β_j are the natural frequency and fraction of critical damping, respectively, of the jth mode. The eigensystem corresponds to the fixed-base modes of the structure.

Substituting eq. 2.10 into eq. 2.9

$$\begin{aligned}
\ddot{\{q\}} + [2\beta_j\omega_j]\dot{\{q\}} + [\omega_j^2]\{q\} = &- \omega^2[\hat{\Phi}]^T[M_1][K_{11}]^{-1}[K_{12}]\{U_2\} \\
&-i\omega[\hat{\Phi}]^T([C_{12}] - [C_{11}][K_{11}]^{-1}[K_{12}])\{U_2\}
\end{aligned} \tag{2.11}$$

where $[\hat{\Phi}]$ denotes the incomplete eigenfunction expansion of U_1^d, i.e. a reduced set of the complete expansion $[\Phi]$. The first term of the right hand side of eq. 2.11 can be further reduced by recognizing the identities:

$$[K_{11}]^{-1} = [\Phi][\omega_j^2]^{-1}[\Phi]^T \tag{2.12a}$$

and

$$[\hat{\Phi}\,|\,0]^T[M_1][\Phi] = \left[\begin{array}{c|c} \hat{I} & 0 \\ \hline 0 & 0 \end{array}\right] \tag{2.12b}$$

The second term is zero, when one assumes damping to be proportional to stiffness. This latter assumption is discussed further in subsequent sections. Hence, eq. 2.11 may be written as:

$$\{\ddot{q}\} + [2\beta_j\omega_j]\{\dot{q}\} + [\omega_j^2]\{q\} = -\omega^2[\omega_j^2]^{-1}[\hat{\Phi}]^T[K_{12}]\{U_2\} \tag{2.13}$$

The solution for q_j in the frequency domain is:

$$\{q\} = -\omega^2[H_j(\omega)][\omega_j^2]^{-1}[\hat{\Phi}]^T[K_{12}]\{U_2\} \tag{2.14}$$

where

$$[H_j(\omega)] = \left(\omega_j^2\left[1-\left(\frac{\omega}{\omega_j}\right)^2 + 2i\beta_j\left(\frac{\omega}{\omega_j}\right)\right]\right)^{-1} \tag{2.15}$$

Combining the solution for U_1^d (eqs. 2.10 and 2.14) with the solution for U_1^s (eq. 2.8) yields:

$$\{U_1\} = -\omega^2[\hat{\Phi}][H_j(\omega)][\omega_j^2]^{-1}[\hat{\Phi}]^T[K_{12}]\{U_2\} + [P]\{U_2\} \tag{2.16a}$$

which is an expression for in-structure kinematic response (displacements or accelerations) in terms of the response of the foundation degrees-of-freedom. For stress response, the stress in member m, $\{\sigma_m\}$, can be written as

$$\{\sigma_m\} = [\hat{S}_{1m}]\{q\} + [\hat{S}_{2m}]\{U_2\} \tag{2.16b}$$

where

$$[\hat{S}_{1m}] = [S_{1m}][\hat{\Phi}]$$

and

$$[\hat{S}_{2m}] = [S_{1m}][P] + [S_{2m}]$$

The matrices $[S_{1m}]$ and $[S_{2m}]$ are stress-displacement relationships relating stresses in member m to structure displacements and foundation displacements respectively.

Foundation response

To determine the unknown foundation response U_2, consider eq. 2.6b. First, note that the load vector P_2 is of the same form as eqs. 2.1 and 2.2, i.e.

$$\{P_2\} = [K_s]\left(\{U_2^*\} - \{U_2\}\right) \tag{2.17}$$

where $\{U_2^*\}$ is the foundation input motion (eq. 2.1) and $\{U_2\}$ is the unknown foundation response including SSI effects. The matrix $[K_s]$ is the foundation impedance matrix. Substituting eqs. 2.16 and 2.17 into eq. 2.6b and rearranging terms leads to:

$$\Big([K^{st}] + [K_s]\Big)\{U_2\} = [K_s]\{U_2^*\} \tag{2.18a}$$

where

$$\begin{aligned}[K^{st}] = &- \omega^2[M_2] + (1 + 2\xi\omega i)\left([K_{22}] - [K_{21}][K_{11}]^{-1}[K_{12}]\right) \\ &- \omega^2(1 + 2\xi\omega i)\left([K_{21}][\hat{\Phi}][H_j(\omega)]\left[\sim\omega_j^2\sim\right]^{-1}[\hat{\Phi}]^T[K_{12}]\right)\end{aligned} \tag{2.18b}$$

and $[C] = 2\xi[K]$ has been assumed.

The matrix $[K^{st}]$ can be thought of as a complex valued impedance matrix for the structure. The first term is the effect of the foundation mass matrix. The second term contains the effect of flexibility of the foundation. The term $([K_{22}]-[K_{21}][K_{11}]^{-1}[K_{12}])$ is denoted the relaxed foundation stiffness matrix and is examined in later sections. The third term contains the effects of dynamic amplification in the structure.

2.2.3 Summary of key steps

The key steps of the analysis procedure are, in general, defining the free-field ground motion, modeling the foundation (which includes, for this discussion, the foundation input motion, foundation impedances, and its structural stiffness), modeling the structure, and combining these elements to perform the SSI analysis. These steps are summarized here and compared with the substructure approach as it is applied to

structures with assumed rigid foundations. The free-field ground motion is treated as described in Sec. 2.2.1 and in Sec. 2.3.1 for the Zion AFT complex.

Modeling the foundation. Modeling the foundation for a flexible foundation SSI analysis entails the following.

- Discretize the foundation into segments which describe its behavior. Each segment is assumed to behave rigidly. In this step, all available information concerning the structure and foundation is used to arrive at the minimum number of segments, which adequately describe the foundation's behavior.

- Model the foundation in the structure model. In so doing, generate the coupling stiffness matrices between structure and foundation degrees-of-freedom (K_{12}) and between foundation degrees-of-freedom themselves (K_{22}). The effective stiffness of the foundation (structure and foundation) is treated exactly through these stiffness matrices.

- Foundation input motion is treated as described in Sec. 2.2.1 and in Sec. 2.3.1 for the present analysis.

- Foundation impedances are generated for each discretized segment including through soil coupling. The impedance matrix is complex valued and frequency dependent, as before. For general three-dimensional behavior, it is 6N x 6N where N is the number of foundation segments.

- Comparing the present foundation model requirements with those for a single rigid foundation, one notes first the obvious difference of discretizing the foundation. Next, one notes the requirement of

modeling the stiffness effects of the foundation including the additional stiffening due to coupling through the structure. Third, one observes the differences in foundation impedances. For a single rigid foundation, the impedance matrix is 6 x 6; whereas, for the flexible foundation, the resulting impedance matrix is 6N x 6N with through soil coupling between segments. Note, the 6N x 6N impedance matrix degenerates to the 6 x 6 impedance matrix for a single rigid foundation when kinematic constraints are applied. Finally, the foundation input motion is treated in the same manner as for the rigid foundation case.

Modeling the structure. A model of the structure, including the foundation, is constructed. From this model, the following information is determined.

- Calculate the fixed-base eigensystem of the structure. Recall that the pseudostatic mode method uses an eigenfunction expansion for the dynamic portion of the structure response -- eqs. 2.10 and 2.11.

- Calculate the pseudostatic modes [P] (eq. 2.8) or influence coefficients which relate structure response to unit support motions.

- Construct the complex valued impedance matrix $[K^{st}]$ for the structure (eq. 2.18). The relaxed foundation stiffness matrix ($[K_{22}] - [K_{21}] [K_{11}]^{-1} [K_{12}]$) is a component of $[K^{st}]$.

- Comparing present flexible foundation structure model requirements with those for a structure founded on a single rigid foundation, extraction of the fixed-base eigensystem is identical. Differences arise in the

additional requirements for the pseudostatic modes and in the development of the equivalent stiffness or impedance matrix (eq. 2.18) vs. the equivalent mass matrix (eq. 2.3). Also, structure response recovery differs for the two cases.

SSI analysis.

- Both the flexible and rigid foundation approaches treat the problem in two steps -- determine foundation response and, subsequently, in-structure response. Differences in the two formulations have been discussed above and most clearly seen by comparing eq. 2.2 with eq. 2.18 and eq. 2.4 with eq. 2.16.

- One key point relates to the treatment of damping in the two approaches. The flexible foundation formulation requires explicit treatment of coupling damping terms which obviously, do not exist for the single rigid foundation case. These damping terms do not lend themselves to a modal representation. Hence, when applying the flexible foundation formulation in a reduced form to a single rigid foundation, a slight difference in the formulations remains. A series of sensitivity studies were performed to investigate the treatment of damping. The conclusion was to treat damping in two ways: for foundation response damping is assumed to be of a hysteretic form; for in-structure response, it is assumed to be viscous modal damping. The differences are small, however, in benchmarking the technique this treatment was necessary.

The basic flexible foundation formulation is that of Luco and Wong [4]. Both the formulation and a pilot computer program were obtained. Extensive modifications to the program and the creation of two large pre-processing programs to permit treatment of large systems such as the Zion AFT complex comprise the final implementation of the methodology.

2.3 Elements of the Zion AFT Complex Analysis

The objective of this study was to investigate the effect on in-structure response of assuming the Zion AFT complex foundation to behave flexibly vs. rigidly. To do so, comparative analyses were performed for these assumptions. The key elements of the two analyses are presented here.

2.3.1 Free-field ground motion

An artificial earthquake composed of three components of motion -- two horizontal, aligned in the east-west (E-W) and north-south (N-S) directions, and vertical -- was used in this study. The horizontal components were scaled to 0.20g; the vertical to 0.13g. The duration of motion was 15 sec. discretized at time intervals of 0.01 sec. The acceleration time histories are plotted in Fig. 2.5; the corresponding spectra for 2% damping are shown in Fig. 2.6. This earthquake was representative of those used in the SSMRP response calculations.

The wave propagation mechanism for the free-field motion was assumed to be vertically propagating waves. This is consistent with the SSMRP response calculations.

2.3.2 Modeling the Zion AFT complex foundation

Figure 2.7 contains a diagram of the finished excavated area for the Zion AFT complex foundation. The complicated geometry and embedment is apparent. A detailed discussion of our modeling of the foundation for the SSMRP response calculations is contained in Ref. 3. The present study concentrated on evaluating the validity of assuming the foundation to behave rigidly. For this purpose, we ignored the effect of embedment and assumed the foundation to be

surface-founded, i.e. the foundation input motion was assumed identical to the free-field ground motion and the foundation impedances were uncorrected for embedment. Note, however, the methodology of Sec. 2.2 is completely general and can treat embedded as well as surface-founded foundations.

The geometry of the foundation model is shown in Fig. 2.8. As mentioned above, we did not include embedment effects. The foundation model was assumed to be surface-founded on a 69 ft. soil layer over bedrock which corresponds to the average depth of soil to bedrock beneath the deeply embedded portions of the Zion AFT complex foundation. Our flexible foundation analysis modeled the Zion AFT complex foundation as a series of eleven rigid segments interconnected by structural elements. Figure 2.8 shows the discretization. The eleven segments were selected based on the physical characteristics of the structure/foundation system. Each segment is assumed to behave in a rigid manner which was easily justified due to the foundation thickness and the structural elements connected to the foundation segment. Impedances are generated for each foundation segment including through soil coupling between segments. For the determination of impedances, each segment was discretized into rectangular subregions; eight to forty-two subregions were used depending on segment size and shape. The subregions are shown in Fig. 2.8. Note, also in Fig. 2.8, the location of the reference points of each of the eleven segments. It is at these points that the foundation motion is determined, i.e. degrees-of-freedom denoted 2 in the formulation.

The foundation model for the rigid foundation assumption is shown in Fig. 2.9 where the discretization here is that used in the calculation of the impedance functions for this case. This model is identical to that used for the SSMRP

response calculations with no correction for embedment. Note the single reference point at which the solution to the SSI analysis is performed.

The Zion site is characterized by approximately 110 ft. of soil overlying a bedrock of Niagara dolomite. The top layer of soil about 36 ft. thick, consists of granular lake deposits of dense, fine to medium sands, together with variable amounts of coarse sand and gravel. The second layer, 30 ft. thick, is a cohesive, firm to hard glacial till. The remaining 45-ft. layer of soil is a cohesionless glacial deposit of dense sands and gravel. Figure 2.2 shows schematically the soil layers. For analysis purposes, this soil configuration was discretized as three soil layers underlain by a half-space. This discretization was the result of numerous sensitivity studies with a finer representation. The soil layers are distinguished by their material properties as shown in Table 2.1. These properties are equivalent linear values corresponding to an earthquake of approximately 0.2g on the surface of the soil. Note, for our purposes, only layer 3 and the underlying half-space are of interest since the foundation is assumed to lie 69 ft. from the bedrock. To assess the effect of varying soil properties on the results, two additional sets of soil properties were considered: a stiffer set, with shear moduli 1.5 times that shown in Table 2.1; and a softer set, with shear moduli 2/3 of those in Table 2.1. Results for all three cases are presented in later sections.

Foundation input motion was assumed identical to the free-field ground motion in the analyses. This reflects the assumptions of a surface-founded foundation and vertically propagating waves.

Foundation impedances were calculated for 35 frequencies in the range of 0 to 25 Hz. For the rigid foundation case, the impedance matrix was 6 x 6; for the

flexible foundation case, it was 66 x 66. The flexible foundation impedances were validated by imposing rigid body constraints on the eleven segments, calculating an effective stiffness of the entire foundation, and comparing it with the rigid foundation impedances. The impedances compared well.

The subsequent section discusses stiffness modeling of the foundation -- coupling stiffnesses between structure and foundation and between foundation degrees-of-freedom themselves.

2.3.3 Modeling the Zion AFT complex structure

The Zion AFT complex consists of the T-shaped auxiliary building, the fuel-handling building, the turbine buildings, and the two diesel generator buildings as shown schematically in Fig. 2.1. These buildings are founded on a common foundation; common floor slabs in the superstructure also provide structural continuity. A complex finite element model of the AFT complex was developed and used in the SSMRP Phases I and II response calculations. The same model was used in the present study.

The AFT complex was modeled with thin plate and shell elements to represent concrete shear walls and floor diaphragms, and beam and truss elements to model the braced frames. To limit the computational size of the model without sacrificing detail, the plane of symmetry through the structure was used. Two half-structure models were developed: one model employed symmetric boundary conditions along the plane of symmetry; the other, antisymmetric boundary conditions. Figure 2.10 shows the half-structure model. The half-model contained 3888 degrees-of-freedom in the structure (denoted 1 in the formulation) and 1482 degrees-of-freedom on the foundation (denoted 2 in the formulation). The foundation was modeled by finite elements as was the superstructure.

The fixed-base eigensystem is required for both the rigid and flexible foundation analyses. Eigenvalue extractions were performed on the symmetric and antisymmetric half-models, important modes determined, and the results merged. A total of 113 fixed-base modes were used; the identical representation used in the SSMRP Phases I and II response calculations.

The pseudostatic modes and the coupling stiffness matrices are added requirements for the flexible foundation analysis. Determining them was a multi-step process. Each half-model was analyzed yielding the quantities of interest for symmetric and antisymmetric assumptions. This yielded 1482 symmetric pseudostatic modes, 1482 antisymmetric pseudostatic modes, and the two sets of corresponding coupling stiffness matrices. The pseudostatic modes and coupling stiffness matrices were then condensed, using rigid body transformations, from 1482 degrees-of-freedom to 66, i.e. six degrees-of-freedom for each of the eleven rigid segments. The 1482 foundation degrees-of-freedom were assigned to rigid segments on the basis of tributary area and an assessment of the behavior of the foundation. After condensation, the symmetric and antisymmetric quantities were merged.

Having assembled the global quantities representing the structure and foundation, pre-processing them into their further condensed form proceeds: form $[M_b(\omega)]$ for the rigid foundation case and $[K^{st}]$ for the flexible foundation case. In addition, response recovery information, eq. 2.4 for the rigid foundation analysis and eq. 2.16 for the flexible foundation case, was developed. All of the pertinent information has been assembled at this stage and the analysis can proceed.

2.4 Comparison of Responses

This section presents a comparison of responses on the foundation and at points in the structure assuming the AFT complex foundation to behave rigidly and flexibly. Three sets of soil properties were considered and results from all three are presented. Before presenting the comparisons, the formulation and its relationship to the standard substructure approach are examined with respect to the AFT complex.

2.4.1 Validation of model and basis of comparison

Numerous small problems were analyzed in the validation phase of the development. To complete the validation, an analysis of the Zion AFT complex was performed using the flexible foundation methodology but assuming the structure to be founded on a single rigid foundation. To do so, the pseudostatic modes and other related quantities were condensed to six foundation degrees-of-freedom and the flexible foundation methodology applied. Results from this analysis and one performed by the standard substructure approach for rigid foundations were compared. The same impedance functions were used in both analyses; they corresponded to the nominal soil case. As noted in Sec. 2.2.3, a difference in the analyses is the manner in which structure damping is treated in the calculation of foundation motions. In this comparison, modal damping of 2% was assumed for the rigid foundation formulation and hysteretic damping of 2% was assumed for the flexible foundation. Both methods used modal damping of 2% for calculation of in-structure response.

Maximum accelerations and response spectra for the six foundation degrees-of-freedom and for the three translations at various elevations and locations in the AFT complex were compared. These locations are shown schematically in Fig. 2.11.

They were selected based on two criteria: locations important to the SSMRP response calculations and locations which demonstrate most clearly the effects of the flexible foundations. Maximum base forces and moments at the foundation reference point were also compared. Table 2.2 compares maximum foundation response which differs by less that 5%. Table 2.3 compares base forces and moments which differ by an average of 12%. Table 2.4 compares in-structure maximum accelerations. These maximum accelrations differed by less than 5% in the horizontal directions and by about 10% in the vertical direction. Response spectra on the foundation are shown in Fig. 2.12. The solid line shows the results for the condensed flexible foundation model, the dashed line for the rigid foundation model. All of the translations and the torsion component compare very well. The rocking components show differences of up to 20% at the spectra peaks. Spectra at typical locations in the structure are shown in Figs. 2.13 - 2.16. The horizontal spectra agree very well, varying by less than about 5%, at the spectra peaks. The vertical spectra show differences over a wider frequency band but generally differ by less than 10%.

On the basis of these results and those of numerous smaller checkout problems, we conclude that the two methodologies are essentially equivalent for the rigid foundation case and the computer algorithm for generating the structural data was performing properly.

For the comparisons of response, quantifying the effects of the flexible foundation, responses attributed to the rigid foundation were calculated by the condensed flexible foundation methodology. This eliminated differences in formulations as a source of differences in response.

2.4.2 Foundation response

Response was calculated and compared at the reference points of each of the eleven segments modeling the foundation. Maximum accelerations and response spectra were compared. Tables 2.5, 2.6, and 2.7 tabulate results for the nominal, stiff, and soft soil properties, respectively. Note, comparisons are presented for the significant foundation segments. The results for the two cases showed that, in general, peak translations did not differ significantly. On the average, the flexible foundation results were within 5% of the rigid foundation results. There was no definite trend, either with respect to directional components or to soil property cases. In the auxiliary building, a primary area of interest, the largest difference in response was about 9%, the average being about 1%. Whereas the largest difference anywhere on the basemat slabs we studied was about 19%. On the other hand, foundation rotations (N-S and E-W rocking and torsion) increased substantially for the flexible foundation case. On the average the flexible foundation analysis gave results 50% higher than those from the rigid foundation analyses for all directions and all soil property assumptions. Variability in these results was large, varying from increases of 35% to 200% for the flexible foundation case. Again, no trend was observed with respect to soil stiffness properties.

Comparisons of foundation response spectra are shown in in Figs. 2.17 - 2.22 for the nominal soil case. Comparisons were generated for the soft soil case and the stiff soil case but are not included here for brevity sake. The solid curve shows the rigid foundation results while the dashed curve shows the flexible foundation results. As with the maximum accelerations, the spectra for foundation translations show little or no difference for all soil cases, while rocking and

torsional spectra showed increases primarily at isolated frequencies. Generally rocking spectra for the larger foundations, i.e., the auxiliary building and the turbine building, showed smaller differences than those for the smaller foundations, and analyses for stiffer soils showed greater differences than those for softer soils. These differences in rocking spectral response included increases of two times that for the rigid foundation and occurred mostly at higher frequencies (10 Hz and above). This is not surprising considering the difference in soil resistance to rocking and torsion for basemats with small plan dimensions relative to those of the entire foundation.

2.4.3 In-structure response

Response was calculated and compared at numerous locations in the structure. Maximum accelerations and response spectra were compared. Tables 2.8, 2.9, and 2.10 tabulate results for the nominal, stiff, and soft soil properties, respectively. Only small differences are seen when comparing maximum accelerations. In the auxiliary building, the average difference was about 3%; the maximum about 10%. In the diesel generator building, the maximum difference was about 15%. In the turbine building, the maximum difference was about 25%. No significant trends with respect to direction or soil properties were evident.

Typical comparisons of response spectra are shown in Figs. 2.23 - 2.37. Again, the solid curve denotes rigid foundation response while the dashed curve shows response due to assuming a flexible foundation. There is surprisingly little difference between the two results. The frequency characteristics of the two are very similar and differences which do occur are in peak spectral accelerations which are

known to be sensitive parameters and dependent on the damping value of the spectra. All spectra shown, herein, are for 2% damping which accentuates the differences. In the auxiliary building, in general, only small differences in spectra were observed; although, a difference of 40% in spectral acceleration at 10 Hz and one location in the auxiliary building is seen. In general, differences were also small in the diesel generator and turbine buildings; although, at selected locations and for isolated frequency ranges, differences of 30% to 40% occurred. In all cases, differences increased slightly at higher elevations and for stiffer soil conditions. North-south accelerations showed the smallest differences and were more uniform through the structure; while vertical accelerations were most different.

2.4.4 Verification of foundation model

Our flexible foundation model discretized the AFT complex foundation into eleven segments. Coupling between the segments occurs in three ways -- through soil coupling of the foundation impedances, stiffness coupling through the superstructure, and direct stiffness coupling between segments. The validity of the latter coupling was investigated further for the AFT complex. One can hypothesize that structural elements directly coupling two foundation segments may experience high stresses, possibly fail, and provide less stiffness than originally assumed. In addition, stresses in these elements may be artificially increased due to the assumption of rigid segment behavior and the possibility of a concentration of strain at the interfaces.

We calculated axial forces, shear forces, and bending moments in walls and slabs at three locations in the auxiliary building -- at the interface with the turbine building, at the

fuel handling building interface, and at the diesel generator building interface. Figure 2.38 shows the locations which are further described below:

- At the interface with the turbine building

  Location A: E-W shear wall, 5 ft. thick, between the basemat at elev. 542 and the floor slab at elev. 560.
  Location B: N-S shear wall, 3 ft. thick, on interface above turbine building basemat between elev. 560 and elev. 579.
  Location C: N-S connection between auxiliary building and turbine building basemats at elev. 542.
  Location D: Floor slab, 2 ft. thick, at elev. 560 in the auxiliary building.

- At the interface with the fuel handling building

  Location E: E-W shear wall, 2 ft. thick, elev. 560 to elev. 579
  Location F: E-W shear wall, 3 ft. thick, elev. 560 to elev. 579
  Location G: N-S exterior wall, 5 ft. thick, between auxiliary building basemat (elev. 542) and fuel handling building basemat (elev. 579).

- At the interface with the diesel generator building

  Location H: N-S shear wall, 5 ft. thick, between the basemat at elev. 542 and the floor slab at elev. 560
  Location I: E-W exterior wall, 3 ft. thick, connecting the auxiliary building basemat (elev. 542) with the diesel generator building basemat (elev. 568)
  Location J: Floor slab, 2 ft. thick, at elev. 560 in the auxiliary building.

The comparison of member forces and capacities at the above locations is summarized in Table 2.11. The table shows axial forces, shear forces, and bending moments normalized per unit length of wall or slab, and their corresponding design capacities. Best estimate capacities would be higher than the design values shown. Hence, these comparisons are conservative. Inspection of Table 2.11 shows that at all locations and force components except two (axial forces at A and G), the calculated member forces were within the design capacities -- generally less than 50% which indicates that the assumption of rigid segments did not lead to significant structure failure or reduction in stiffness.

The axial forces in the shear walls at Locations A and G in Fig. 2.38 were higher than the design capacities for combined axial force and bending. However, the ultimate tensile capacities of these members are at least 70% higher than the design values, so actual failure would not occur. We would expect some stiffness degradation in these members and a consequent redistribution of loads. This appearws to be a minor consideration relative to the overall model.

2.5 Observations and Conclusions

The assumption made in the SSMRP response calculations that the Zion AFT complex foundation behaves rigidly was reasonable. Further, this study showed that some variability in response due to the flexible vs. rigid foundation assumption occurs but no clear conservative or unconservative bias is observed. Hence, these foundation modeling assumptions lead to variability in response but not necessarily a change in its best estimate value. The overall frequency characteristics of the response remained the same independent of foundation modeling assumptions. This is a result of the unimportance of the

flexible foundation assumption for the Zion AFT complex rather than a general conclusion.

It is clear from this study that, in all flexible foundation assessments, it is essential to account for the stiffening effects of structural members on the foundation's stiffness. That is, an effective stiffness of the foundation exists due to the foundation itself and the interconnecting structural members, such as walls. Simplified models, e.g. in two dimensions, which model a foundation as being flexible should develop its effective stiffness from three-dimensional structure and foundation considerations. To demonstrate the concept of effective stiffness, we examined the relative stiffnesses due to the soil and structure for foundation degrees-of-freedom. We concentrated on static stiffnesses, i.e. at zero frequency. Table 2.12 shows the comparison for the foundation segment of the auxiliary building. The values shown give the forces that must be applied to produce unit displacements for each basemat degree-of-freedom, keeping all other basemats fixed. The table shows the resistance to displacement due to the structure is from one to two orders of magnitude greater than that due to the soil stiffness. This comparison is typical of other basemats as well. Although the plan area of the AFT complex is large, there are numerous shear walls and floor slabs continuously connected to basemat slabs which greatly stiffen the foundation.

This study was performed on a single specific structure and three related site conditions which is inadequate to draw generic conclusions concerning the importance of flexible foundations. A systematic evaluation of likely structure and site conditions is required to do so. However it would appear that shear wall structures typical to nuclear power plants provide significant additional stiffness to their foundations which permits their foundations to behave rigidly.

Table 2.1 Zion Soil Characteristics - Nominal Values.

Layer Number	Description	Layer Thickness (ft)	Unit Weight (lb/ft^3)	Poisson's Ratio	Shear Modulus ($10^6 lb/ft^2$)	Damping Ratio
1	Lake Deposits above Water Table	6	116	0.39	1.46	.018
2	Lake Deposits below Water Table	30	131	0.39	3.46	.026
3	Cohesive Glacial Till and Cohesionless Glacial Deposits	75	142	0.46	8.57	.025
4	Niagara Dolomite	--	160	0.27	423.	.01

Table 2.2: Comparison of Maximum Foundation Accelerations - Condensed Flexible Foundation Model vs. Rigid Foundation Model

	Condensed Flexible Foundation Model	Rigid Foundation Model
E-W Translation (x)	7.71 ft./sec.^{2}	7.91 ft./sec.^{2}
N-S Translation (y)	8.71	9.26
Vertical Translation (z)	4.71	4.69
N-S Rocking (xx)	.0043 rad./sec.^{2}	.0041 rad./sec.^{2}
E-W Rocking (yy)	.0201	.0192
Torsion (zz)	.0068	.0067

Table 2.3: Comparison of Maximum Base Forces and Moments - Condensed Flexible Foundation Model vs. Rigid Foundation Model

	Condensed Flexible Foundation Model	Rigid Foundation Model
E-W Shear Force (x)	117 x 10 kips	138 x 10 kips
N-S Shear Force (y)	102 x 10	118 x 10
Vertical Force (z)	37 x 10	48 x 10
N-S Overturning Moment (xx)	7.2 x 10 kip-ft.	8.0 x 10 kip-ft.
E-W Overturning Moment (yy)	10.1 x 10	11.4 x 10
Torsional Moment (zz)	4.1 x 10	4.0 x 10

Table 2.4: Comparison of Maximum In-Structure Accelerations (ft./sec.^{2}) -- Condensed Flexible Foundation Model vs. Rigid Foundation Model

Location	Node Number	Elevation	Condensed Flex. Found. Model E-W Trans.	N-S Trans.	Vertical	Rigid Foundation Model E-W Trans.	N-S Trans.	Vertical
Auxiliary building -- center	506	560	7.99	9.19	5.04	8.13	9.80	4.62
	1008	579	8.36	9.36	5.54	8.40	9.98	5.12
	1510	592	8.28	9.40	5.88	8.29	10.04	5.44
	2012	617	12.28	11.06	5.92	12.30	11.42	5.48
	2502	630	15.45	11.39	5.95	15.58	11.59	5.50
	3006	642	15.74	11.87	5.96	15.85	11.89	5.52
	3511	666	15.59	12.10	5.98	15.69	12.08	5.53
Diesel generator building	2118	617	7.68	9.69	5.21	8.29	10.31	4.64
	2534	630	16.67	10.43	5.97	15.96	11.18	5.48
	3105	642	15.81	10.87	5.99	15.59	11.62	5.43
	3584	666	15.21	10.90	6.03	15.79	11.61	5.43
Fuel handling building--centerline west end	2001	617	8.02	9.57	6.85	8.09	10.22	6.72
	3001	642	10.20	10.69	6.87	10.35	11.85	6.72
Turbine building-- centerline east end	3012	642	16.58	24.21	5.14	16.73	-	5.93
	3516	666	35.67	35.04	5.14	31.51	35.77	5.93
	4005	712	8.02	22.34	5.14	8.12	23.19	5.93
Turbine building-- southeast corner	4065	712	10.28	22.39	5.76	10.44	23.24	6.60

Table 2.5: Comparison of Maximum Foundation Accelerations - Flexible vs. Rigid Foundation -- Nominal Soil Properties

	Flexible Foundation						Rigid Foundation					
Fdn. No.	E-W Trans.	N-S Trans.	Vert. Trans.	N-S Rock	E-W Rock	Torsion	E-W Trans.	N-S Trans.	Vert. Trans.	N-S Rock	E-W Rock	Torsion
1	7.59	9.07	4.61	.0047	.013	.011	7.71	8.83	4.61	.0043	.020	.0067
2	7.49	8.83	5.72	.0045	.020	.011	7.71	8.57	4.82	"	"	"
4	6.53	9.01	5.05	.0075	.019	.010	7.43	8.78	5.10	"	"	"
7	6.49	8.82	5.94	.0064	.020	.011	7.44	8.57	5.24	"	"	"
8	8.64	9.00	4.14	.0077	.022	.011	7.99	8.78	4.21	"	"	"
11	8.60	8.82	5.19	.0066	.021	.011	7.97	8.57	4.51	"	"	"

Table 2.6: Comparison of Maximum Foundation Accelerations - Flexible vs. Rigid Foundation -- Stiff Soil Properties

	Flexible Foundation						Rigid Foundation					
Fdn. No.	E-W Trans.	N-S Trans.	Vert. Trans.	N-S Rock	E-W Rock	Torsion	E-W Trans.	N-S Trans.	Vert. Trans.	N-S Rock	E-W Rock	Torsion
1	6.68	6.21	5.05	.0038	.014	.0072	6.41	6.38	5.40	.0026	.0137	.0066
2	6.63	6.43	5.17	.0033	.017	.0073	6.41	6.57	4.79	"	"	"
4	6.54	6.20	5.08	.0080	.015	.0076	7.02	6.41	5.43	"	"	"
7	6.55	6.41	5.06	.0049	.017	.0074	6.98	6.57	4.99	"	"	"
8	6.96	6.24	4.76	.0075	.019	.0076	6.32	6.41	5.12	"	"	"
11	6.94	6.45	5.01	.0056	.018	.0074	6.31	6.57	4.61	"	"	"

Table 2.7: Comparison of Maximum Foundation Accelerations - Flexible vs. Rigid Foundation -- Soft Soil Properties

	Flexible Foundation						Rigid Foundation					
Fdn. No.	E-W Trans.	N-S Trans.	Vert. Trans	N-S Rock	E-W Rock	Torsion	E-W Trans.	N-S Trans.	Vert. Trans.	N-S Rock	E-W Rock	Torsion
1	10.08	9.27	4.24	.0067	.016	.012	9.68	9.34	4.65	.0045	.021	.0079
2	9.94	9.29	5.43	.0065	.030	.012	9.68	9.22	4.96	"	"	"
4	10.13	9.26	4.62	.0098	.026	.012	10.04	9.30	4.39	"	"	"
7	10.10	9.30	5.40	.0081	.030	.012	10.02	9.22	5.02	"	"	"
8	9.88	9.24	4.51	.0101	.031	.011	9.32	9.30	4.58	"	"	"
11	9.87	9.26	5.34	.0082	.030	.011	9.34	9.22	5.12	"	"	"

Table 2.8: Comparison of Maximum In-Structure Accelerations - Flexible vs. Rigid Foundation -- Nominal Soil Properties

Location	Node Number	Elevation	Flexible Foundation E-W Trans.	Flexible Foundation N-S Trans.	Flexible Foundation Vert. Trans.	Rigid Foundation E-W Trans.	Rigid Foundation N-S Trans.	Rigid Foundation Vert. Trans.
Auxiliary building -- center	506	560	7.80	9.44	4.98	7.99	9.19	5.04
	1008	579	8.08	9.56	5.34	8.36	9.36	5.54
	1510	592	8.00	9.57	5.66	8.28	9.40	5.88
	2012	617	11.86	10.76	5.71	12.28	11.06	5.93
	2502	630	14.95	11.06	5.73	15.45	11.39	5.95
	3006	642	15.15	11.50	5.74	15.74	11.87	5.97
	3511	666	15.91	11.73	5.76	15.59	12.10	5.98
Diesel generator building	2118	617	8.14	9.94	5.11	7.68	9.69	5.21
	2534	630	15.49	10.73	5.17	16.67	10.43	5.97
	3105	642	14.74	11.15	5.31	15.81	10.87	5.99
	3584	666	13.66	11.27	5.26	15.21	10.90	6.03
Turbine building-- centerline east end	3012	642	15.89	24.28	6.50	16.58	24.21	5.14
	3516	666	39.46	39.29	6.50	35.67	35.04	5.14
	4005	712	8.08	24.41	6.50	8.02	22.34	5.14
Turbine building-- southeast corner	4065	712	10.59	24.45	6.94	10.28	22.39	5.76

Table 2.9: Comparison of Maximum In-Structure Accelerations - Flexible vs. Rigid Foundation -- Stiff Soil Properties

Location	Node Number	Elevation	Flexible Foundation E-W Trans.	Flexible Foundation N-S Trans.	Flexible Foundation Vert. Trans.	Rigid Foundation E-W Trans.	Rigid Foundation N-S Trans.	Rigid Foundation Vert. Trans.
Auxiliary building -- center	506	560	6.75	6.53	5.31	6.68	6.76	5.76
	1008	579	6.92	6.62	5.53	6.93	6.87	5.93
	1510	592	6.93	6.62	5.62	6.72	6.90	6.00
	2012	617	8.97	7.21	5.63	9.63	7.47	6.00
	2502	630	11.44	7.51	5.63	12.32	7.68	6.01
	3006	642	12.23	8.09	5.64	12.94	8.17	6.01
	3511	666	12.89	8.47	5.64	14.32	8.50	6.01
Diesel generator building	2118	617	7.81	7.22	5.52	8.23	7.18	5.89
	2534	630	16.54	7.97	5.89	15.93	7.72	6.39
	3105	642	16.31	8.51	6.02	15.28	8.04	6.51
	3584	666	15.37	8.46	6.10	14.49	8.18	6.58
Turbine building-- centerline east end	3012	642	12.30	18.67	5.15	13.69	17.23	4.47
	3516	666	34.79	26.17	5.15	32.84	27.17	4.47
	4005	712	8.21	19.92	5.15	7.98	19.37	4.47
Turbine building-- southeast corner	4065	712	9.63	19.97	5.35	9.33	19.42	4.90

Table 2.10: Comparison of Maximum In-Structure Accelerations - Flexible vs. Rigid Foundation -- Soft Soil Properties

Location	Node Number	Elevation	Flexible Foundation E-W Trans.	Flexible Foundation N-S Trans.	Flexible Foundation Vert. Trans.	Rigid Foundation E-W Trans.	Rigid Foundation N-S Trans.	Rigid Foundation Vert. Trans.
Auxiliary building -- center	506	560	10.31	9.77	4.53	9.80	9.91	4.86
	1008	579	10.65	10.03	4.72	9.97	10.18	5.14
	1510	592	10.70	10.13	4.82	9.90	10.29	5.34
	2012	617	11.64	11.87	4.83	11.50	11.44	5.37
	2502	630	14.64	12.18	4.84	14.45	11.76	5.38
	3006	642	14.89	12.64	4.85	14.76	12.26	5.40
	3511	666	16.27	12.88	4.85	14.65	12.56	5.40
Diesel generator building	2118	617	11.37	10.79	4.86	9.90	10.70	4.57
	2534	630	16.39	11.80	5.30	14.66	11.67	5.21
	3105	642	15.99	12.38	5.43	14.36	12.23	5.34
	3584	666	15.55	13.28	5.50	14.11	12.78	5.40
Turbine building-- centerline east end	3012	642	15.52	18.28	6.46	15.65	19.72	5.49
	3516	666	28.08	30.38	6.46	28.72	31.45	5.49
	4005	712	8.55	28.25	6.46	8.29	26.41	5.49
Turbine building-- southeast corner	4065	712	11.22	28.28	6.61	9.25	26.46	5.67

Table 2.11: Comparison of Calculated Member Forces and Capacities in the Auxiliary Building

Description	Location (Fig. 2.50)	Calculated Member Forces			Design Member Capacities		
		Axial k/ft	Shear k/ft	Bending k-ft/ft	Tension k/ft	Shear k/ft	Bending k-ft/ft
At Turbine Bldg.							
E-W Shear Wall, Elev. 542-560	A	36.0	20.7	--	26.4	41.6	--
N-S Boundary Wall, Elev. 560-579	B	14.9	38.4	1.5	93.6	62.8	164.
N-S Basemat Connection, Elev. 542	C	138.	9.6	152.	159.	115.	614.
Floor Slab, Elev. 560	D	10.6	10.6	1.0	139.	51.2	46.3
At Fuel Handling Bldg.							
E-W Shear Wall, Elev. 560-579	E	11.5	16.2	--	26.4	41.6	--
E-W Shear Wall, Elev. 560-579	F	46.2	27.9	--	125.	61.0	--
N-S Ext. Wall Between Basemats, Elev. 560-579	G	114.	45.5	24.9	93.6	117.	268.
At Diesel Generator Bldg.							
N-S Shear Wall, Elev. 542-560	H	83.5	19.9	--	125.	57.7	--
E-W Ext. Wall Between Elev. 542-560	I	103.	27.5	0.3	125.	57.7	198.
Floor Slab, Elev. 560	J	4.7	2.2	1.6	139.	51.2	46.3

Table 2.12: Comparison of Structural and Soil Stiffnesses for Auxiliary Building Foundation Segment

Foundation Component	Structural Stiffness	Soil Stiffness	Ratio
E-W Translation (k/ft)	1.4×10^{9}	1.0×10^{7}	133
N-S Translation (k/ft)	8.7×10^{8}	8.3×10^{6}	105
Vertical Translation (k/ft)	4.0×10^{8}	2.4×10^{7}	16
N-S Rocking (k-ft/ft)	4.3×10^{12}	1.1×10^{11}	39
E-W Rocking (k-ft/ft)	1.4×10^{12}	5.4×10^{10}	26
Torsion (k-ft/ft)	1.6×10^{13}	7.8×10^{10}	205

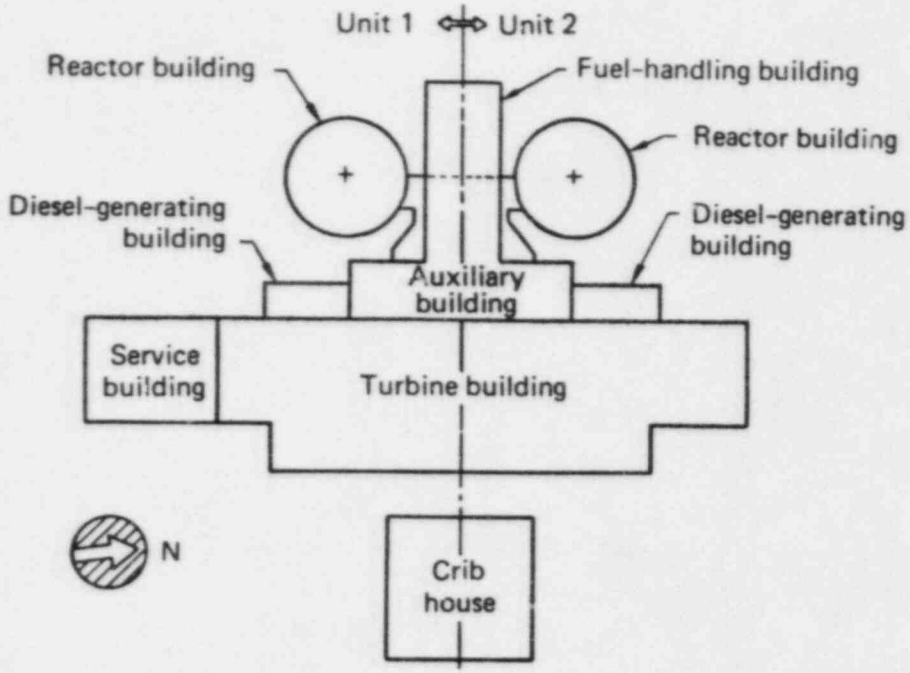

Fig. 2.1 Plan view of the Zion Nuclear Power Plant.

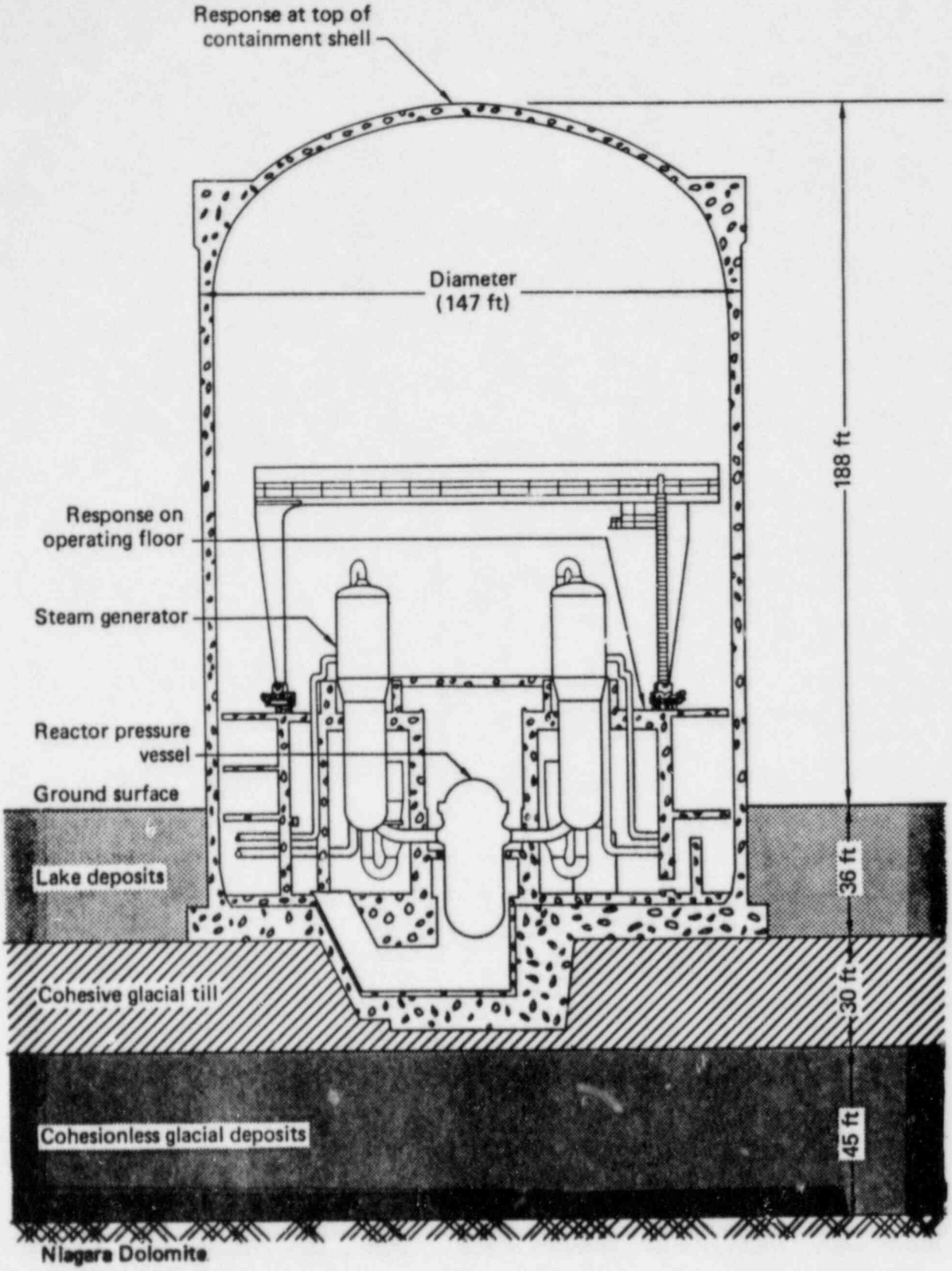

Fig. 2.2 Simplified elevation view of Unit 1 Reactor Building, facing west.

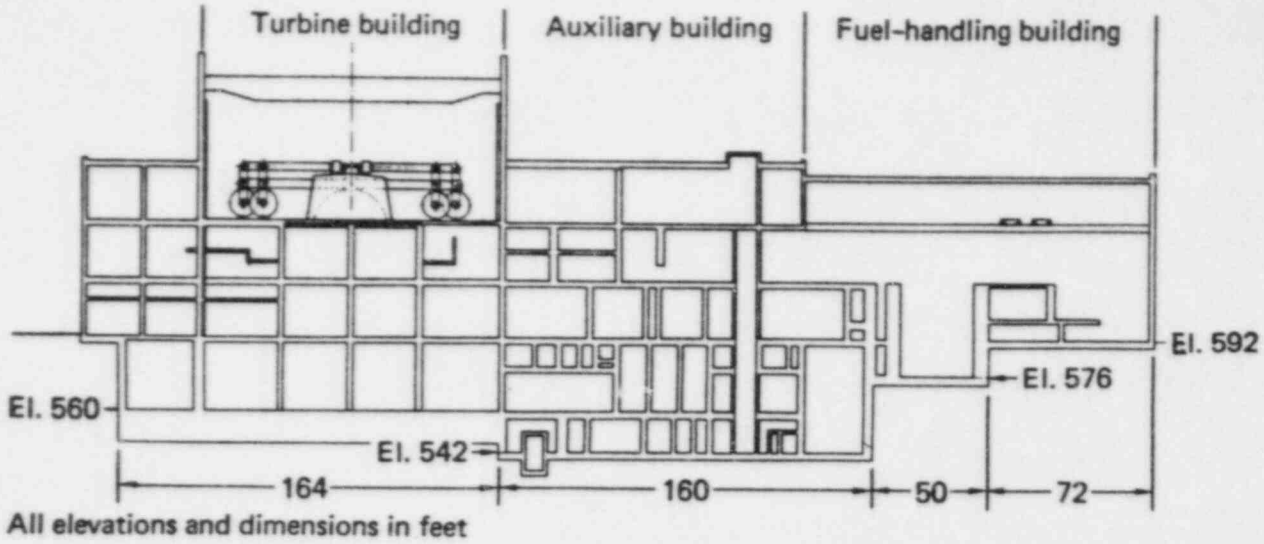

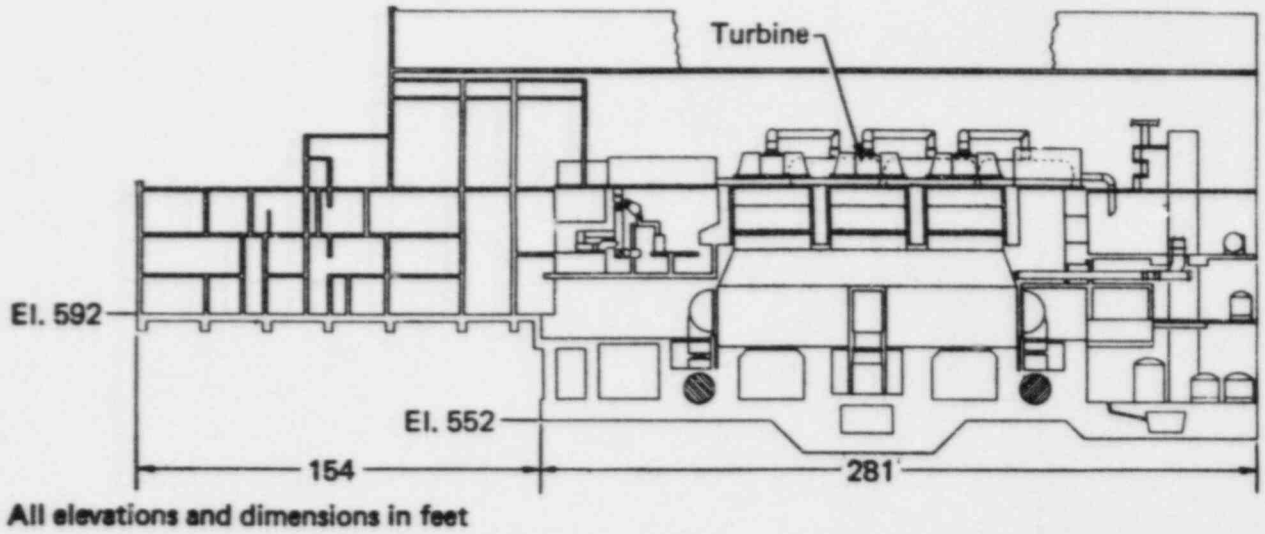

Fig. 2.3 Simplified elevation views of the auxiliary/fuel-handling/turbine (AFT) building complex. The top figure shows the view through the auxiliary building centerline, facing south; the bottom figure shows the view through the centerline of the turbines, facing west.

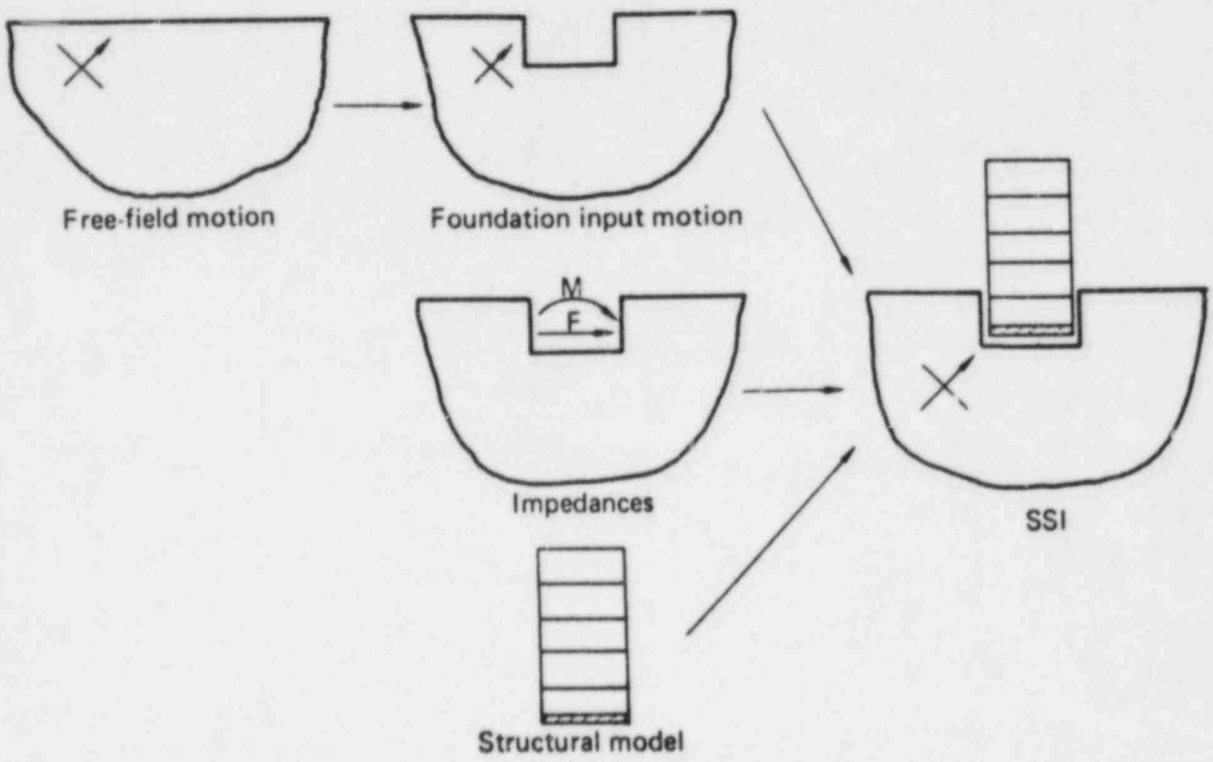

Fig. 2.4 Schematic representation of the elements of the substructure approach to SSI analysis.

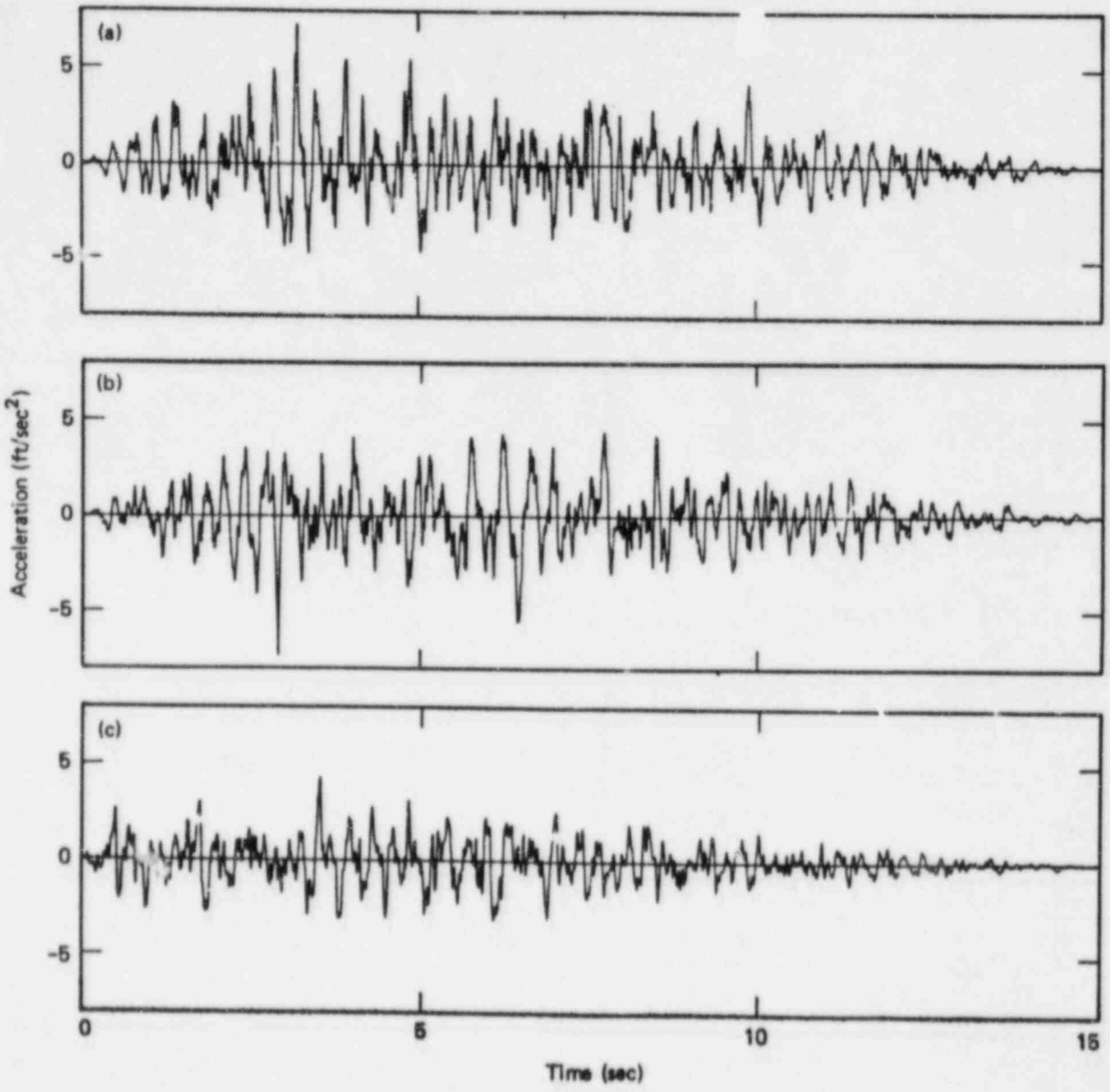

Fig. 2.5 Synthetic earthquake accelerograms. Shown are (a) E-W translation, (b) N-S translation, and (c) vertical translation.

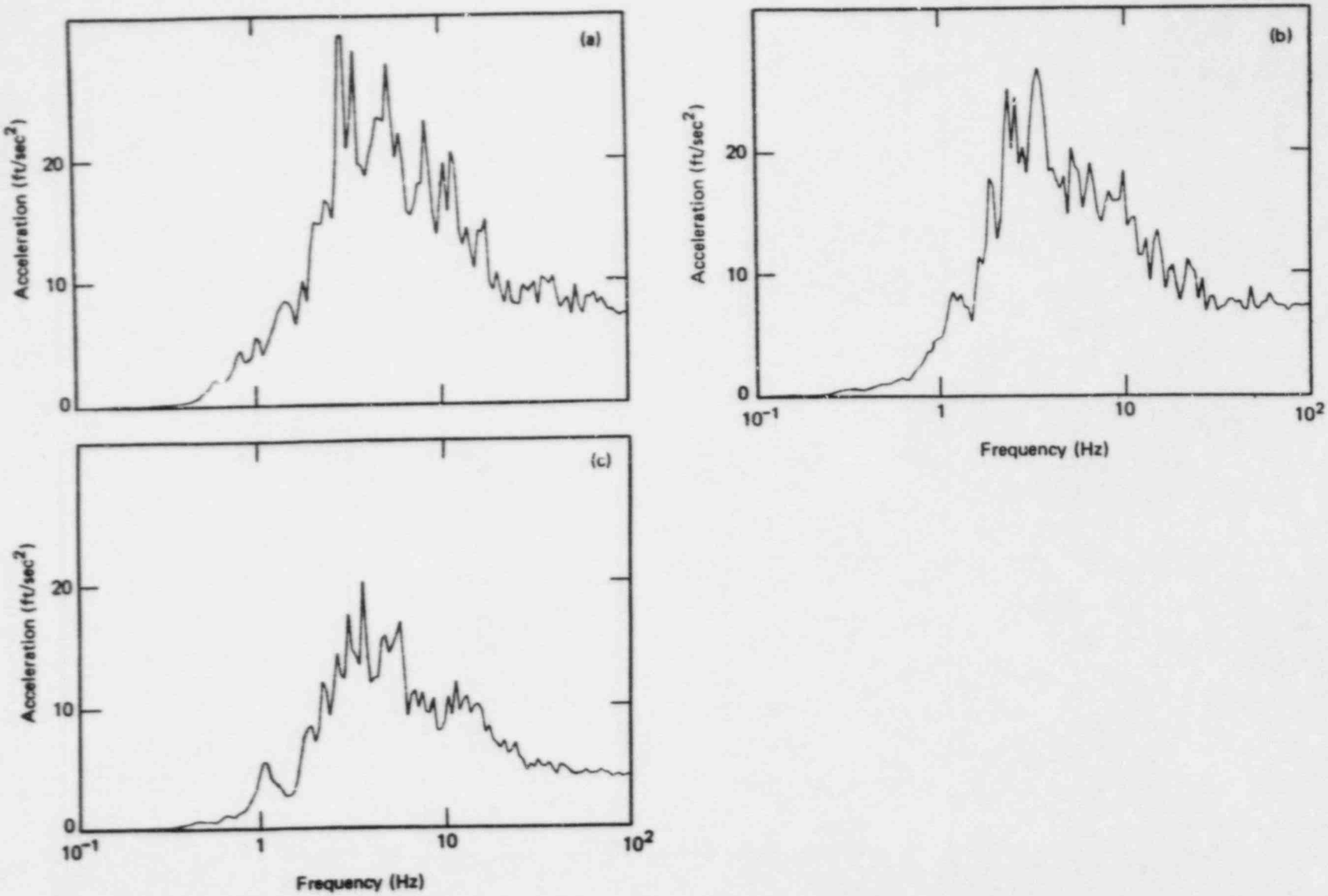

Fig. 2.6 Synthetic earthquake response spectra at 2% damping. Shown are (a) E-W translation, (b) N-S translation, and (c) vertical translation.

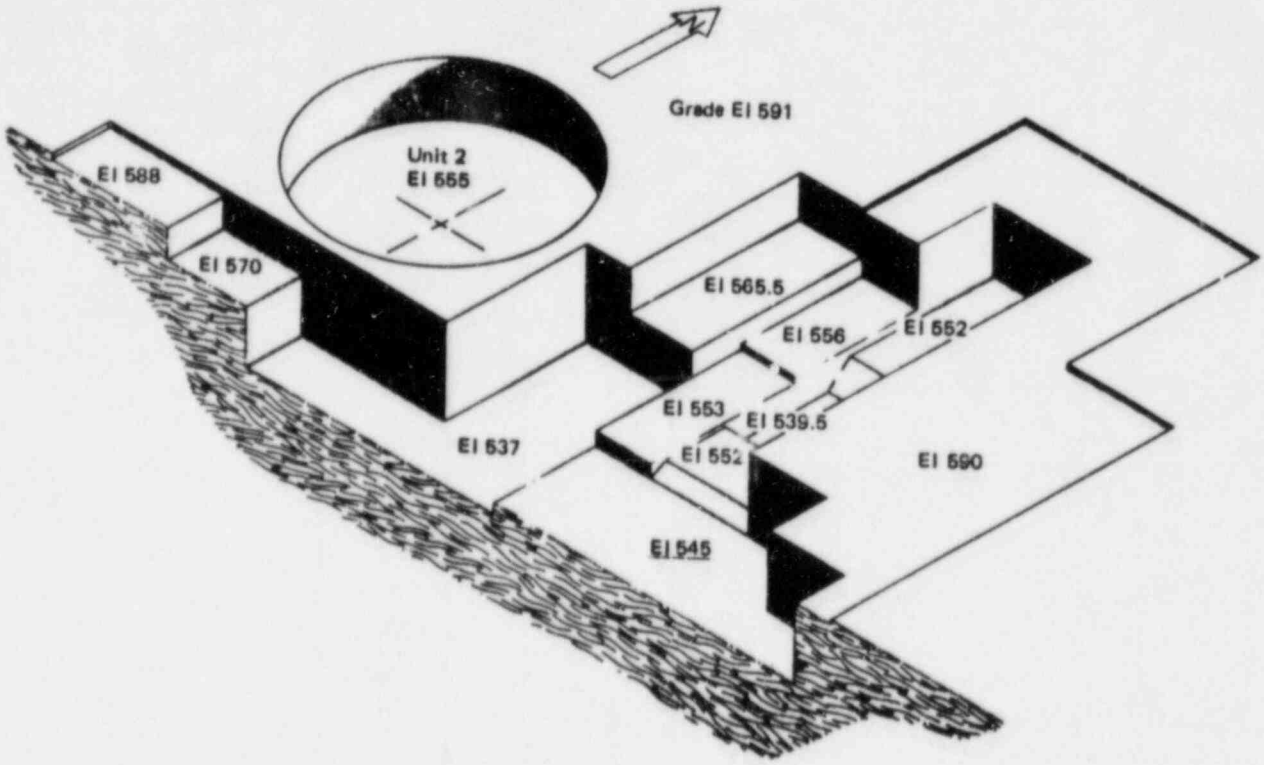

Fig. 2.7 Isometric view of the Zion foundation excavation configuration.

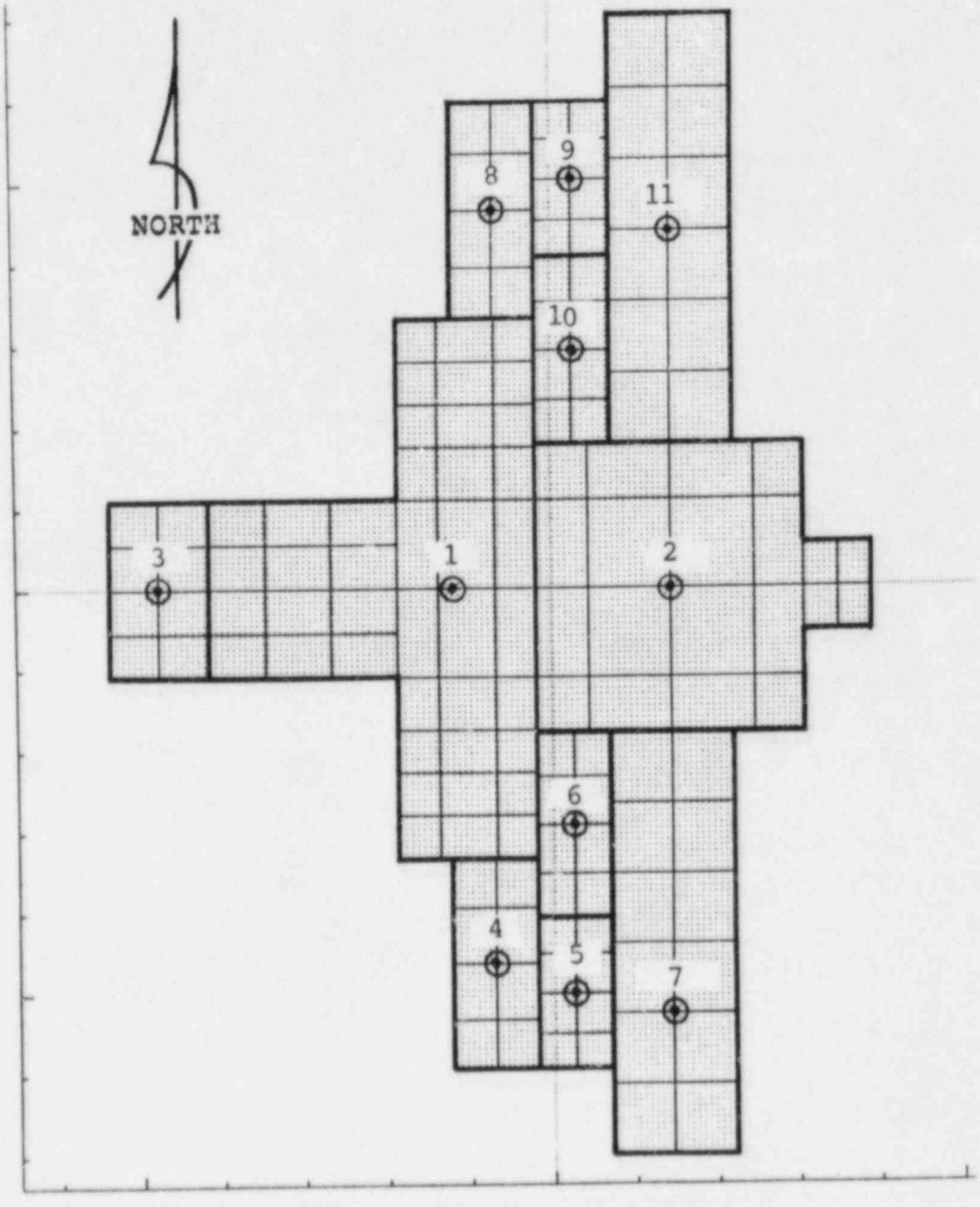

Fig. 2.8 Plan view of the AFT complex surface-foundation model -- discretization for eleven rigid segments.

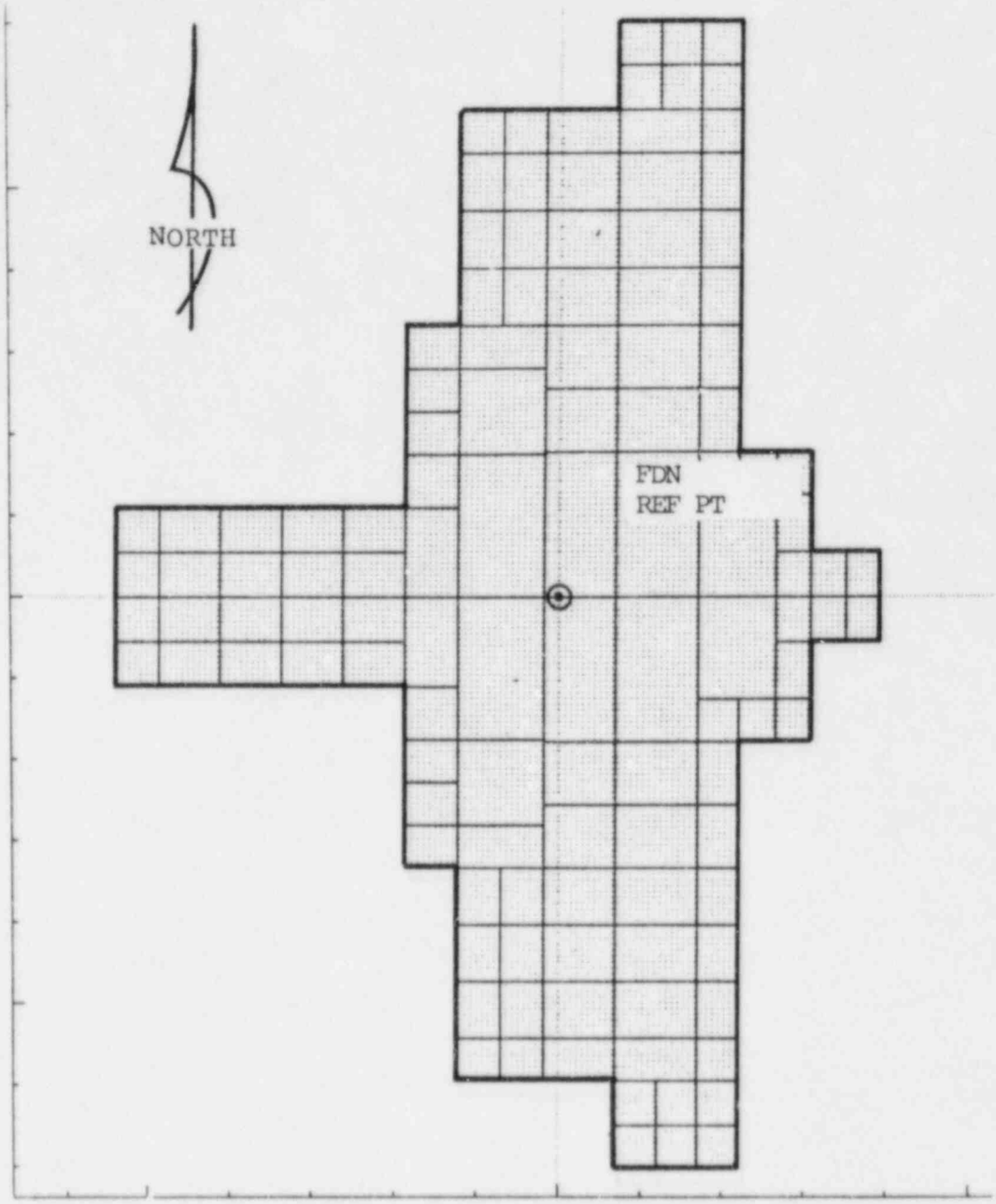

Fig. 2.9 Plan view of the AFT complex surface-foundation model -- rigid behavior, discretization for calculating impedances (Fig. 7 Ref. 3).

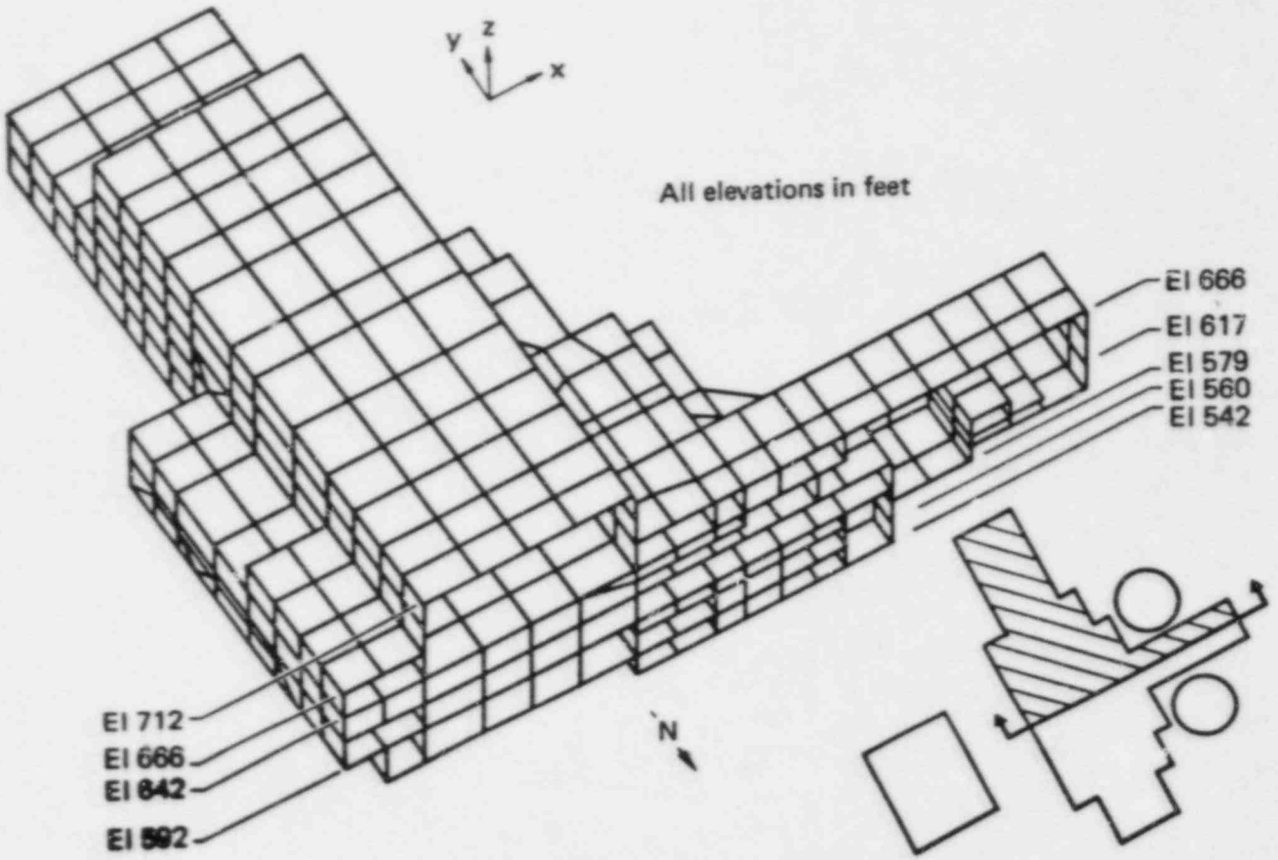

Fig. 2.10 Finite element half-structure model of the AFT complex; shaded area of the inset sketch shows the portion of the structure modeled.

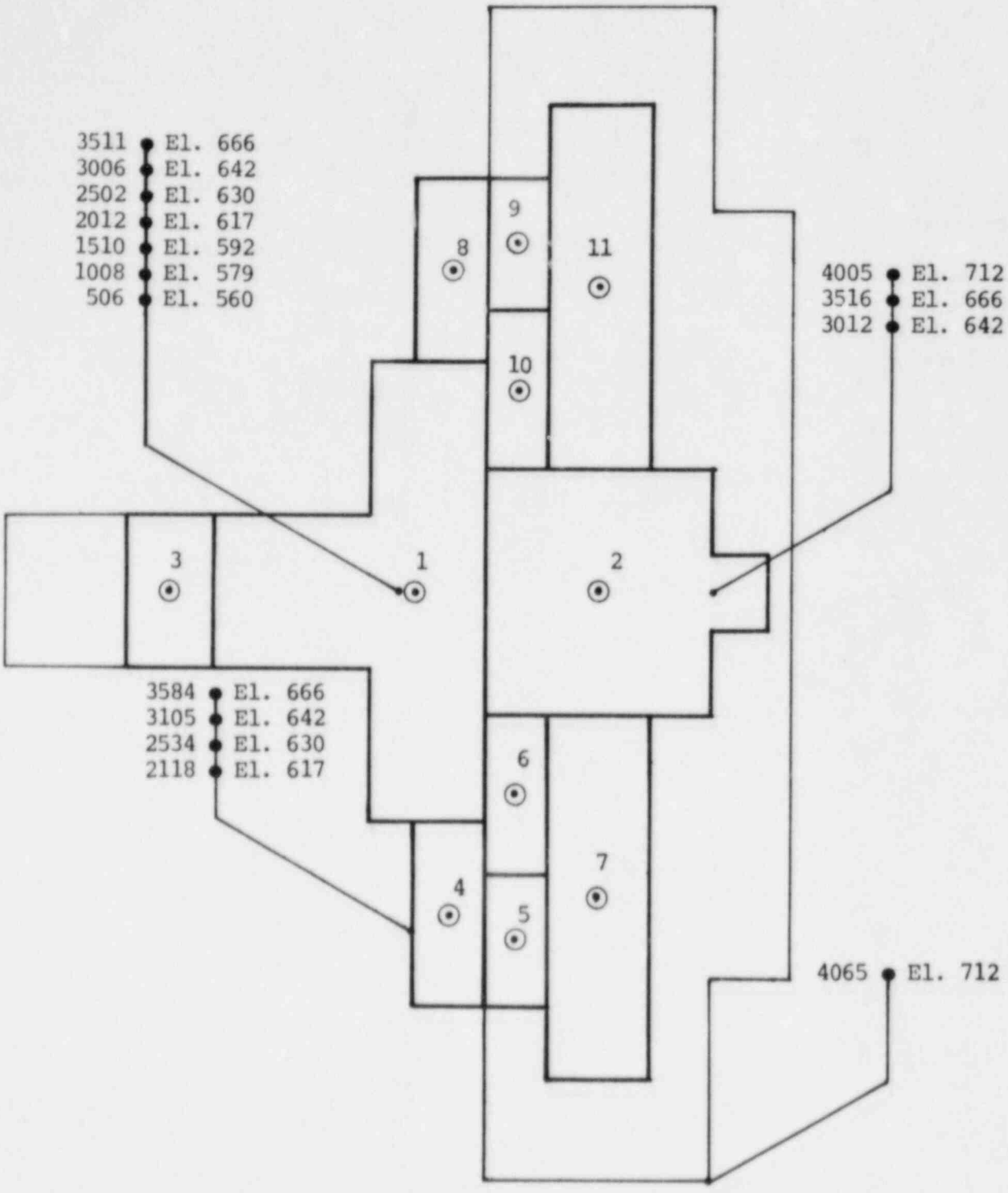

Fig. 2.11 Response locations in AFT complex.

a) E-W Translation

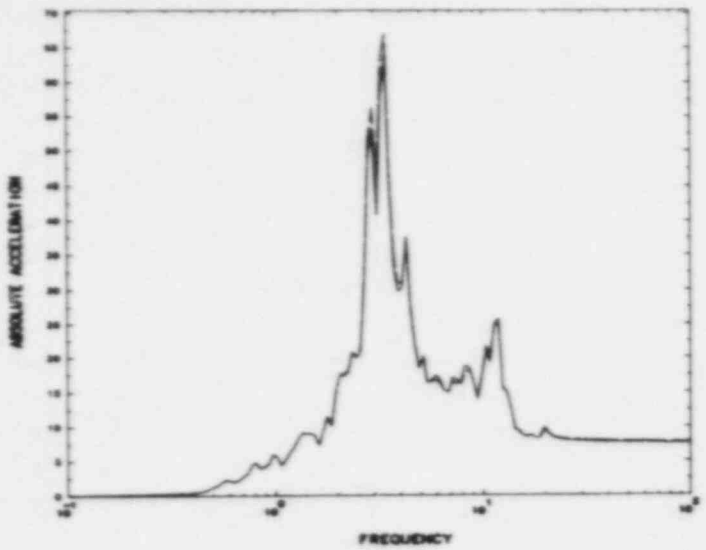

b) N-S Translation

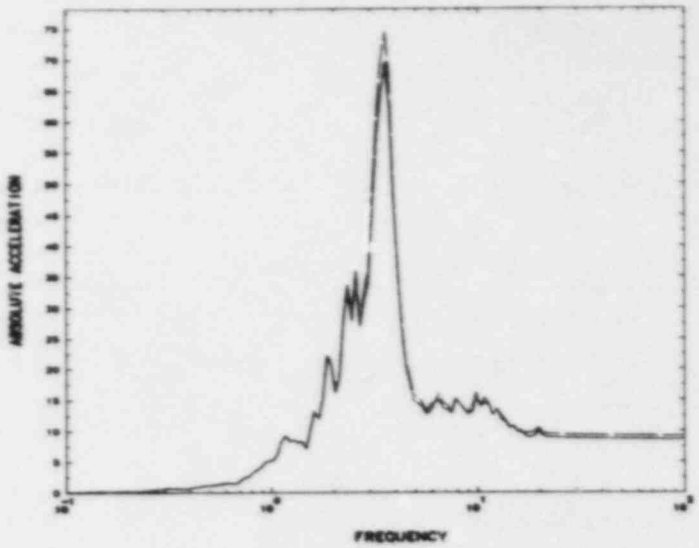

c) Vertical Translation

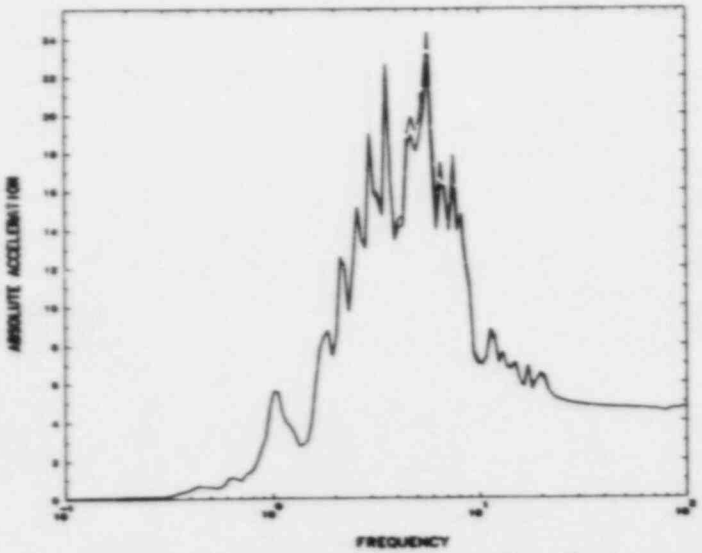

Legend

Condensed Flexible Foundation Model ————————

Rigid Foundation Model - - - - - -

Notes

All spectra at 2% damping

Frequencies in Hz

Translations in ft/sec^2 -

Fig. 2.12 Comparison of foundation response spectra -- condensed flexible foundation model vs. rigid foundation model (a) E-W translation, (b) N-S translation, (c) vertical translation, (d) N-S rocking, (e) E-W rocking, and (f) torsion.

d) N-S Rocking

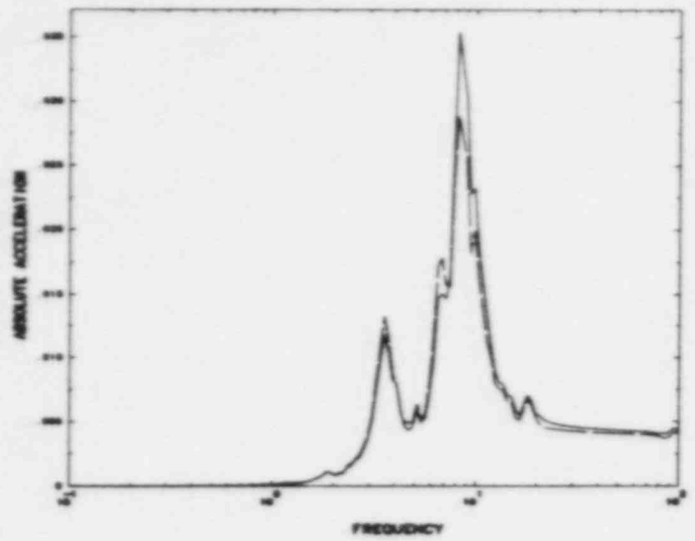

e) E-W Rocking

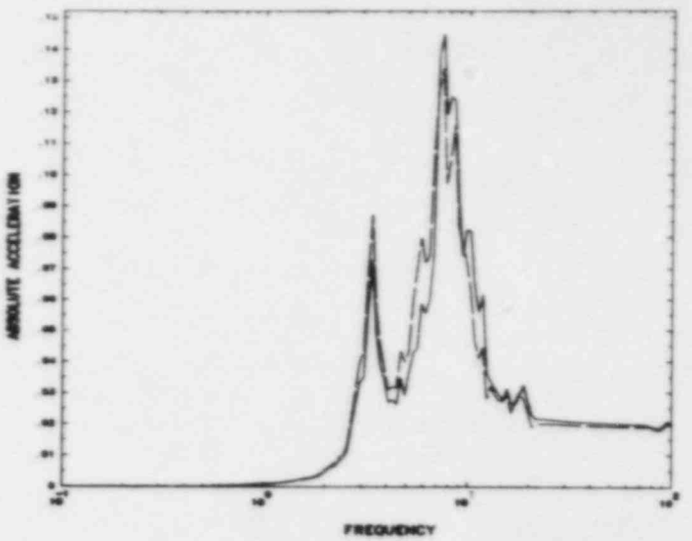

f) Torsion

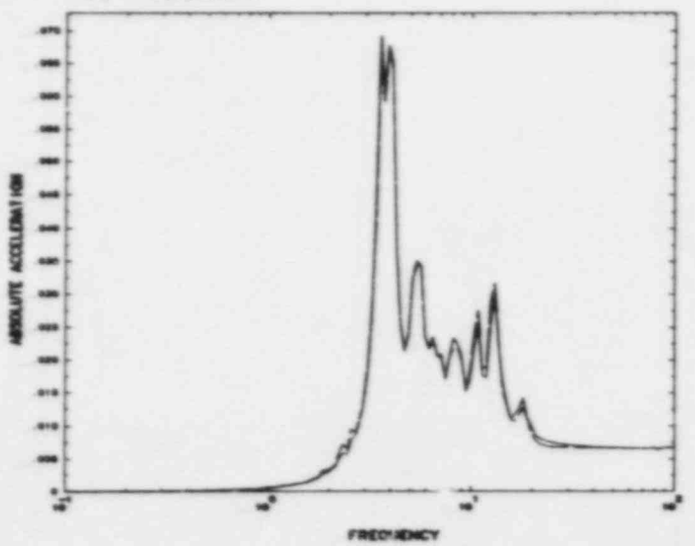

Legend

Condensed Flexible Foundation Model ————————

Rigid Foundation Model - - - - - - -

Notes

All spectra at 2% damping

Frequencies in Hz

Rotations in rad/sec^2 -

Fig. 2.12 (continued)

a) E-W Translation

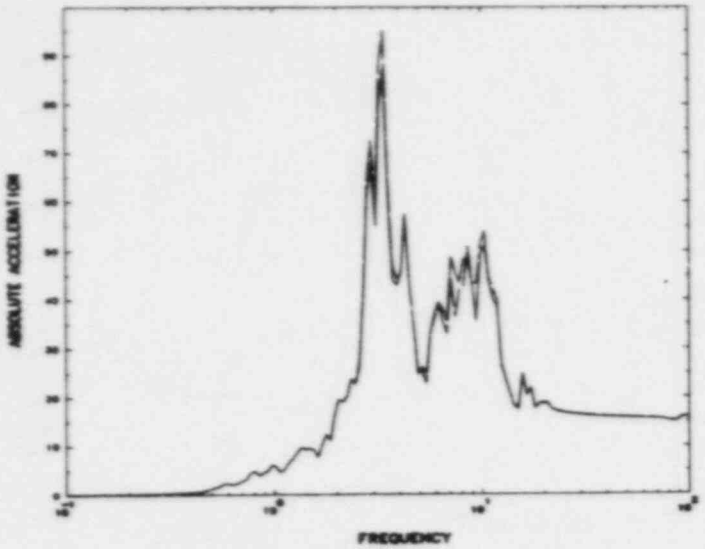

b) N-S Translation

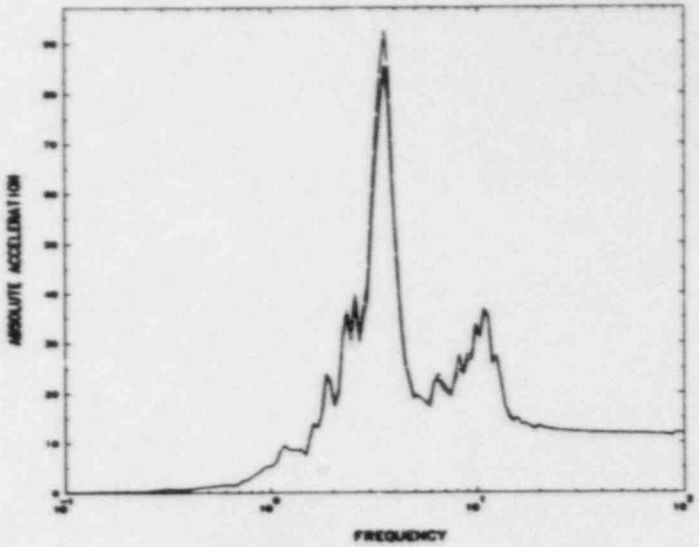

c) Vertical Translation

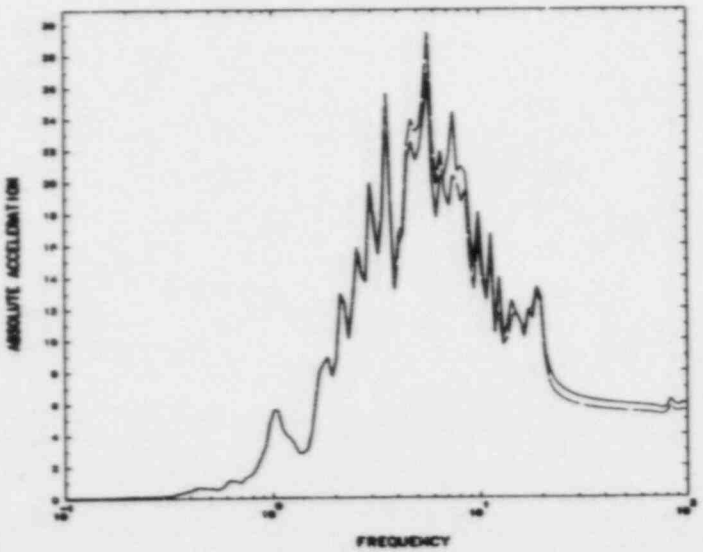

Legend

Condensed Flexible Foundation Model ————————

Rigid Foundation Model - - - - - -

Notes

All spectra at 2% damping
Frequencies in Hz
Translations in ft/sec^2

Fig. 2.13 Comparison of response spectra in the auxiliary building control room, node 3006, elevation 642' -- condensed flexible foundation model vs. rigid foundation model (a) E-W translation (b) N-S translation, (c) vertical translation.

a) E-W Translation

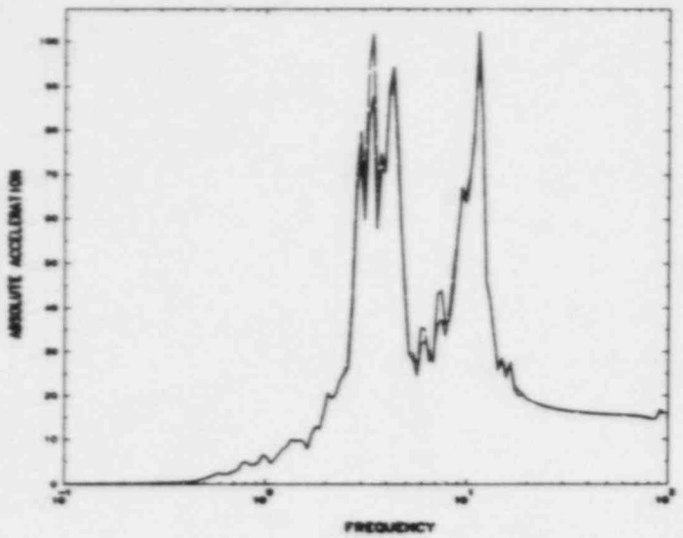

b) N-S Translation

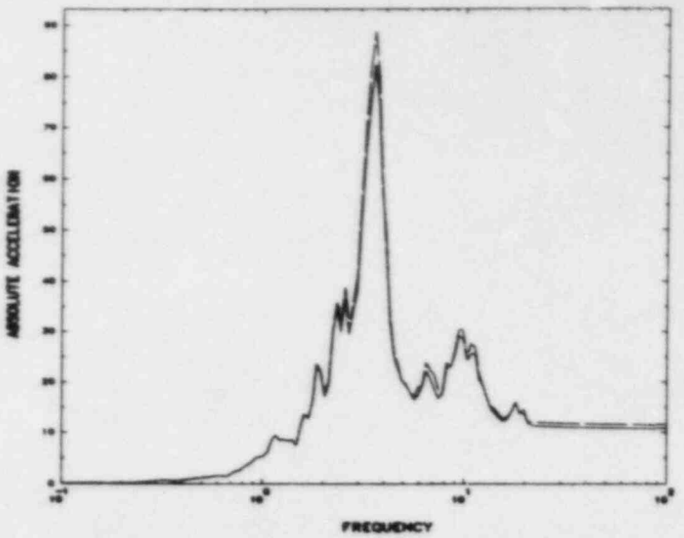

c) Vertical Translation

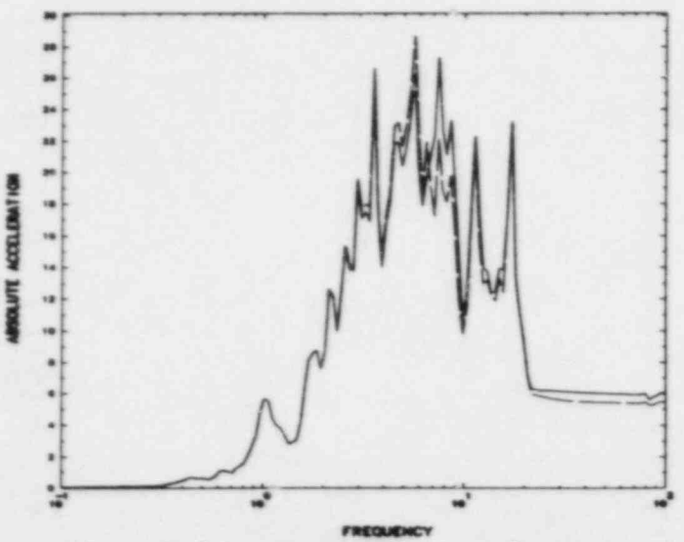

Legend

Condensed Flexible Foundation Model ————————

Rigid Foundation Model - - - - - - -

Notes

All spectra at 2% damping
Frequencies in Hz
Translations in ft/sec^2

Fig. 2.14 Comparison of response spectra in the diesel generator building, west wall, node 3105, elevation 642' -- condensed flexible foundation model vs. rigid foundation model (a) E-W translation, (b) N-S translation, and (c) vertical translation.

a) E-W Translation

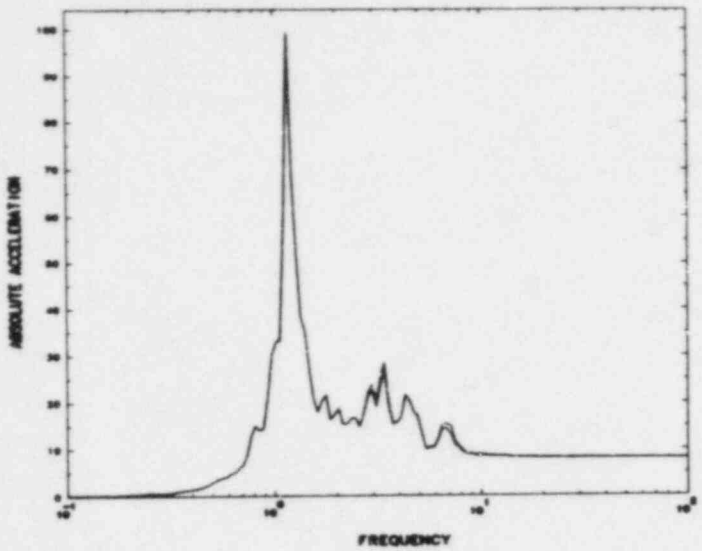

b) N-S Translation

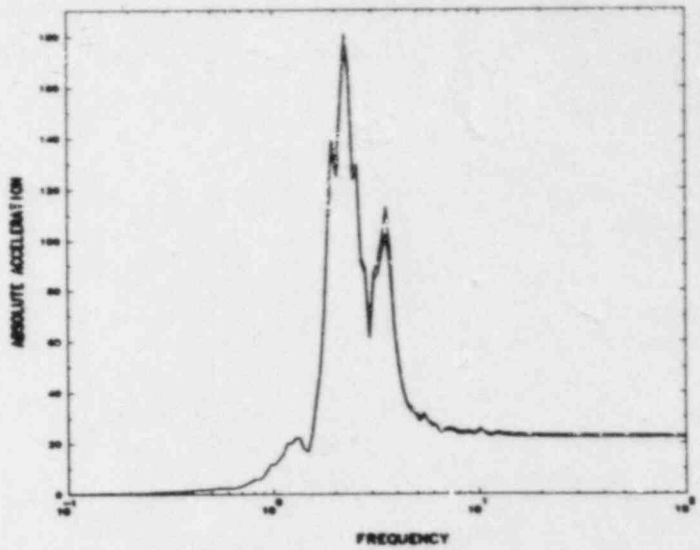

Legend

Condensed Flexible Foundation Model ————————

Rigid Foundation Model - - - - - -

Notes

All spectra at 2% damping

Frequencies in Hz

Translations in ft/sec^2

c) Vertical Translation

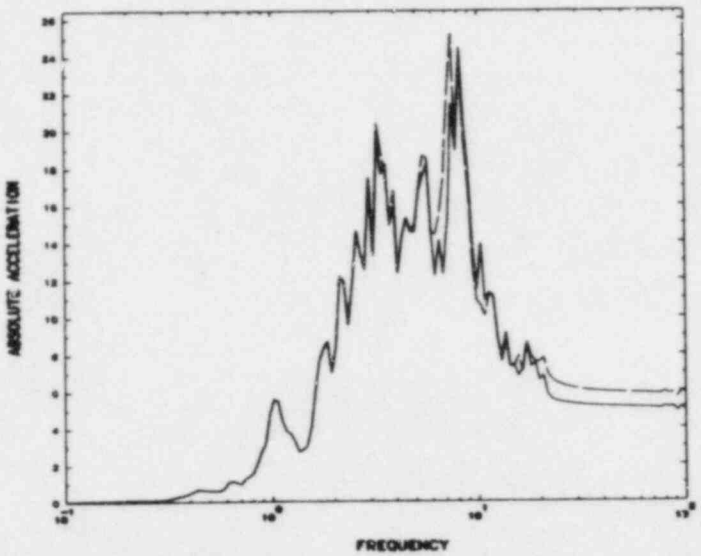

Fig. 2.15 Comparison of response spectra in the turbine building, center line east end, node 4005, elevation 712' -- condensed flexible foundation model vs. rigid foundation model (a) E-W translation, (b) N-S translation, and (c) vertical translation.

a) E-W Translation

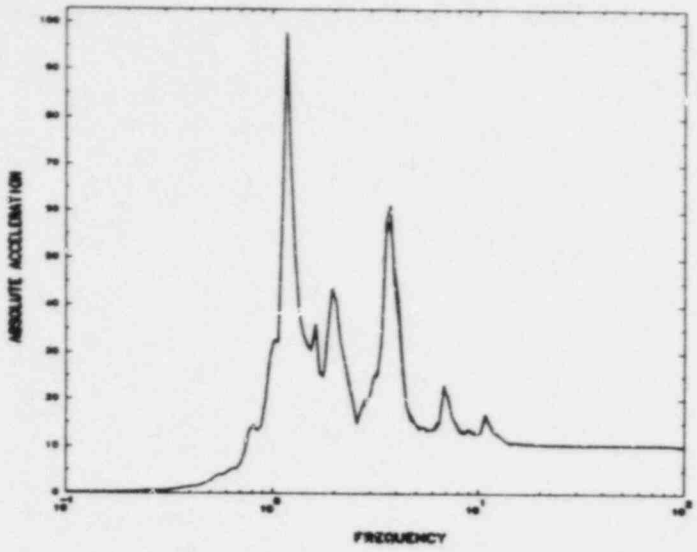

b) N-S Translation

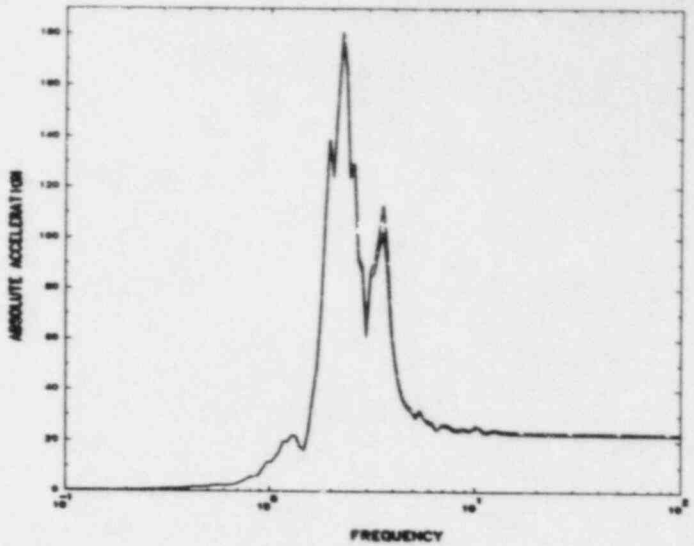

c) Vertical Translation

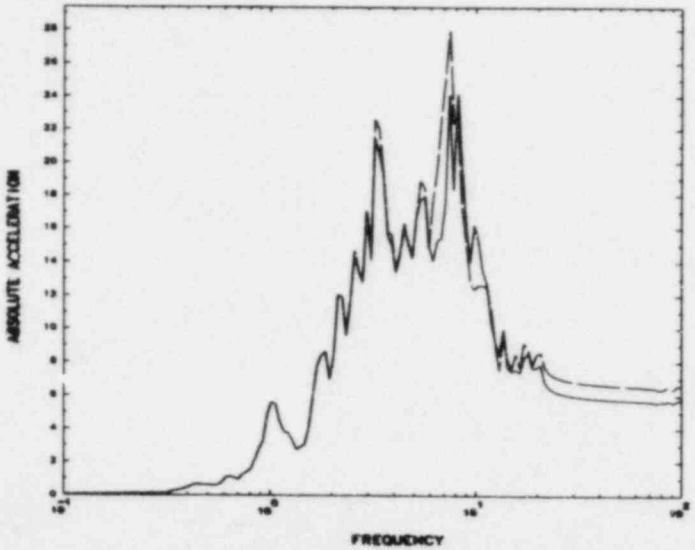

Legend

Condensed Flexible Foundation Model ————————

Rigid Foundation Model - - - - - -

Notes

All spectra at 2% damping
Frequencies in Hz
Translations in ft/sec^2

Fig. 2.16 Comparison of response spectra in the turbine building, southeast corner, node 4065, elevation 712' -- condensed flexible foundation model vs. rigid foundation model (a) E-W translation, (b) N-S translation, and (c) vertical translation.

a) E-W Translation

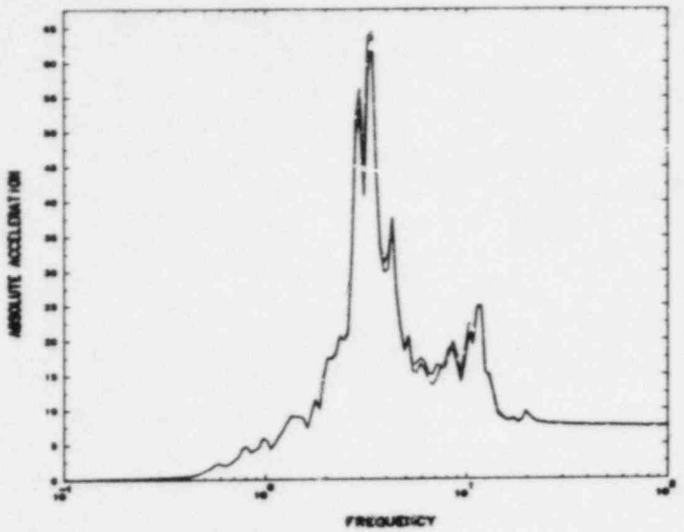

b) N-S Translation

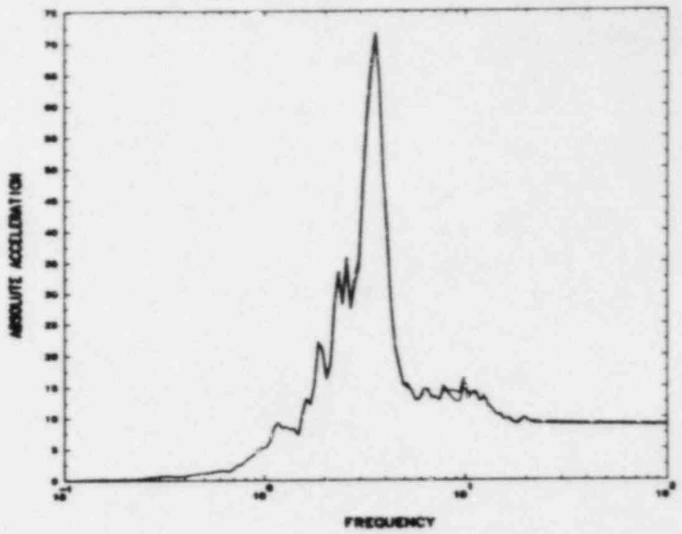

Legend

Rigid Foundation Model ————————
Flexible Foundation Model - - - - - - -

c) Vertical Translation

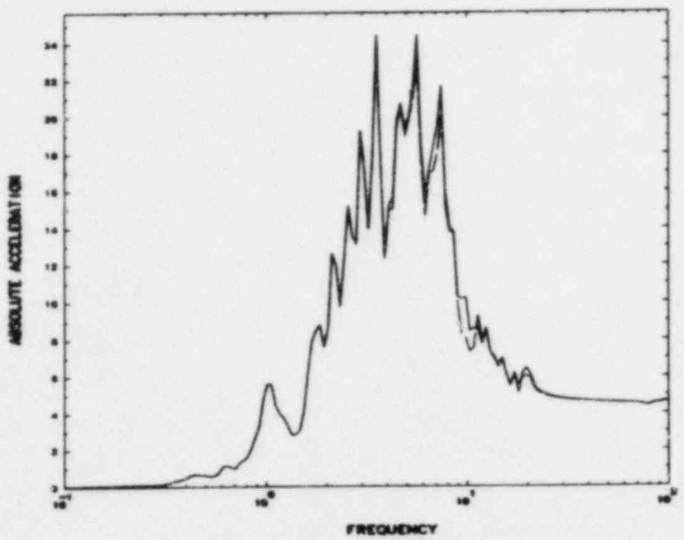

Notes

All spectra at 2% damping
Frequencies in Hz
Translations in ft/sec^2

Fig. 2.17 Comparison of response spectra on foundation segment 1, nominal soil properties -- flexible vs. rigid foundation, (a) E-W translation, (b) N-S translation, (c) vertical translation, (d) N-S rocking, (e) E-W rocking, and (f) torsion.

d) N-S Rocking

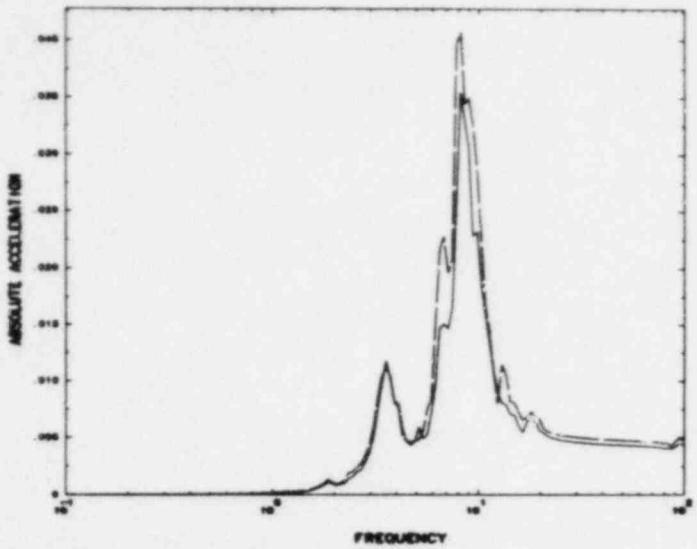

e) E-W Rocking

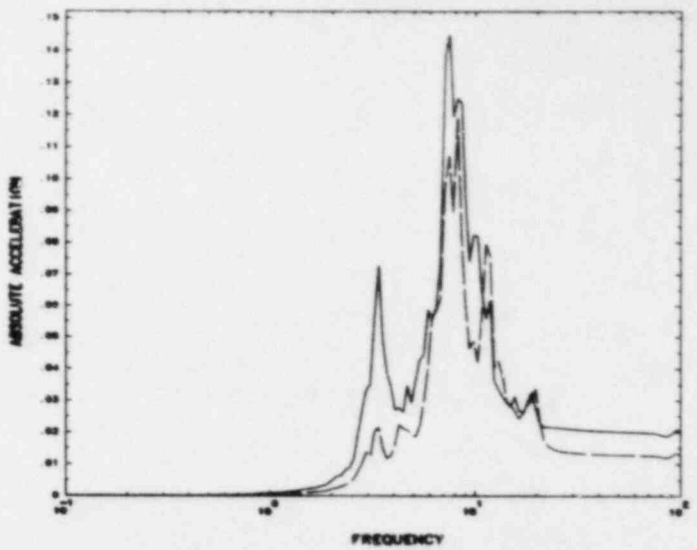

Legend

Rigid Foundation Model ————————

Flexible Foundation Model - - - - - -

Notes

All spectra at 2% damping
Frequencies in Hz
Rotations in rad/sec^2

f) Torsion

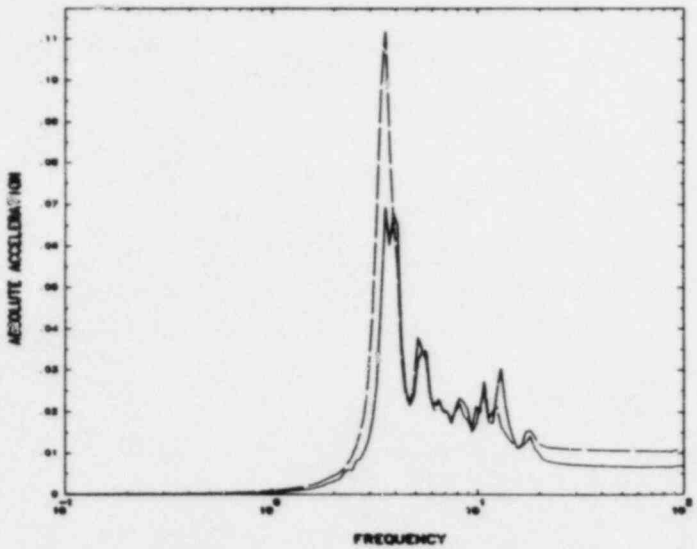

Fig. 2.17 (continued)

a) E-W Translation

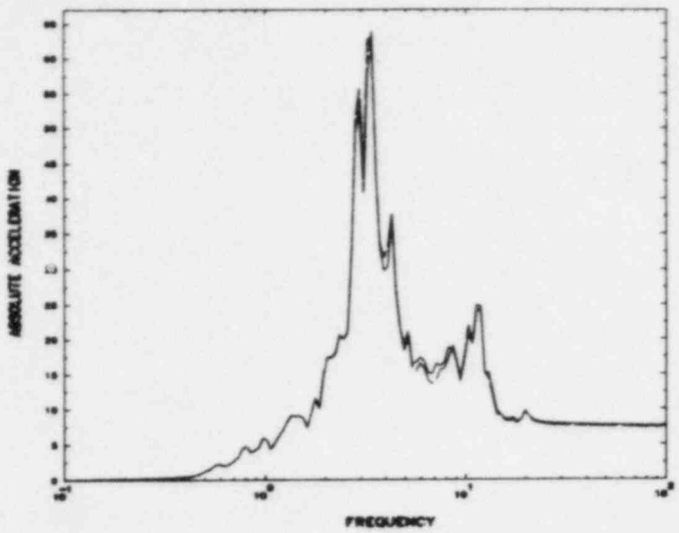

b) N-S Translation

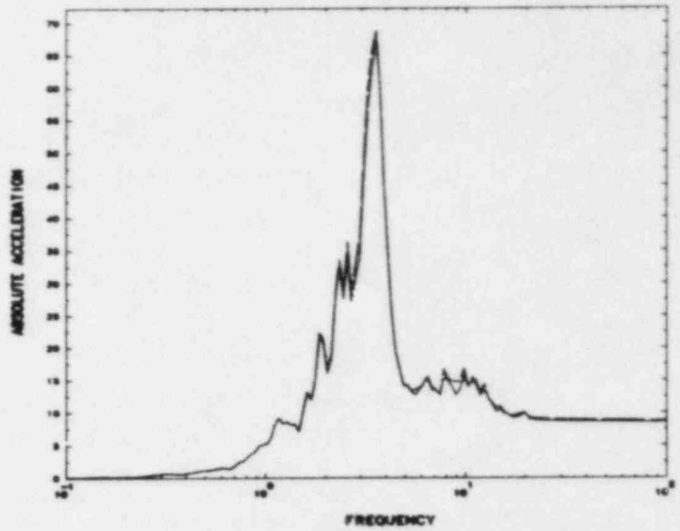

Legend

Rigid Foundation Model ————————
Flexible Foundation Model - - - - - -

Notes

All spectra at 2% damping
Frequencies in Hz
Translations in ft/sec^2

c) Vertical Translation

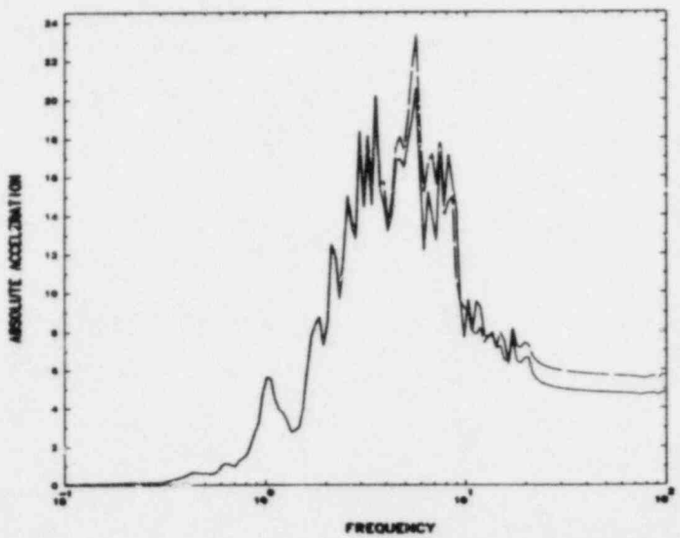

Fig. 2.18 Comparison of response spectra on foundation segment 2, nominal soil properties -- flexible vs. rigid foundation, (a) E-W translation, (b) N-S translation, (c) vertical translation, (d) N-S rocking, (e) E-W rocking, and (f) torsion.

d) N-S Rocking

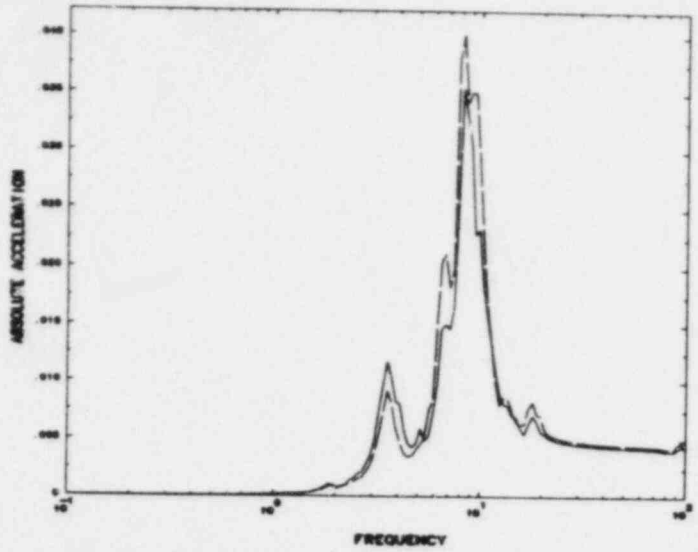

e) E-W Rocking

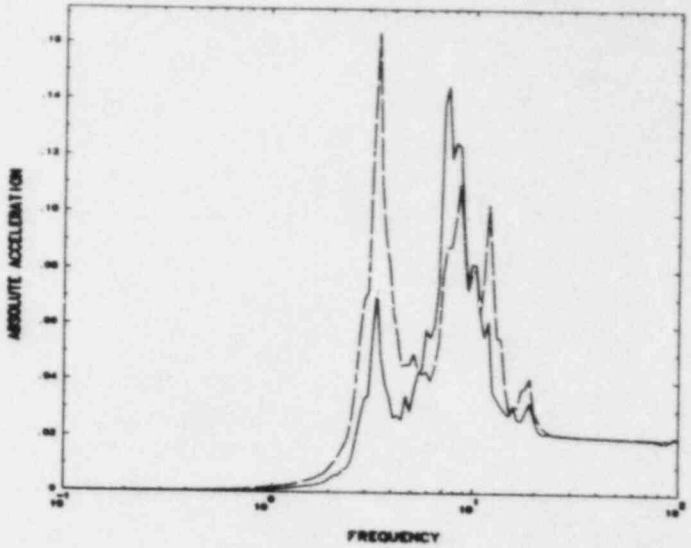

Legend

Rigid Foundation Model ————————
Flexible Foundation Model - - - - - -

Notes

All spectra at 2% damping
Frequencies in Hz
Rotations in rad/sec^2

f) Torsion

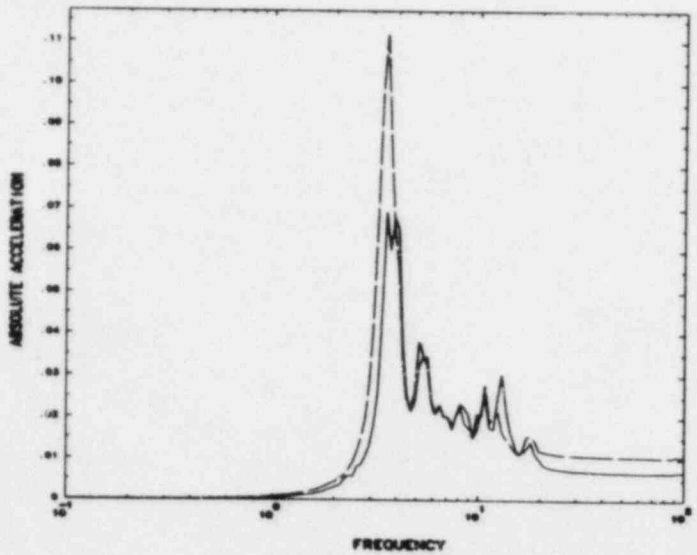

Fig. 2.18 (continued)

a) E-W Translation

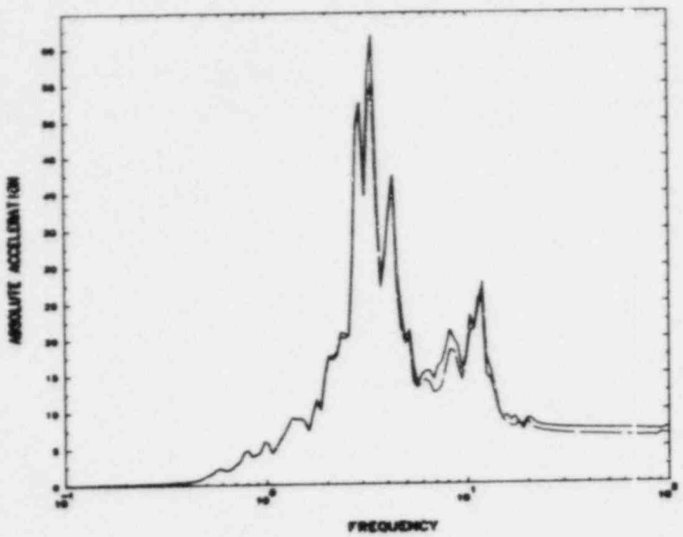

b) N-S Translation

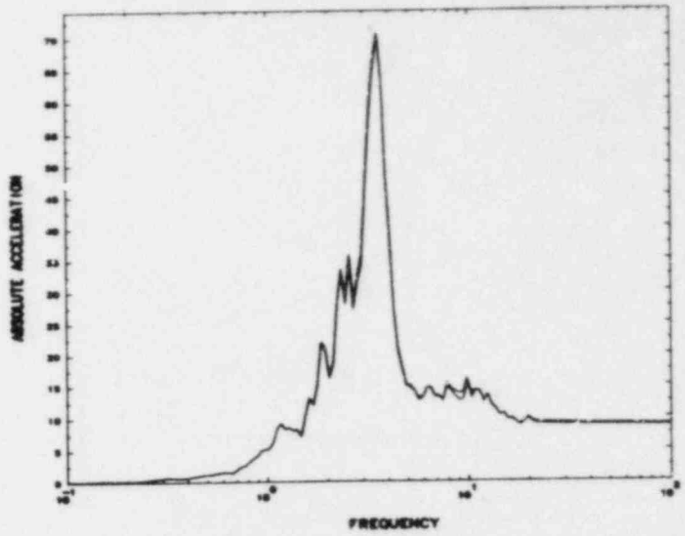

Legend

Rigid Foundation Model ————————
Flexible Foundation Model - - - - - - -

Notes

All spectra at 2% damping
Frequencies in Hz
Translations in ft/sec^2

c) Vertical Translation

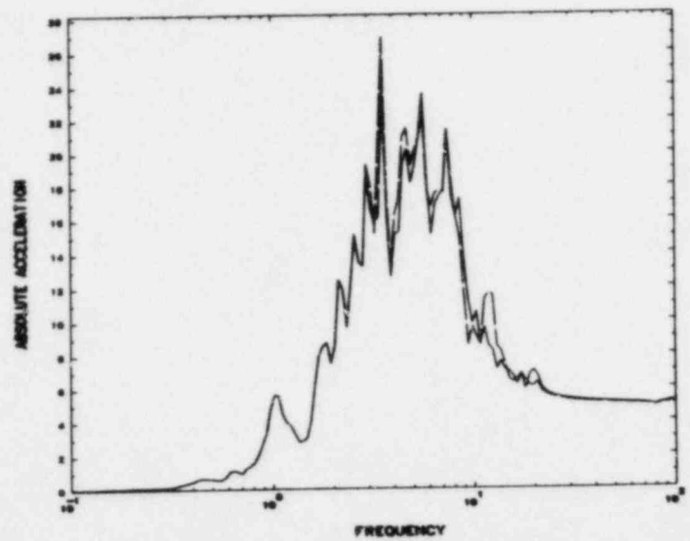

Fig. 2.19 Comparison of response spectra on foundation segment 4, nominal soil properties -- flexible vs. rigid foundation, (a) E-W translation, (b) N-S translation, (c) vertical translation, (d) N-S rocking, (e) E-W rocking, and (f) torsion.

d) N-S Rocking

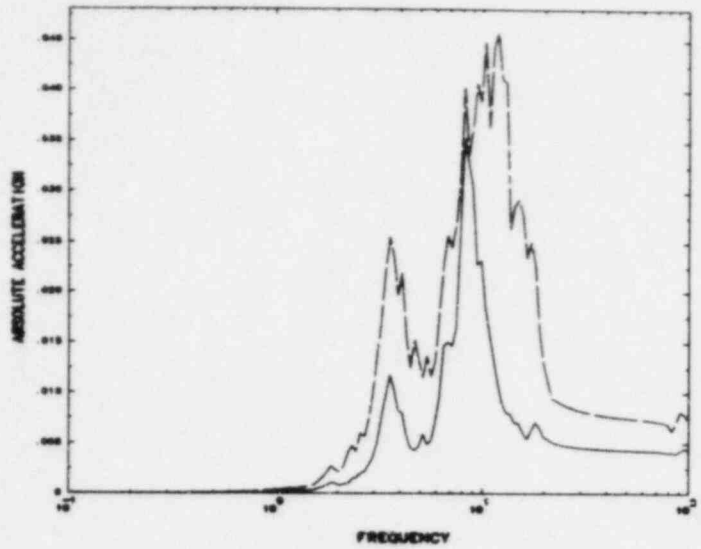

e) E-W Rocking

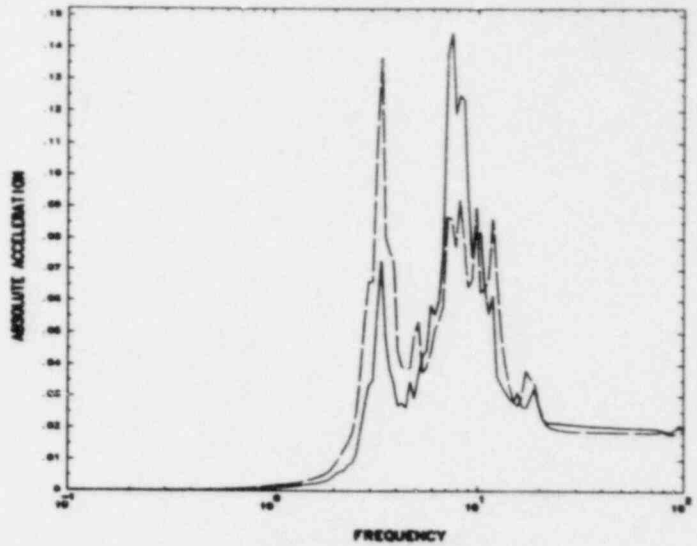

f) Torsion

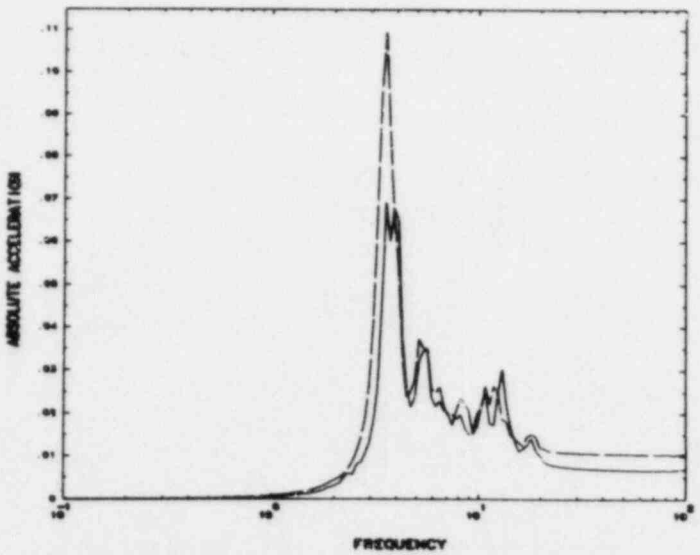

Legend

Rigid Foundation Model ————————
Flexible Foundation Model - - - - - - - -

Notes

All spectra at 2% damping
Frequencies in Hz
Rotations in rad/sec^2

Fig. 2.19 (continued)

a) E-W Translation

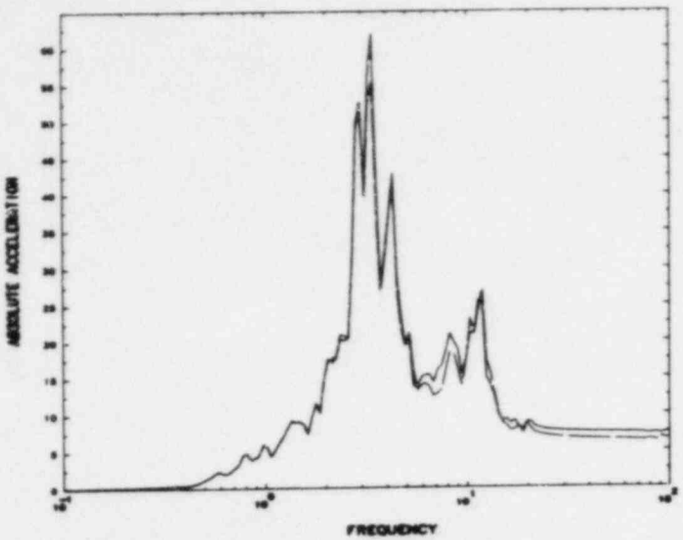

b) N-S Translation

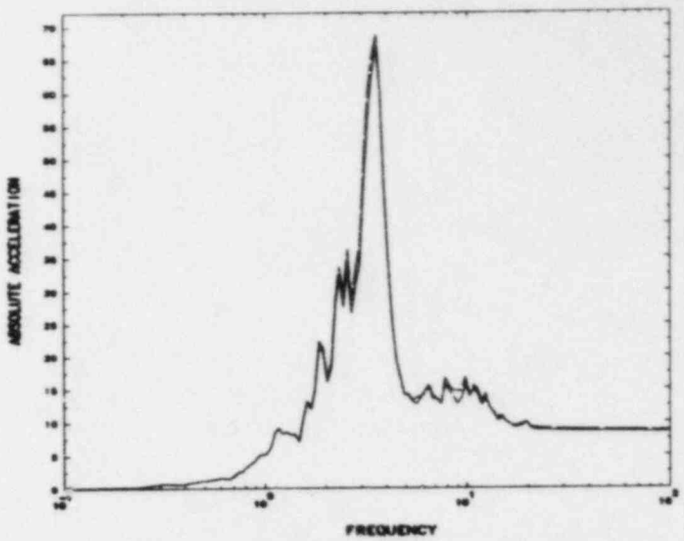

Legend

Rigid Foundation Model ————————
Flexible Foundation Model - - - - - -

Notes

All spectra at 2% damping
Frequencies in Hz
Translations in ft/sec^2

c) Vertical Translation

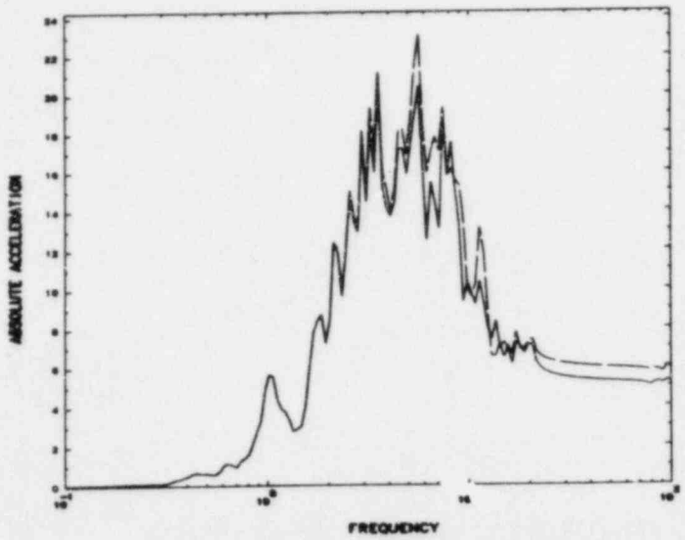

Fig. 2.20 Comparison of response spectra on foundation segment 7, nominal soil properties -- flexible vs. rigid foundation, (a) E-W translation, (b) N-S translation, (c) vertical translation, (d) N-S rocking, (e) E-W rocking, and (f) torsion.

d) N-S Rocking

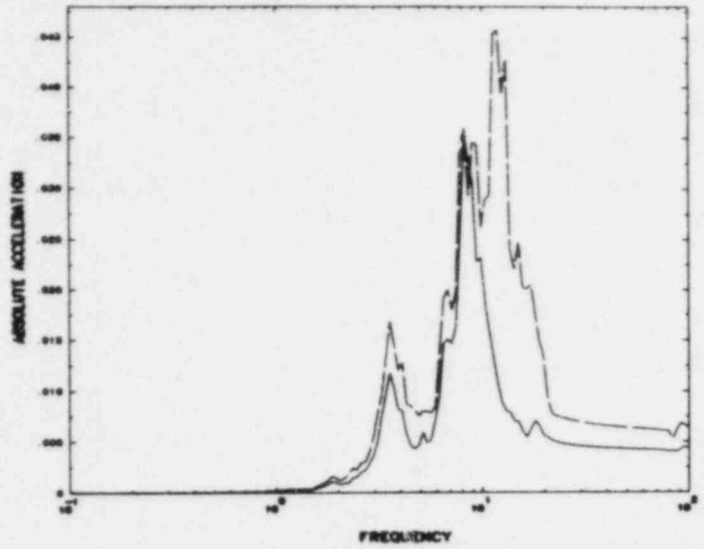

e) E-W Rocking

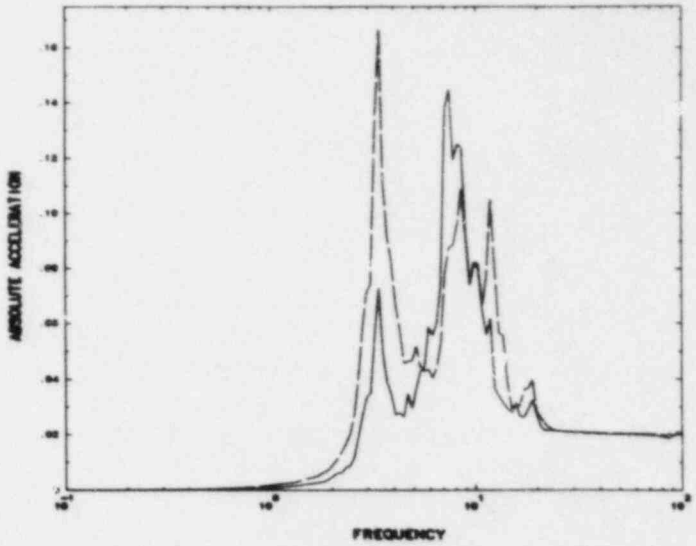

Legend

Rigid Foundation Model ————————
Flexible Foundation Model - - - - - -

Notes

All spectra at 2% damping
Frequenicies in Hz
Rotations in rad/sec^2

f) Torsion

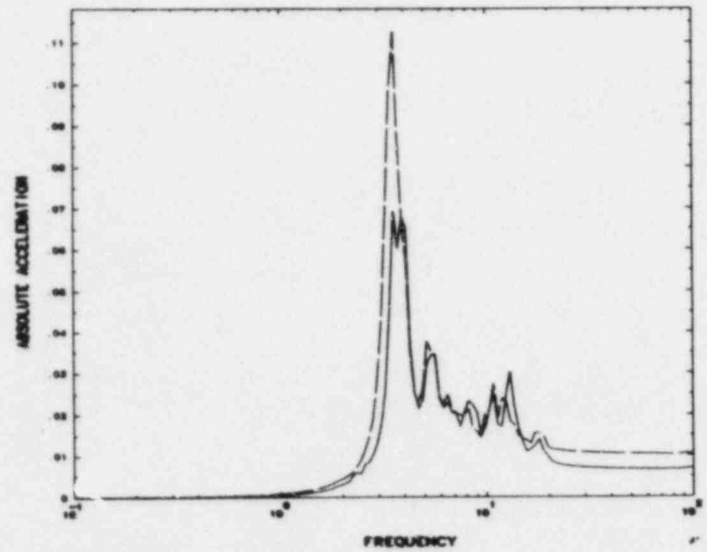

Fig. 2.20 (continued)

a) E-W Translation

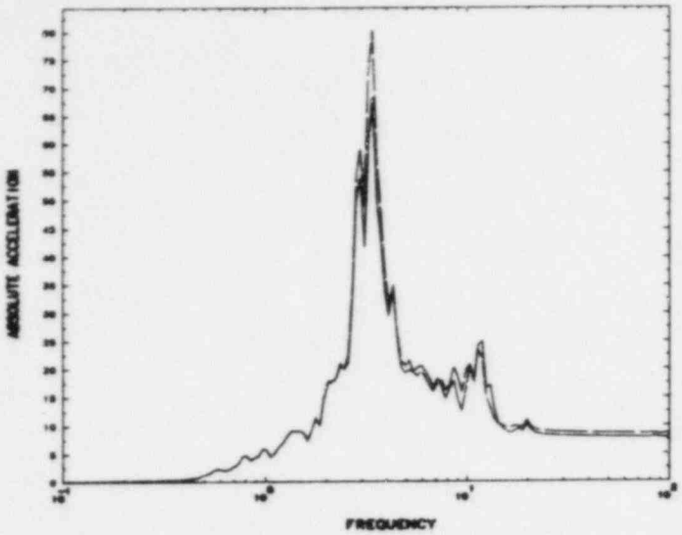

b) N-S Translation

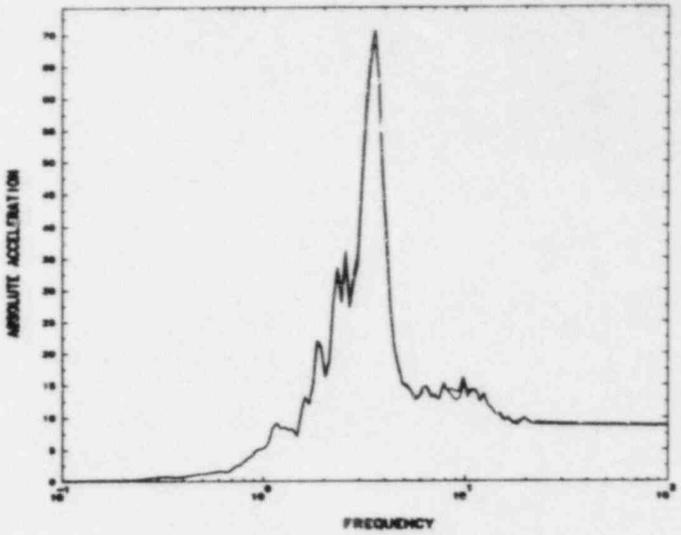

Legend

Rigid Foundation Model ————————
Flexible Foundation Model - - - - - - -

c) Vertical Translation

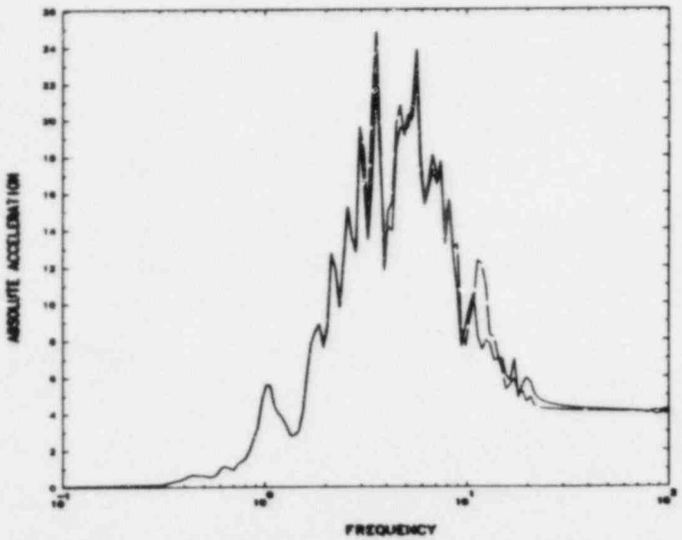

Notes

All spectra at 2% damping
Frequencies in Hz
Translations in ft/sec^2

Fig. 2.21 Comparison of response spectra on foundation segment 8, nominal soil properties -- flexible vs. rigid foundation, (a) E-W translation, (b) N-S translation, (c) vertical translation, (d) N-S rocking, (e) E-W rocking, and (f) torsion.

d) N-S Rocking

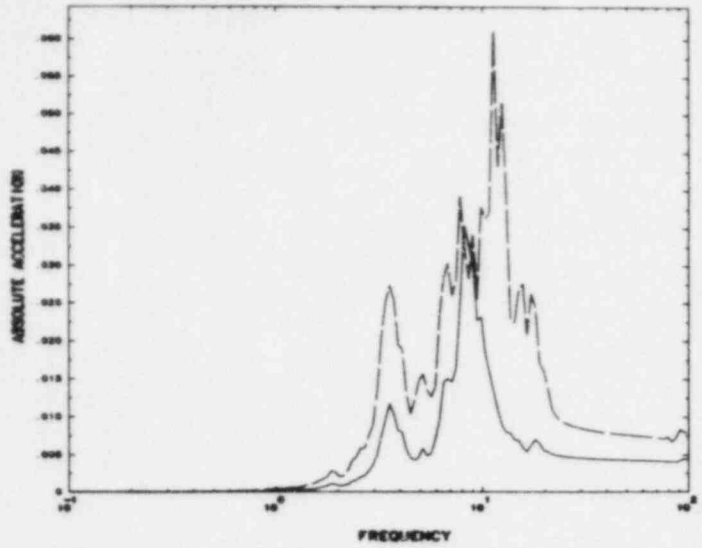

e) E-W Rocking

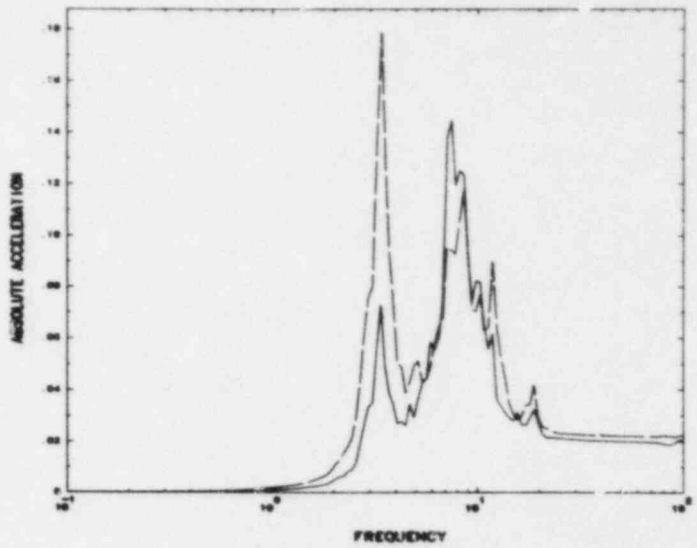

Legend

Rigid Foundation Model ————————
Flexible Foundation Model - - - - - -

Notes

All spectra at 2% damping
Frequencies in Hz
Rotations in rad/sec^2

f) Torsion

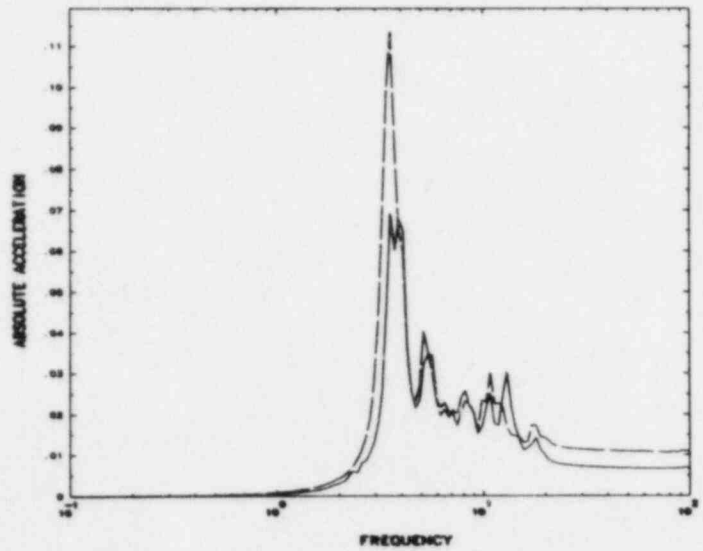

Fig. 2.21 (continued)

a) E-W Translation

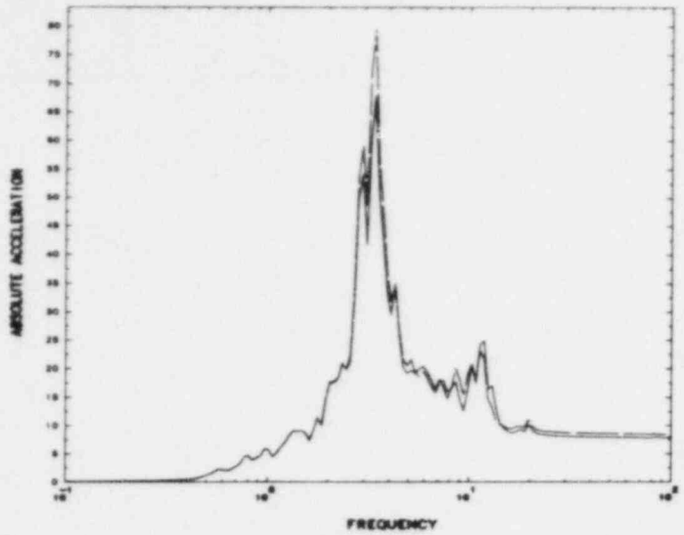

b) N-S Translation

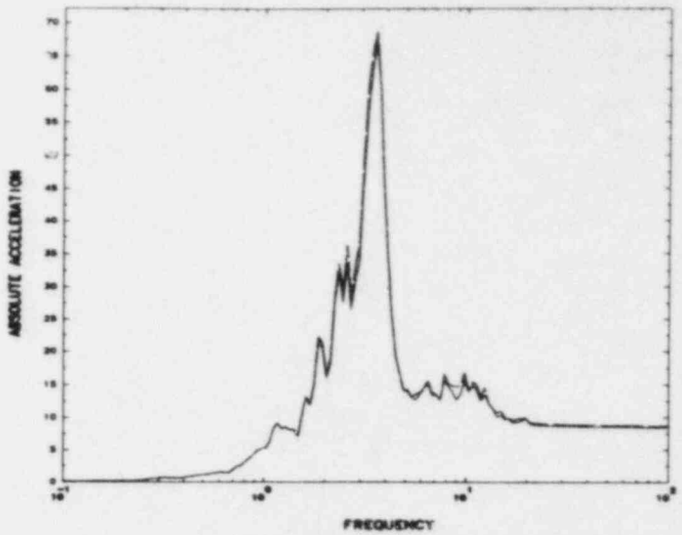

Legend

Rigid Foundation Model ————————
Flexible Foundation Model - - - - - - -

Notes

All spectra at 2% damping
Frequencies in Hz
Translations in ft/sec^2

c) Vertical Translation

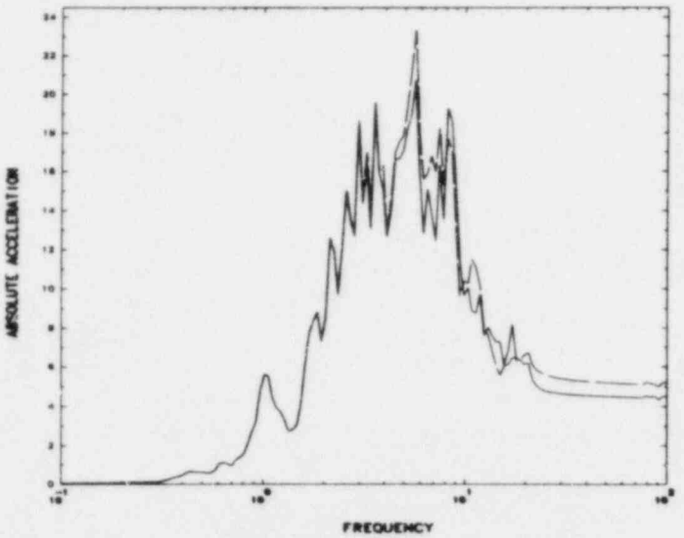

Fig. 2.22 Comparison of response spectra on foundation segment 11, nominal soil properties -- flexible vs. rigid foundation, (a) E-W translation, (b) N-S translation, (c) vertical translation, (d) N-S rocking, (e) E-W rocking, and (f) torsion.

d) N-S Rocking

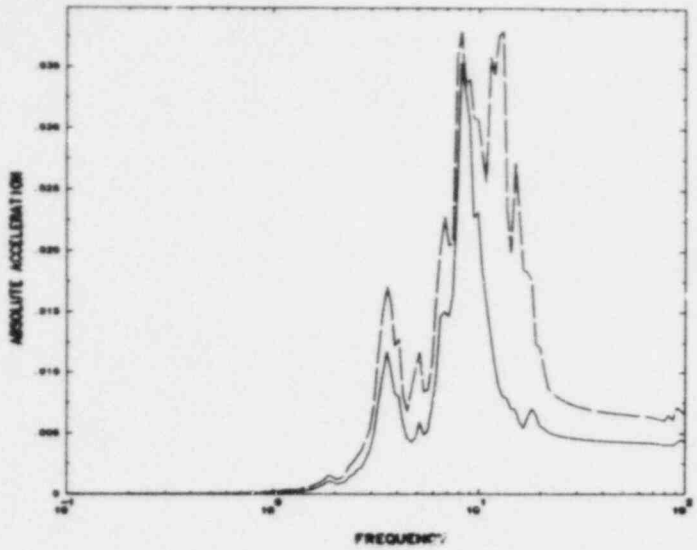

e) E-W Rocking

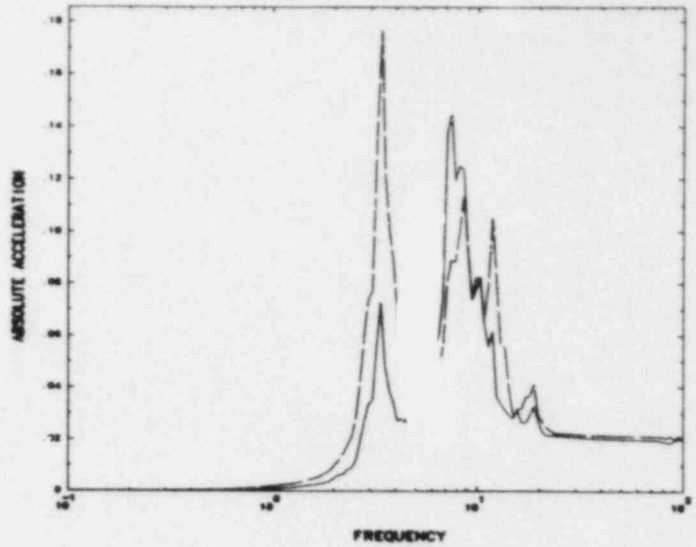

Legend

Rigid Foundation Model ————————
Flexible Foundation Model - - - - - -

Notes

All spectra at 2% damping
Frequencies in Hz
Rotations in rad ft/sec^2

f) Torsion

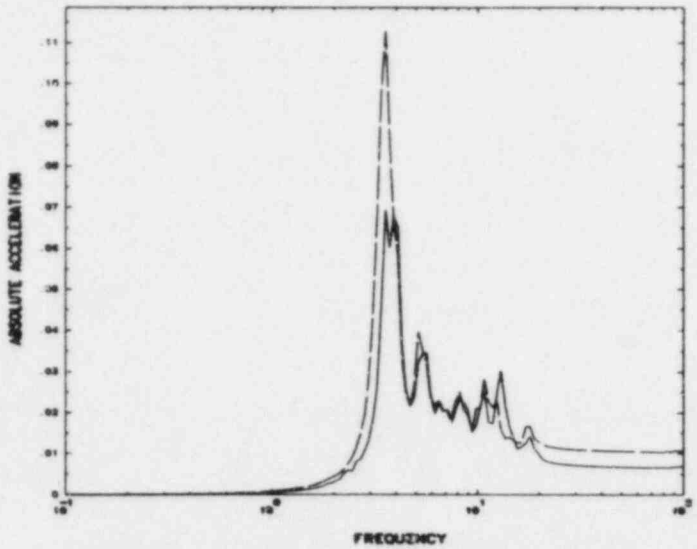

Fig. 2.22 (continued)

a) E-W Translation

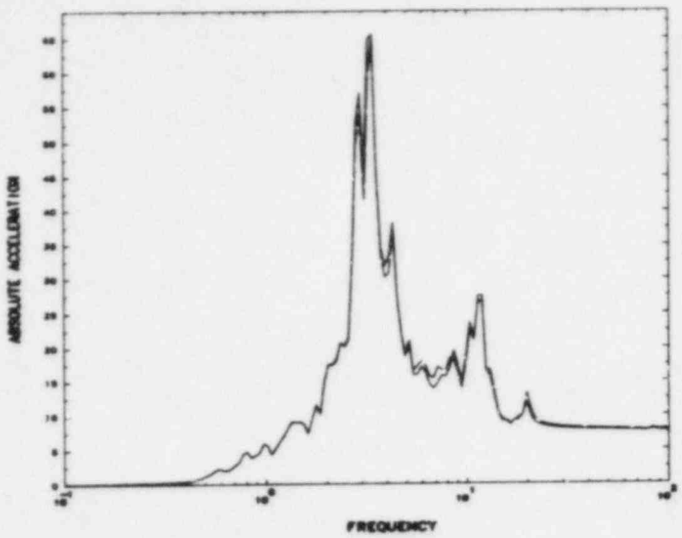

b) N-S Translation

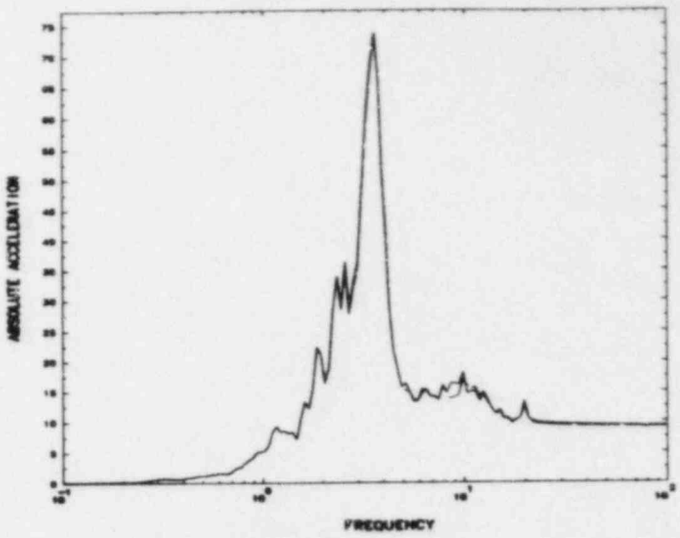

Legend

Flexible Foundation Model————————
Rigid Foundation Model - - - - - -

Notes

All spectra at 2% damping
Frequencies in Hz
Translations in ft/sec^2

c) Vertical Translation

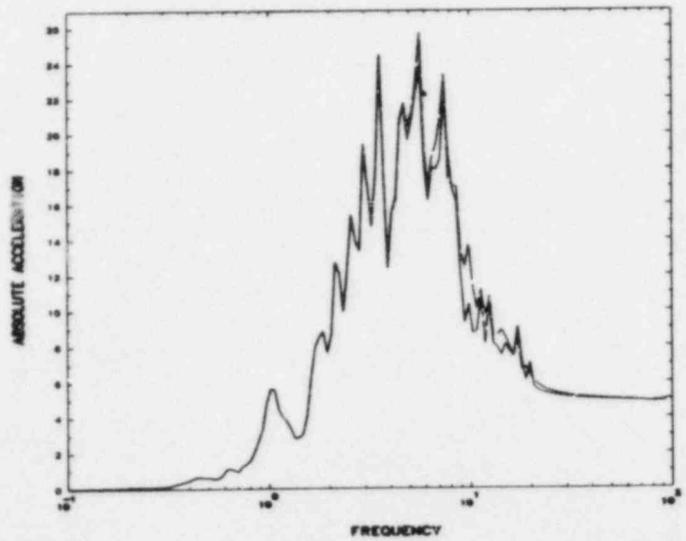

Fig. 2.23 Comparison of response spectra in the auxiliary building, node 506, elevation 560; nominal soil properties -- flexible vs. rigid foundation, (a) E-W translation, (b) N-S translation, and (c) vertical translation.

a) E-W Translation

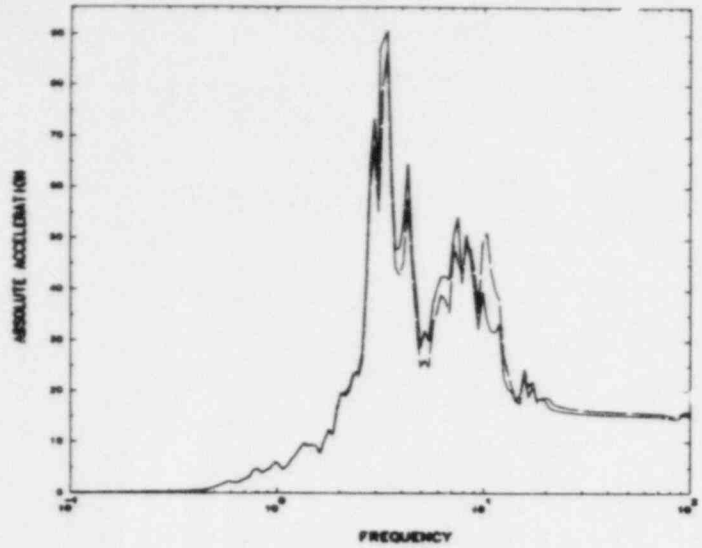

b) N-S Translation

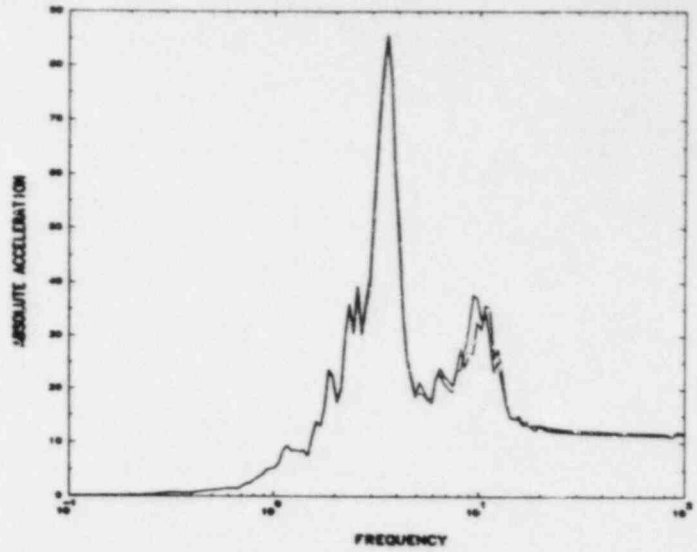

Legend

Flexible Foundation Model ————————
Rigid Foundation Model - - - - - -

Notes

All spectra at 2% damping
Frequencies in Hz
Translations in ft/sec^2

c) Vertical Translation

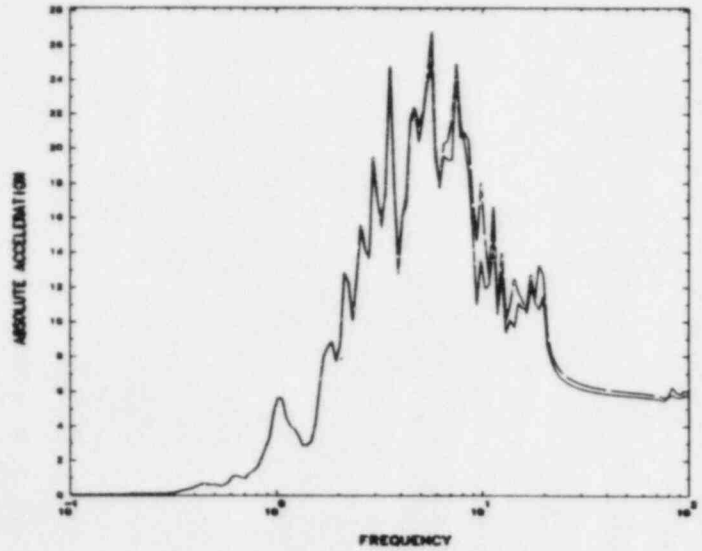

Fig. 2.24 Comparison of response spectra in the auxiliary building, node 3006, elevation 642', nominal soil properties -- flexible vs. rigid foundation, (a) E-W translation, (b) N-S translation, and (c) vertical translation.

a) E-W Translation

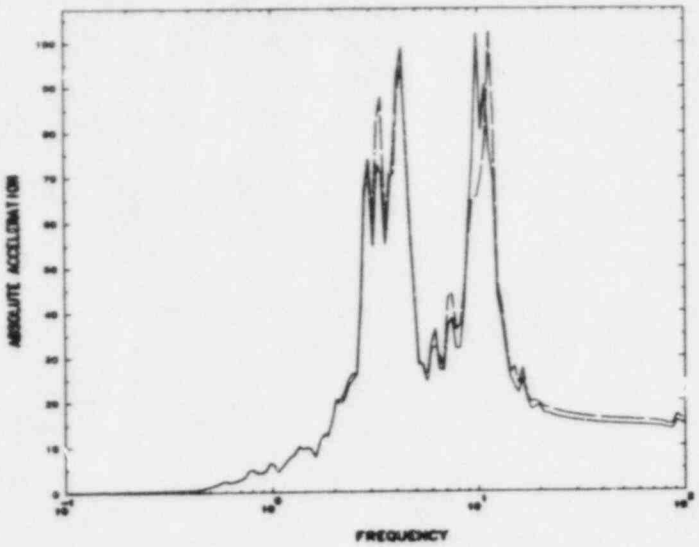

b) N-S Translation

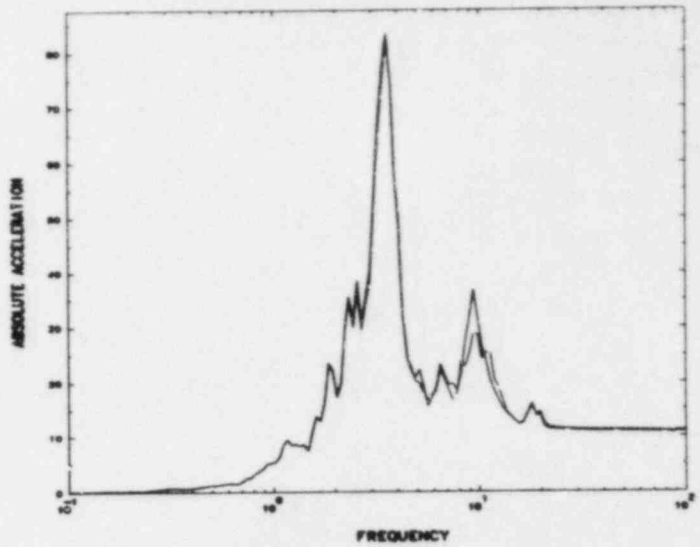

Legend

Flexible Foundation Model————————
Rigid Foundation Model - - - - - - -

Notes

All spectra at 2% damping
Frequencies in Hz
Translations in ft/sec^2

c) Vertical Translation

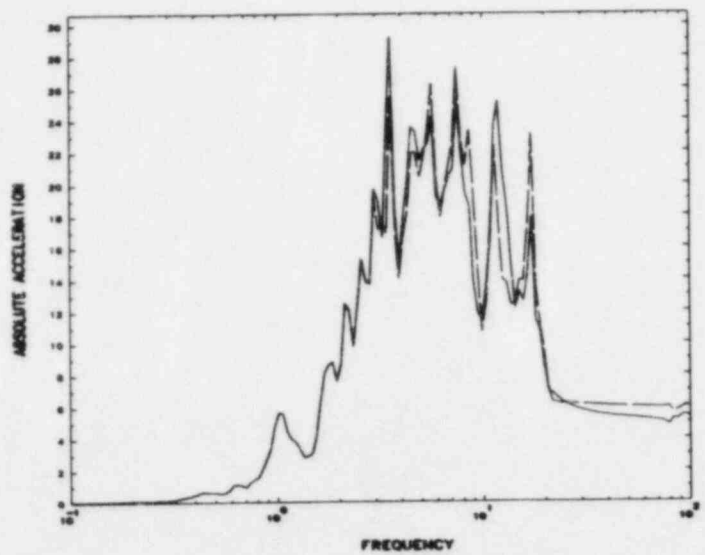

Fig. 2.25 Comparison of response spectra in the diesel generator building, west wall, node 3105, elevation 642', nominal soil properties -- flexible vs. rigid foundation, (a) E-W translation, (b) N-S translation, and (c) vertical translation.

a) E-W Translation

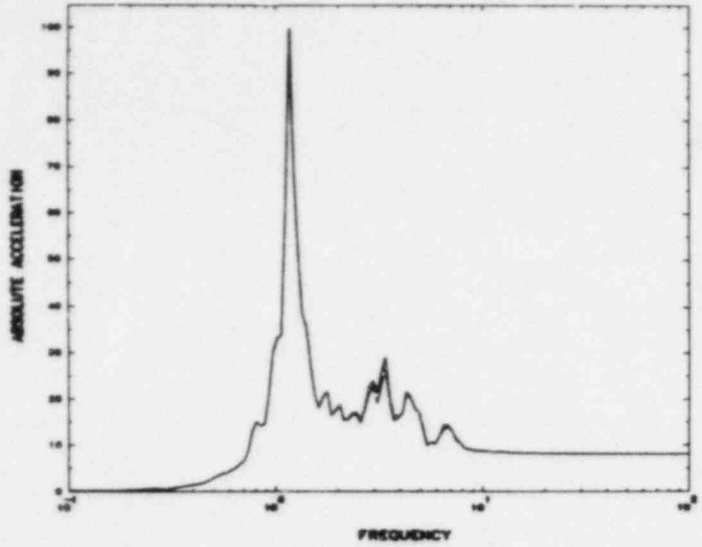

b) N-S Translation

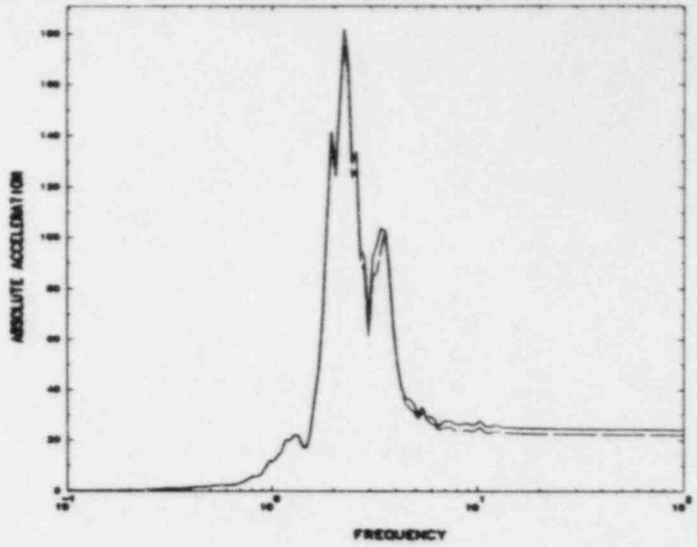

Legend

Flexible Foundation Model ————————
Rigid Foundation Model - - - - - -

Notes

All spectra at 2% damping
Frequencies in Hz
Translations in ft/sec^2

c) Vertical Translation

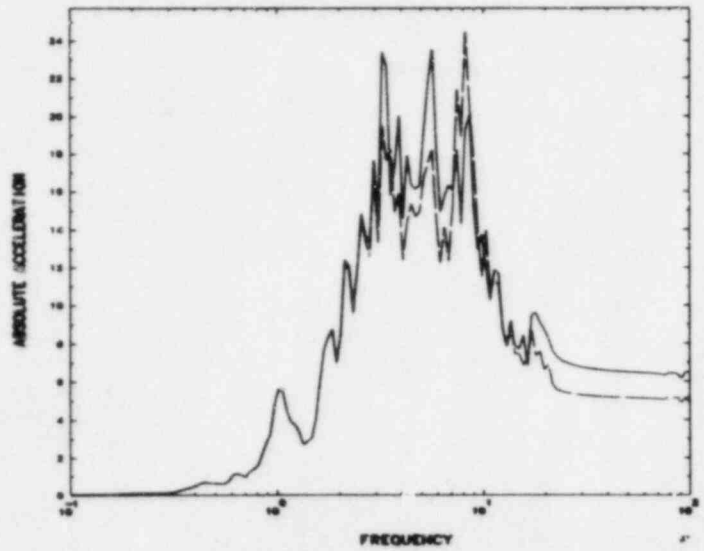

Fig. 2.26 Comparison of response spectra in the turbine building, centerline east end, node 4005, elevation 712', nominal soil properties -- flexible vs. rigid foundation, (a) E-W translation, (b) N-S translation, and (c) vertical translation.

a) E-W Translation

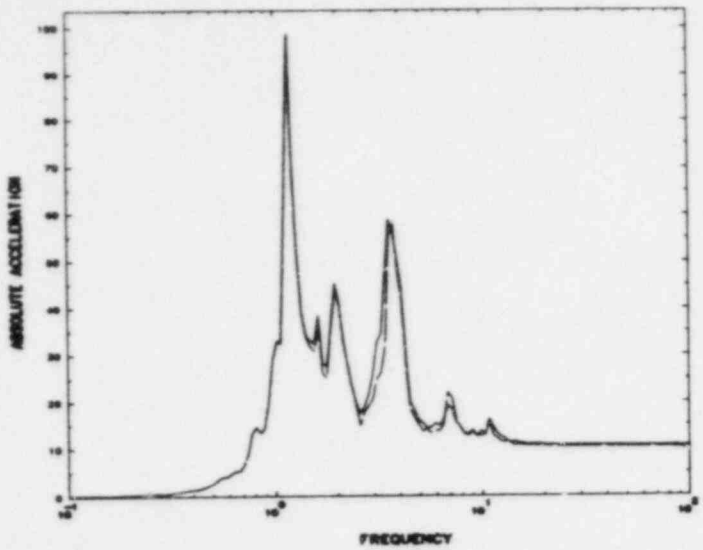

b) N-S Translation

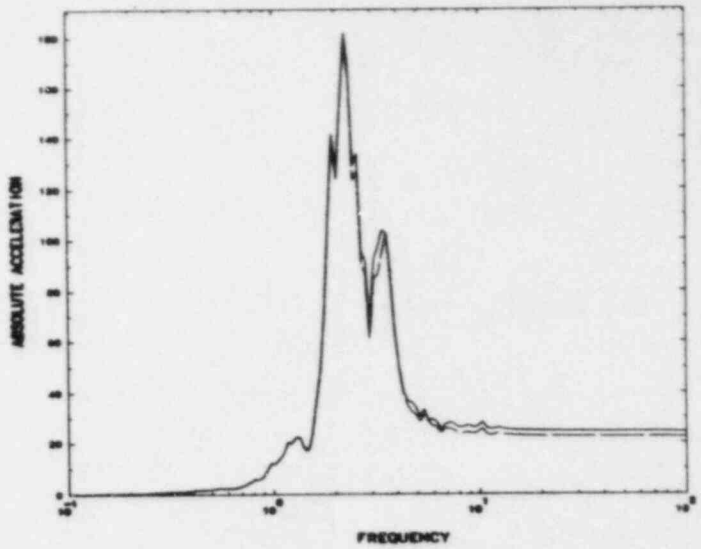

Legend

Flexible Foundation Model ————————
Rigid Foundation Model - - - - - -

Notes

All spectra at 2% damping
Frequencies in Hz
Translation in ft/sec^2

c) Vertical Translation

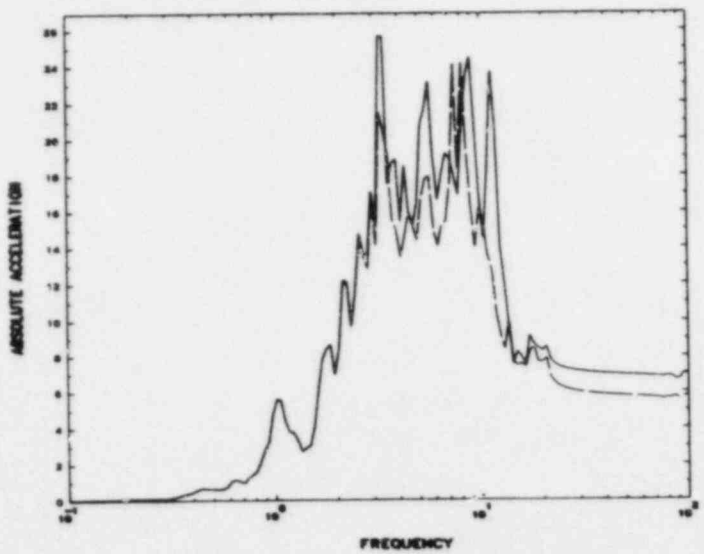

Fig. 2.27 Comparison of response spectra in the turbine building, southeast corner, node 4065, elevation 712', nominal soil properties -- flexible vs. rigid foundation, (a) E-W translation, (b) N-S translation, and (c) vertical translation.

a) E-W Translation

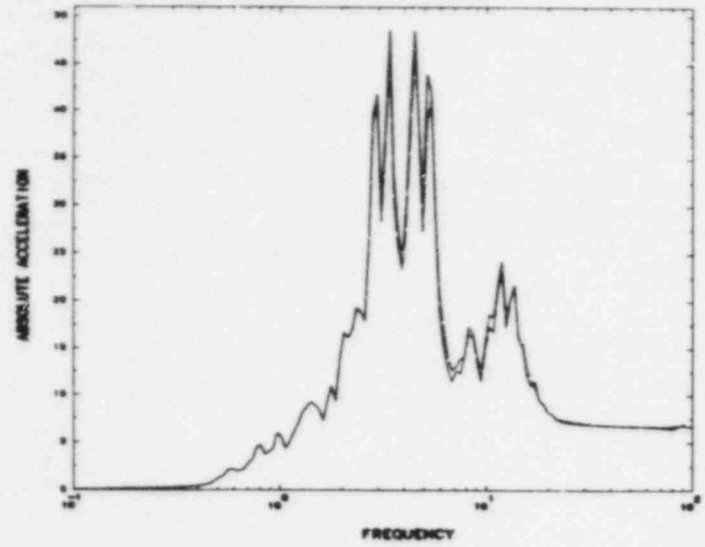

b) N-S Translation

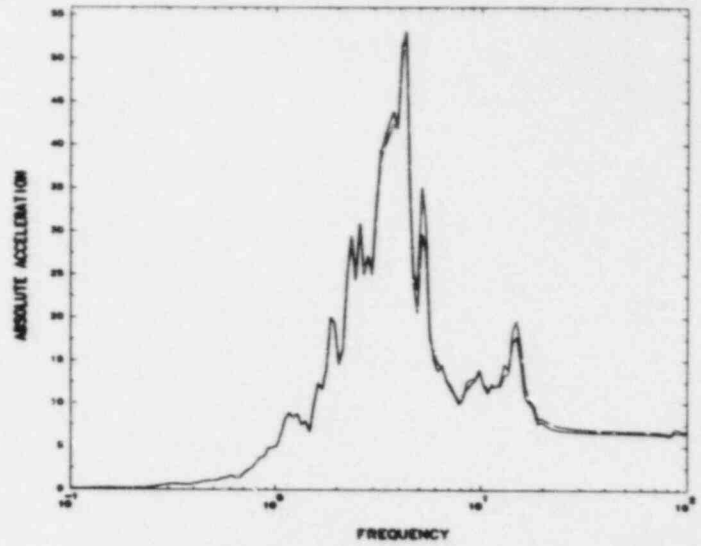

c) Vertical Translation

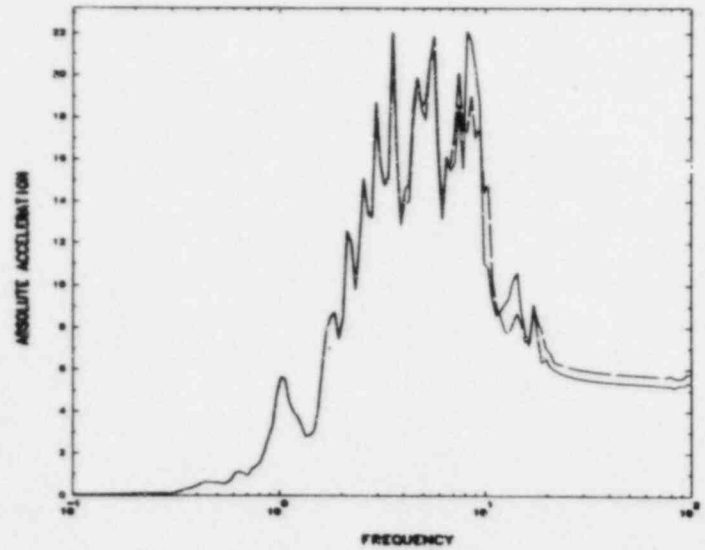

Legend

Flexible Foundation Model ————————
Rigid Foundation Model - - - - - -

Notes

All spectra at 2% damping
Frequencies in Hz
Translations in ft/sec^2

Fig. 2.28 Comparison of response spectra in the auxiliary building, node 506, elevation 560', stiff soil properties -- flexible vs. rigid foundation, (a) E-W translation, (b) N-S translation, and (c) vertical translation.

a) E-W Translation

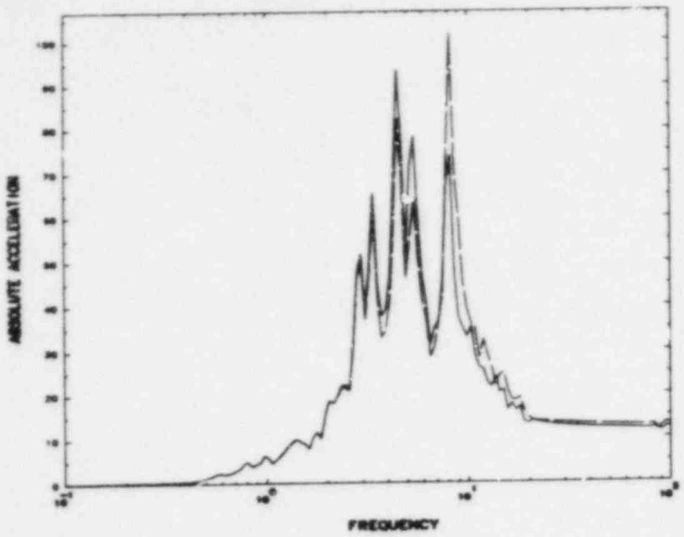

b) N-S Translation

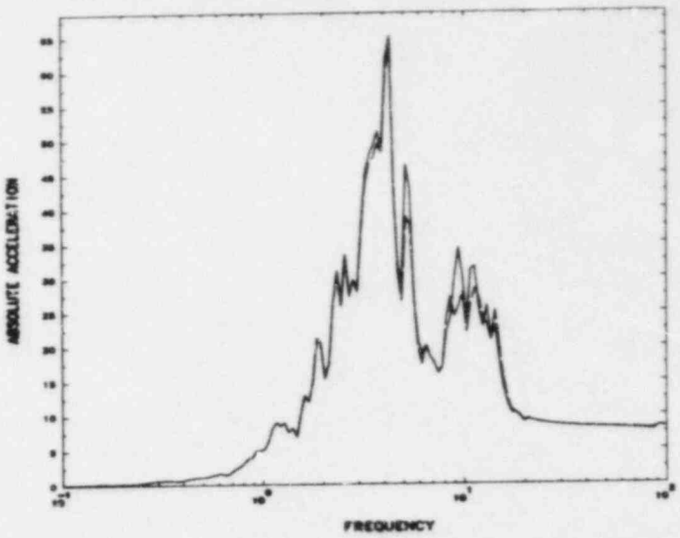

c) Vertical Translation

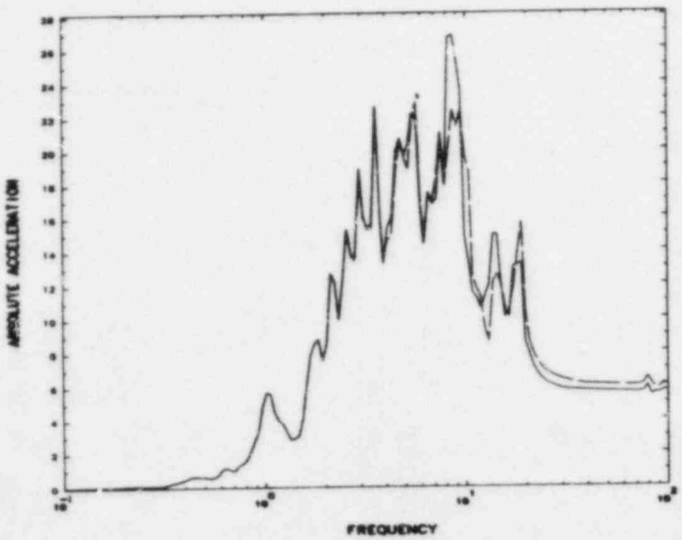

Legend

Flexible Foundation Model ————————
Rigid Foundation Model - - - - - - -

Notes

All spectra at 2% damping
Frequencies in Hz
Translations in ft/sec^2

Fig. 2.29 Comparison of response spectra in the auxiliary building, node 3006, elevation 642', stiff soil properties -- flexible vs. rigid foundation, (a) E-W translation, (b) N-S translation, and (c) vertical translation.

a) E-W Translation

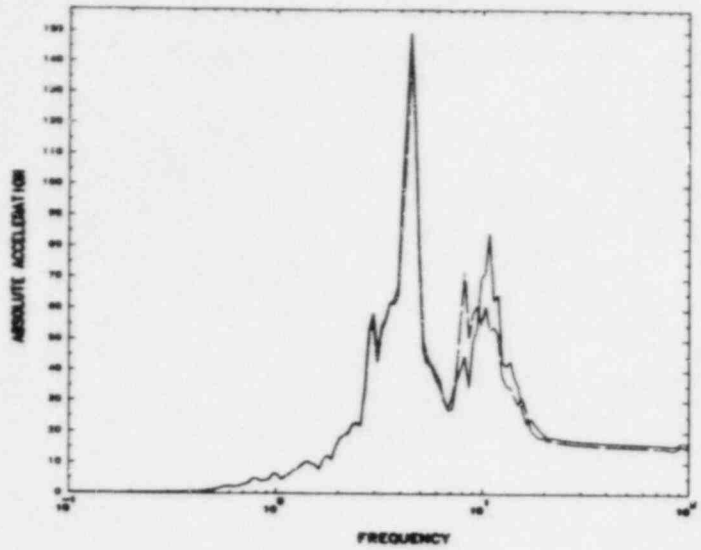

b) N-S Translation

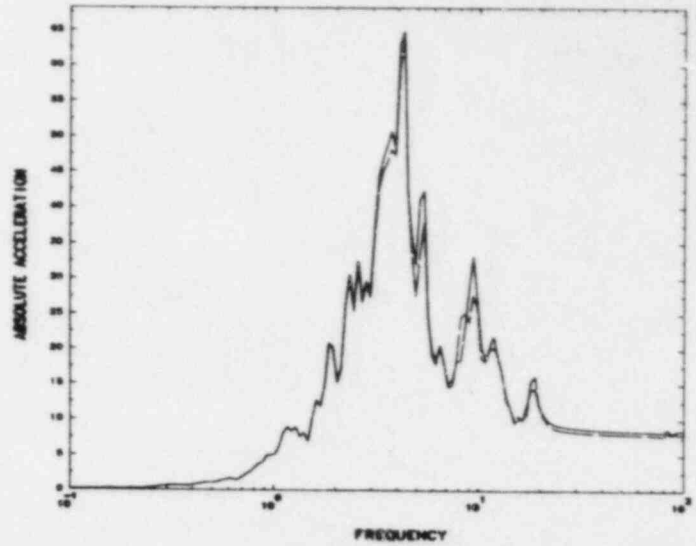

c) Vertical Translation

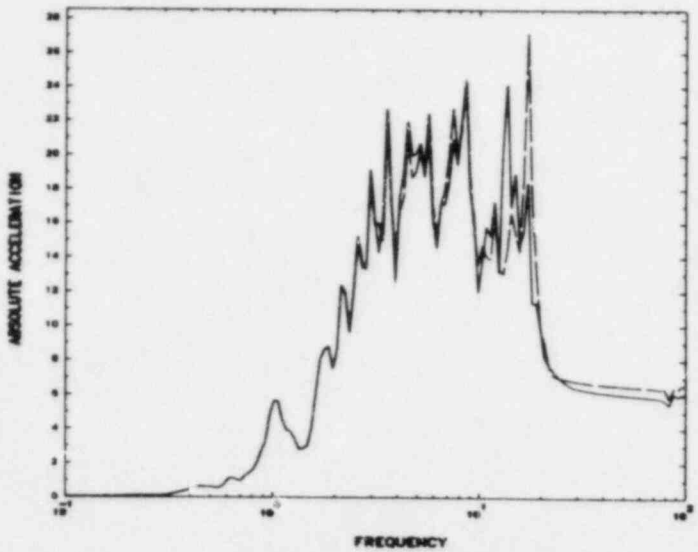

Legend

Flexible Foundation Model ————————
Rigid Foundation Model - - - - - -

Notes

All spectra at 2% damping
Frequencies in Hz
Translations in ft/sec^2

Fig. 2.30 Comparison of response spectra in the diesel generator building, west wall, node 3105, elevation 642', stiff soil properties -- flexible vs. rigid foundation, (a) E-W translation, (b) N-S translation, and (c) vertical translation.

a) E-W Translation

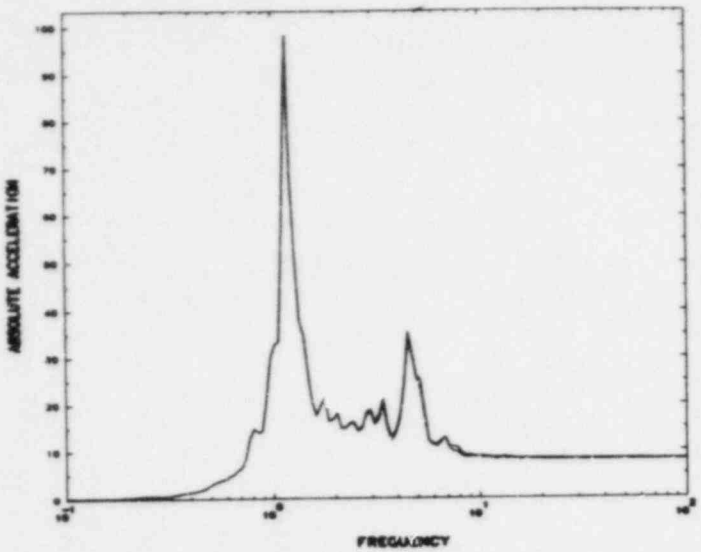

b) N-S Translation

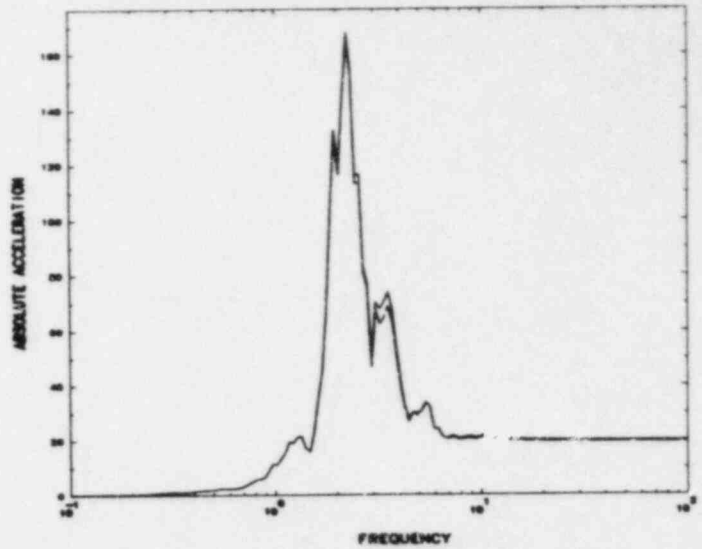

Legend

Flexible Foundation Model ————————
Rigid Foundation Model - - - - - -

c) Vertical Translation

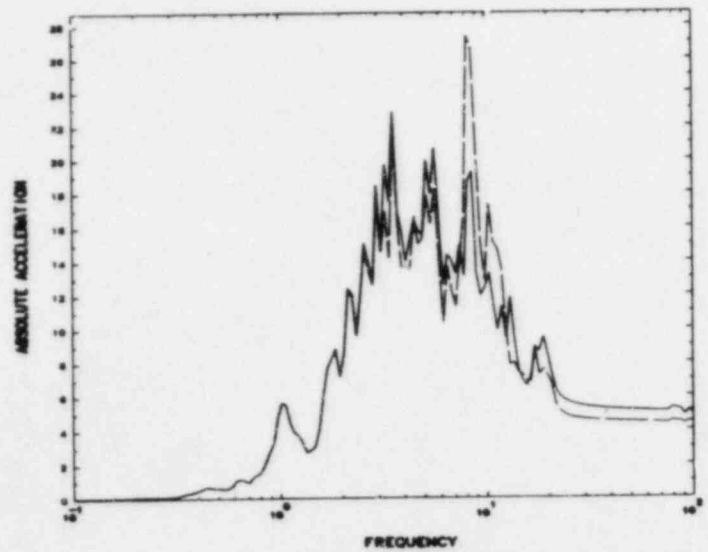

Notes

All spectra at 2% damping
Frequencies in Hz
Translations in ft/sec^2

Fig. 2.31 Comparison of response spectra in the turbine building, centerline east end, node 4005, elevation 712', stiff soil properties -- flexible vs. rigid foundation, (a) E-W translation, (b) N-S translation, and (c) vertical translation.

a) E-W Translation

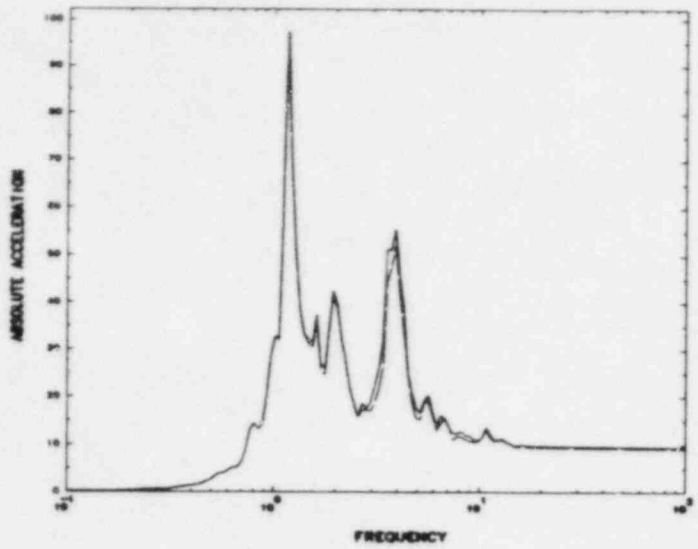

b) N-S Translation

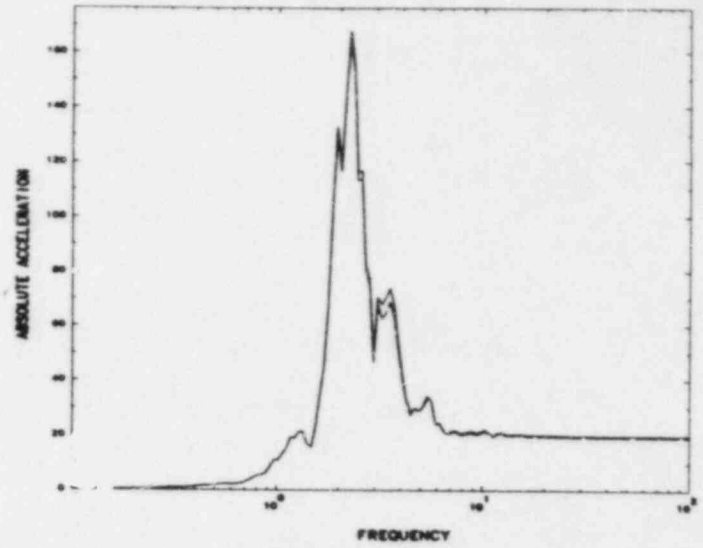

c) Vertical Translation

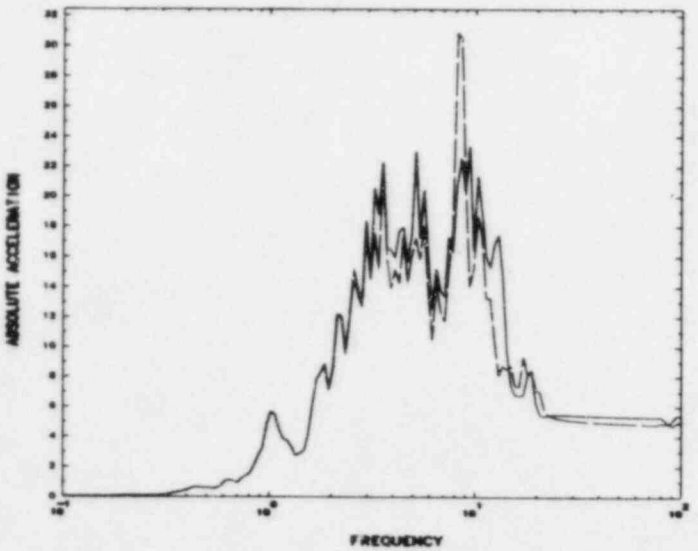

Legend

Flexible Foundation Model ————————
Rigid Foundation Model - - - - - -

Notes

All spectra at 2% damping
Frequencies in Hz
Translations in ft/sec^2

Fig. 2. 32 Comparison of response spectra in the turbine building, southeast corner, node 4065, elevation 712', stiff soil properties -- flexible vs. rigid foundation, (a) E-W translation, (b) N-S translation, (c) vertical translation.

a) E-W Translation

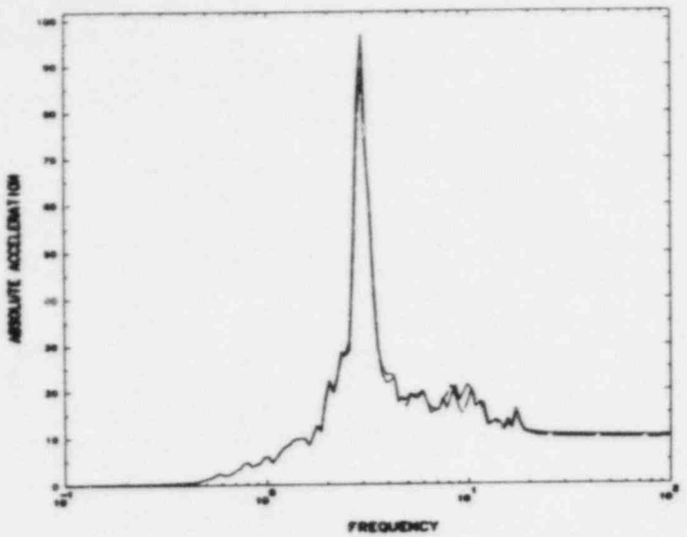

b) N-S Translation

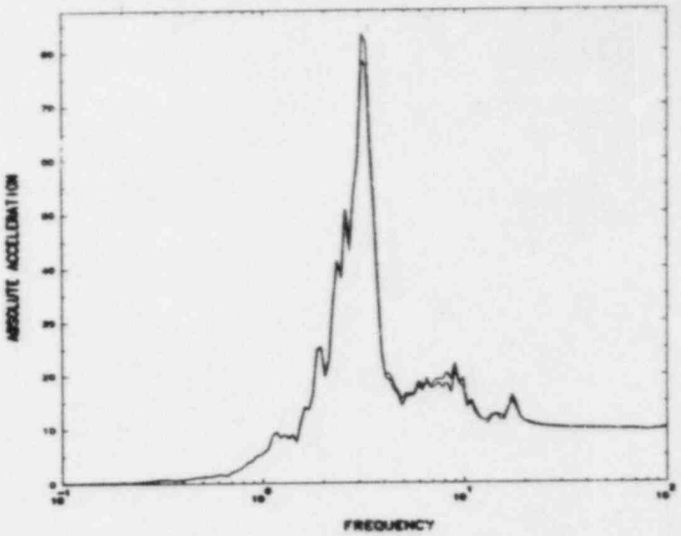

Legend

Flexible Foundation Model ————————
Rigid Foundation Model - - - - - - -

c) Vertical Translation

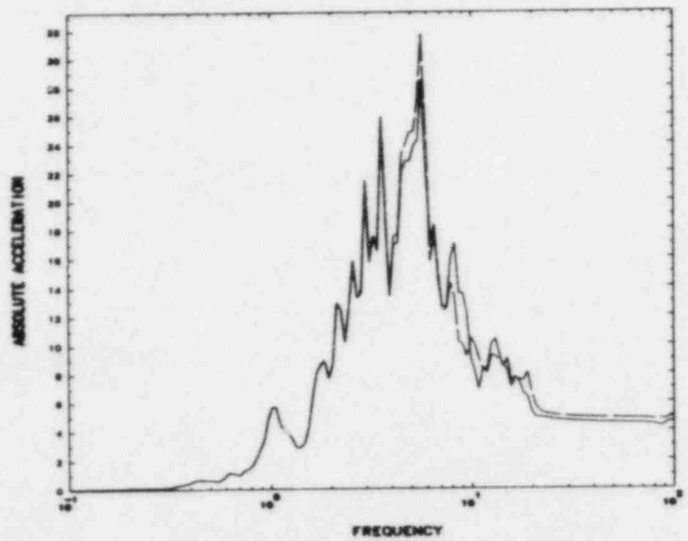

Notes

All spectra at 2% damping
Frequencies in Hz
Translations in ft/sec^2

Fig. 2.33 Comparison of response spectra in the auxiliary building, node 506, elevation 560', soft soil properties -- flexible vs. rigid foundation, (a) E-W translation, (b) N-S translation, and (c) vertical translation.

a) E-W Translation

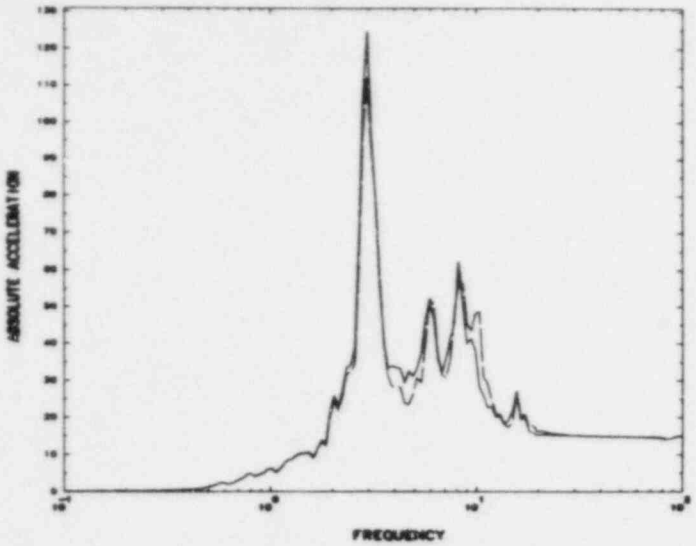

b) N-S Translation

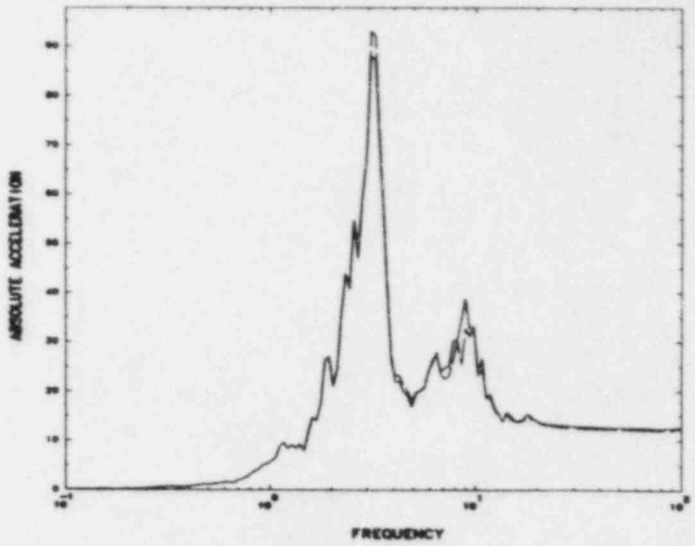

c) Vertical Translation

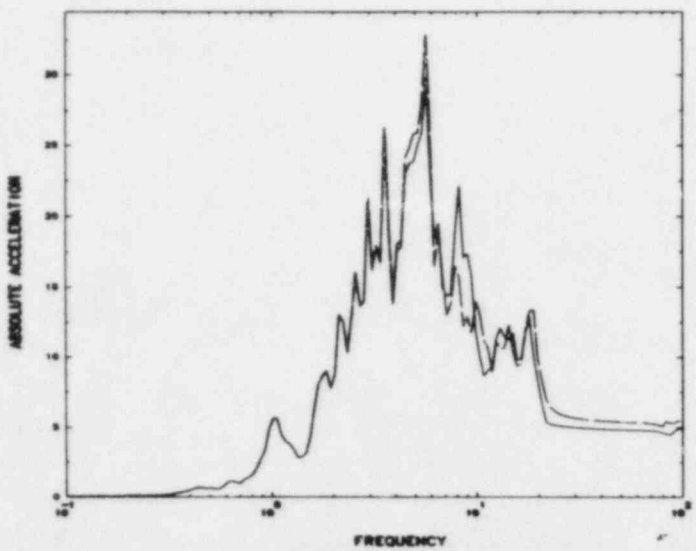

Legend

Flexible Foundation Model ————————
Rigid Foundation Model - - - - - -

Notes

All spectra at 2% damping
Frequencies in Hz
Translation in ft/sec^2

Fig. 2.34 Comparison of response spectra in the auxiliary building, node 3006, elevation 642', soft soil properties -- flexible vs. rigid foundation, (a) E-W translation, (b) N-S translation, and (c) vertical translation.

a) E-W Translation

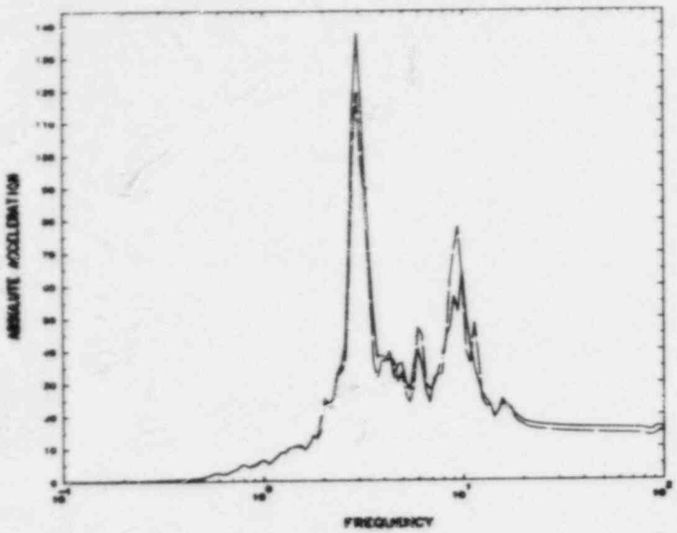

b) N-S Translation

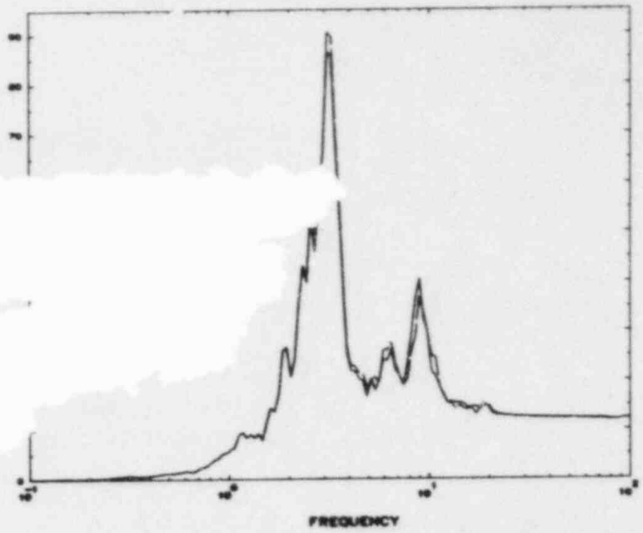

Legend

Flexible Foundation Model ————————
Rigid Foundation Model - - - - - - -

c) Vertical Translation

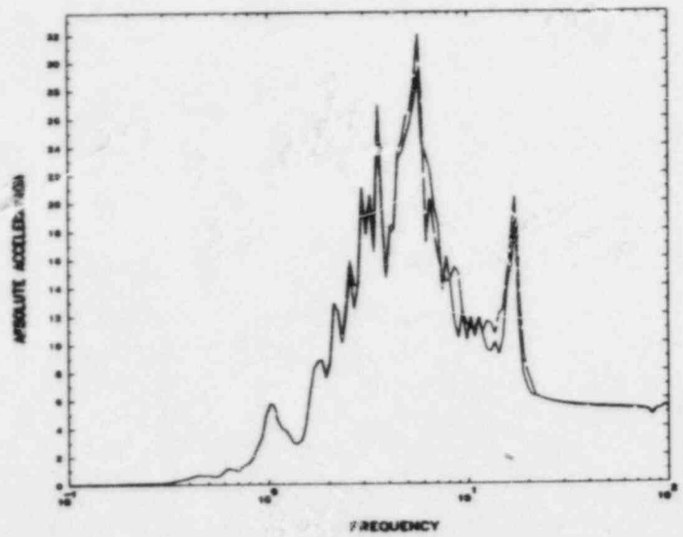

Notes

All spectra at 2% damping
Frequencies in Hz
Translations in ft/sec^2

Fig. 2.35 Comparison of response spectra in the diesel generator building, west wall, node 3105, elevation 642', soft soil properties -- flexible vs. rigid foundation, (a) E-W translation, (b) N-S translation, and (c) vertical translation.

a) E-W Translation

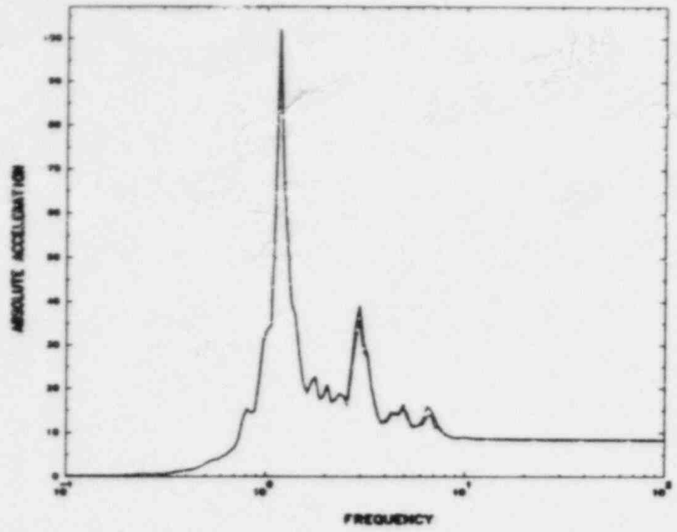

b) N-S Translation

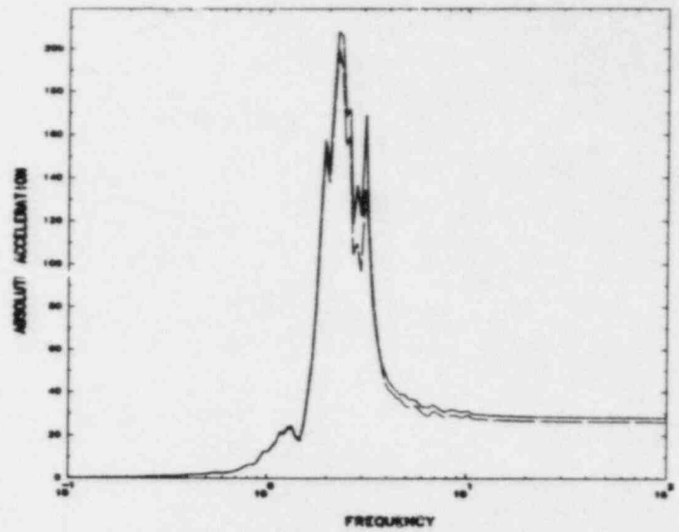

Legend

Flexible Foundation Model ————————
Rigid Foundation Model - - - - - - -

Notes

All spectra at 2% damping
Frequencies in Hz
Translations in ft/sec^2

c) Vertical Translation

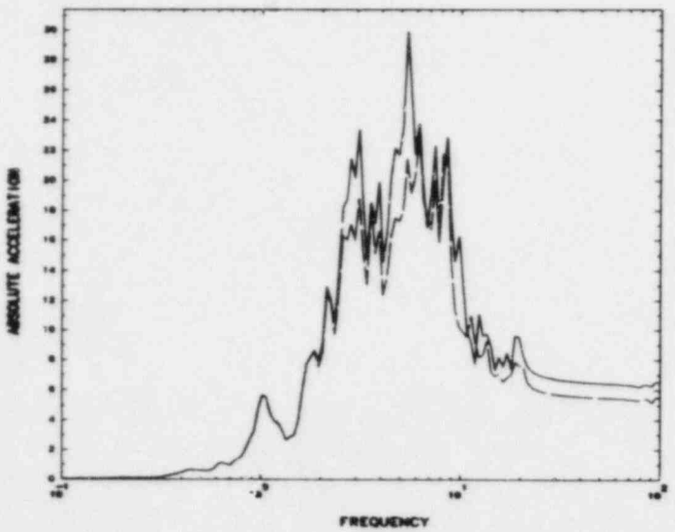

Fig. 2.36 Comparison of response spectra in the turbine building, centerline east end, node 4005, elevation 712', soft soil properties -- flexible vs. rigid foundation, (a) E-W translation, (b) N-S translation, and (c) vertical translation.

a) E-W Translation

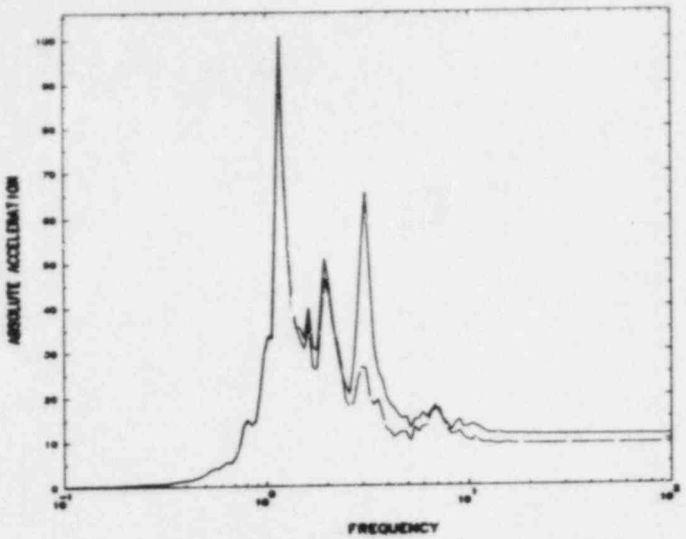

b) N-S Translation

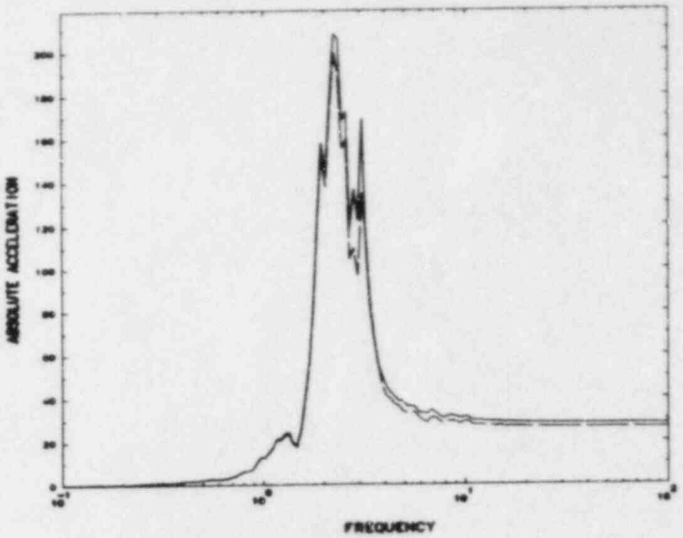

c) Vertical Translation

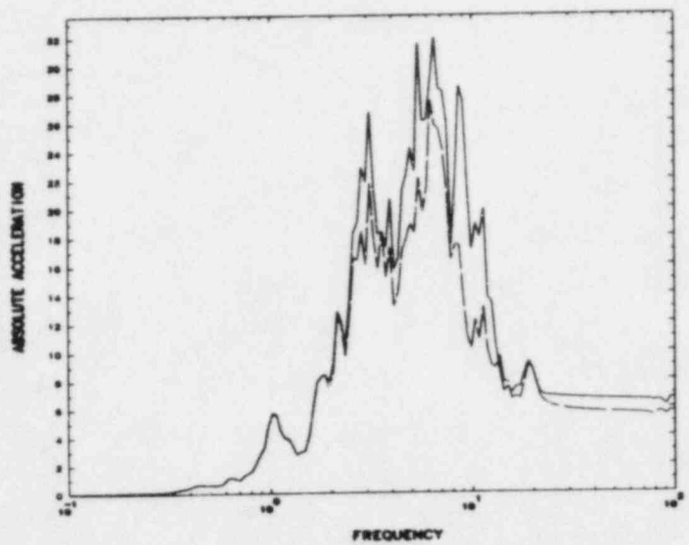

Legend

Flexible Foundation Model ————————
Rigid Foundation Model - - - - - -

Notes

All spectra at 2% damping
Frequencies in Hz
Translations in ft/sec^2

Fig. 2.37 Comparison of response spectra in the turbine building, southeast corner, node 4065, elevation 712', soft soil properties -- flexible vs. rigid foundation, (a) E-W translation, (b) N-S translation, and (c) vertical translation.

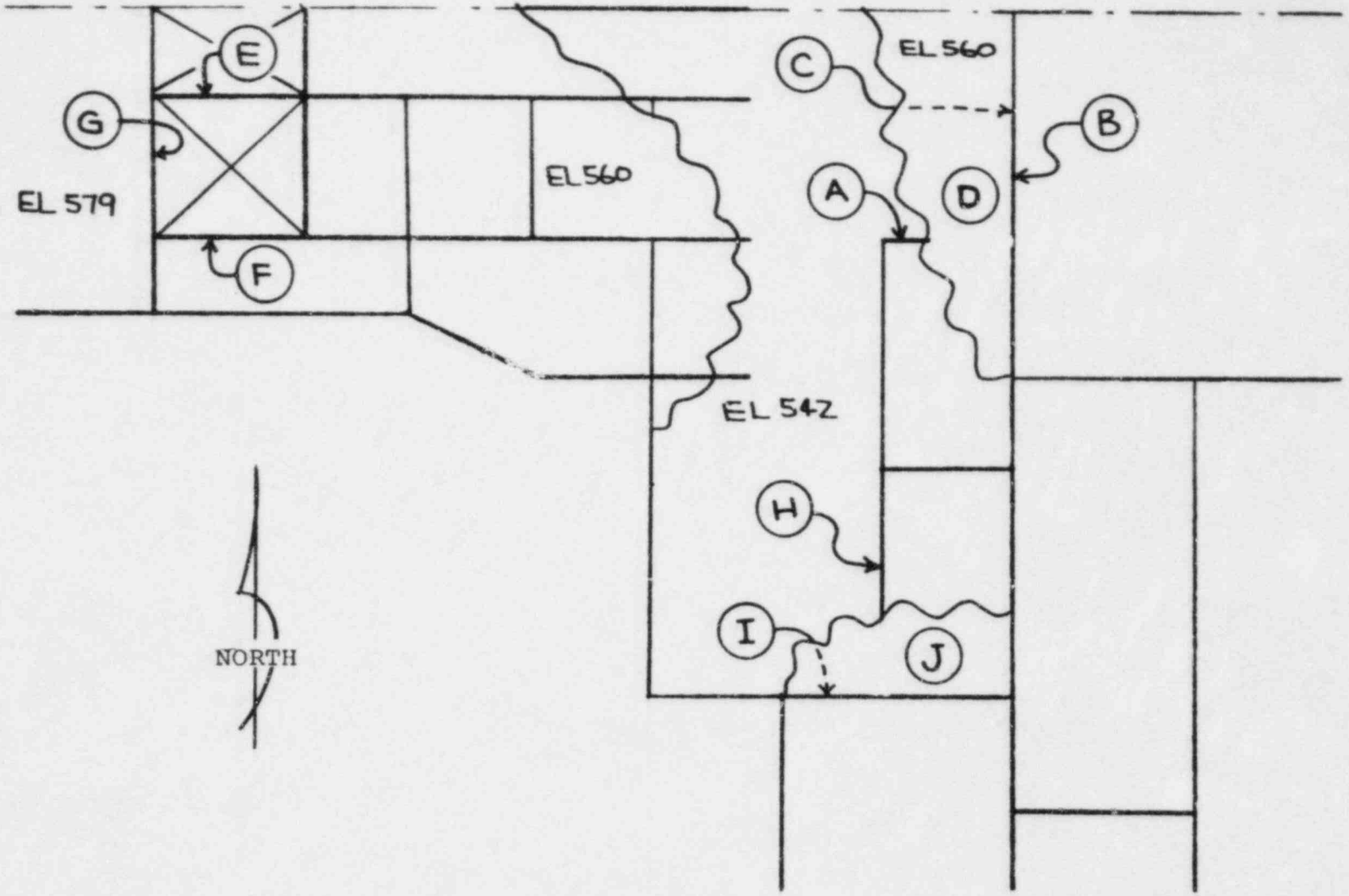

Fig. 2.38 Locations of stress evaluations.

3. STRUCTURE-TO-STRUCTURE INTERACTION

3.1 Modeling the Zion Nuclear Power Plant

During an earthquake, the vibration of one structure can affect the motion of another. This coupling through the soil is denoted structure-to-structure interaction. It is of potential significance at a nuclear power plant because of the small distances which separate adjacent structures and the large massive structure-foundation systems involved. Two characteristics of the structures and foundations affect structure-to-structure interaction -- the relative size of the foundations and the relative mass of the structures. In both cases, the larger of the two affects the smaller.

For the Zion nuclear power plant, structures on three foundations were considered in the response calculations -- two containment building foundations and the AFT complex (Fig. 2.1). The AFT complex foundation is significantly larger than either containment building foundation. In addition, the mass of the AFT complex is approximately five times greater than the mass of either containment building. Hence, both important characteristics of the structure-foundation system indicate structure-to-structure interaction will have a greater effect on response of the containment building than on the AFT complex.

For Phase II of the SSMRP, structure-to-structure interaction was considered in two ways: the effect was modelled explicitly in the SSMRP Phase II response calculations with SMACS; and the effect of structure-to-structure interaction on seismic response and seismic risk was assessed. Results of the latter sensitivity studies are discussed here and summarized in Ref. 2.

Before proceeding with the discussion, recall the five steps of a seismic risk analysis: seismic hazard characterization (seismic hazard curve, frequency characteristics of the motion); seismic response of structures and components; structure and component failure descriptions; plant logic models (fault trees and event trees); and probabilistic failure and release calculations. Structure-to-structure interaction enters explicitly into the calculation of seismic responses of structures and components; the results of which are used in the final step -- calculating the frequency of: failure of structures and components, failure of a group of structures and components, and radioactive release. Seismic responses are calculated by the computer program SMACS (Sec. 2.1). Treatment of structure-to-structure interaction enters in the SSI model as described below. An additional point is that the seismic response and systems analyses are performed for discretizations of the seismic hazard curve and the hazard curve is then convolved with these conditional results as a final step in the process. This point is relevant to the present discussion because comparisons of seismic responses are presented here for each discretized interval of the seismic hazard curve -- six intervals were analyzed. Reference 2 discusses in detail the SSMRP seismic risk analysis methodology and its application to the Zion nuclear power plant.

To assess the effect of structure-to-structure interaction on seismic response and seismic risk, two sets of calculations were performed. Seismic responses of structures and components were calculated for one case including structure-to-structure interaction and for a second case ignoring it. The two sets of responses were then used in two separate seismic risk analyses. Comparisons were made at the response and systems level to assess the impact of structure-to-structure interaction.

The substructure method was described in Sec. 2.2.1 as it applies to structures whose foundations are assumed to behave rigidly. For the SSMRP Phase II response calculations, the containment buildings' foundations and the foundation of the AFT complex were assumed to behave rigidly. Section 2 presented our evaluation of this assumption for the AFT complex and concluded it was reasonable. The present study of structure-to-structure interaction makes the same assumption. Assuming the AFT complex foundation to be flexible rather than rigid would have some effect on structure-to-structure interaction; however, in light of the results presented in Sec. 2, it is anticipated that the effect would be small.

The key elements in the SSI model are the scattering matrices and foundation impedances. Two sets of scattering matrices and impedances were generated -- with and without foundation-to-foundation interaction effects. First, a brief description of these parameters for the isolated foundation case is presented. Next, modifications to incorporate foundation-to-foundation interaction effects are discussed. In all instances, SSI models were developed for the soil properties itemized in Table 2.1. These are considered to be nominal values for an earthquake with peak horizontal acceleration of 0.2g. The nominal soil properties change with excitation level i.e. each discretized interval of the seismic hazard curve has associated with it a set of nominal soil properties which reflect the size of the earthquake. Also, within an interval soil properties are assigned a probability distribution and varied according to an experimental design. Details of these aspects are contained in Ref. 2.

For the isolated foundation case, scattering matrices and foundation impedances were developed assuming no interaction between the three foundations -- each containment building and the AFT complex. Each containment building foundation was

modeled as a circular cylinder, 157 ft. in diameter, embedded 36 ft. The scattering matrices and foundation impedances were developed using CLASSI and reported in detail in Ref. 3. Modeling the AFT complex foundation was significantly more complicated. Impedances for the AFT complex were generated for a flat surface foundation identical in shape to the AFT complex, resting on a soil layer of depth equal to the average soil depth under the real foundation. This model is identical to that described in Sec. 2.3.2 and shown in Fig. 2.9. This representation maintains the general characteristics of the foundation's dynamic behavior--differing horizontal translation and rocking impedances in each direction and appropriate coupling terms. To account for embedment, we considered an equivalent cylindrical shape with dimensions obtained by matching the total volume and the area of the deepest portions of the foundation. Scattering matrices were generated for this equivalent cylinder and were used in our analysis. Several two-dimensional analyses were performed to gain insight into the effect of irregular foundation geometry on the scattering matrices. These studies aided the selection of equivalent dimensions. To correct the impedances for embedment, a correction term was obtained by comparing impedances for the equivalent cylinder with those for an assumed circular disk resting on the same soil layer as the AFT foundation. This comparison yielded minimal differences for most components; however, embedment had a significant effect on horizontal translations, due largely to radiation damping effects. The details of this process and intermediate results are presented in Ref. 3.

To incorporate the effects of foundation-to-foundation interaction, we proceeded as follows. We modeled the two containment building foundations and the AFT complex foundation as surface foundations in much the same manner as we modeled the AFT complex foundation previously. The discretization is shown

in Fig. 3.1. In the CLASSI algorithm, which was used, the compliance matrix is computed first and then inverted to obtain the impedance matrix. Hence, we obtained an 18 x 18 compliance matrix for the three foundations shown in Fig. 3.1. The 6 x 6 diagonal blocks of the compliance matrix were modified to be identical to compliances for the isolated foundation case, i.e. corrected for embedment. The coupling blocks were for the mutiple surface foundation case. Inversion of the coupled compliance matrix results ir an impedance matrix in which diagonal blocks have been modified from the isolated case to include approximate coupling effects. Reference 6 compares the isolated and coupled impedances in detail. In summary, the AFT complex impedances show little difference in diagonal block terms and coupling terms with the containment building foundation are small relative to diagonal block elements. Hence, structure-to-structure interaction effects would appear to be minimal for the AFT complex, as expected. Selected differences in diagonal block terms for the containment building were observed but the largest impact appears to be the magnitude of coupling terms between the AFT complex and the containment building. These coupling terms are large compared to diagonal block elements, hence, significant coupling effects are expected.

3.2 Effect of Structure-to-Structure Interaction on Response

In the seismic response step of performing a seismic risk analysis, responses of structures and components for all basic events in the fault trees and for the calculation of initiating events are required. These responses must be compatible with fragility descriptions of the structures and components and must be estimated for the range of earthquakes represented by the seismic hazard curve (Sec. 3.1). Three aspects of seismic response are necessary for seismic risk

analysis: median response, variability of response, and correlation of response. In the SSMRP, responses are described by lognormal distributions; the two parameters of particular interest being the median value and the lognormal standard deviation -- denoted beta herein. Correlation is described by correlation coefficients. The computer program SMACS calculates these three aspects of seismic response for the SSMRP. To assess the effect of structure-to-structure interaction on seismic responses, two sets of calculations were performed; one including the phenomenon and a second excluding it.

For the analysis of the Zion nuclear power plant, responses in three structures and twenty piping systems were calculated with SMACS. Table 3.1 itemizes a comparison of responses on the foundation (peak and spectral acceleration) in the structures (peak and spectral acceleration), and in piping systems (peak accelerations and resultant moments). Comparisons of median values and betas are included and discussed below. In general, all median responses tended to remain the same or increase when structure-to-structure interaction was included; exceptions being horizontal response in the AFT complex and peak accelerations in four piping systems which decreased slightly. Table 3.1 shows results for acceleration range 2 which are typical of all six acceleration ranges.

- Foundation response. Response on the containment building foundation only has been saved for input to the systems analysis. Horizontal response of the containment building foundation is minimally affected by structure-to-structure interaction. Vertical response, however, is increased by 56%. Note, increases in vertical response are observed throughout the containment building structures (containment shell and internal structure). This is due principally to additional induced vertical motion resulting from rocking of the AFT complex. Betas of response change up to 10% as shown.

- Structure response. Response in three structures is tabulated in Table 3.1 -- containment shell, internal structure, and AFT complex. In the containment shell, response at only one point was saved for input to the systems analysis. Horizontal and vertical accelerations were both increased when structure-to-structure interaction is included; vertical response increased most (64%) as discussed above. The flexible nature of the containment shell vs. the internal structure leads to the greater impact of structure-to-structure interaction. Note response at several additional points on the containment shell were calculated and used as input to piping systems. Hence, changes in response of the containment shell manifest themselves in piping system response. Horizontal response in the internal structure changes by up to 11% with the average increases being 2% and 6% in each direction. Vertical response again changes the most with an average of 55% and a maximum increase of 78%. The AFT complex is least affected by structure-to-structure interaction, as shown by the ratios of Table 3.1 and as expected.

- Piping system response. Two forms of response are calculated for piping systems -- peak accelerations and resultant moments. Table 3.1 tabulates results for both. Piping systems may be categorized by location within the Zion unit 1 structures as follows:
- Outside containment and the AFT complex, e.g., in the crib house or underground. Two piping systems fall in this category. Their response is unaffected by structure-to-structure interaction and not included in Table 3.1.
- Inside containment, supported on the internal structure alone or on the internal structure and containment shell. Eight piping systems fall in this category.
- Supported entirely in the AFT complex. Three piping systems are in this category.

- Supported in the AFT complex and one support on the containment shell or internal structure. Seven piping systems fit this category.

Some observations can be made concerning piping system responses.

- In general, accelerations in piping systems were affected least by structure-to-structure interaction -- median responses varied - 4% to +17%.
- Responses (accelerations and moments) were minimally effected for piping systems supported entirely in the AFT complex, as expected.
- For piping systems supported inside containment and running between containment and the AFT complex, increases in piping moments occur. Average values are shown in Table 3.1. It appears that increased accelerations in the internal structure produce increased piping moments. Also, all piping system elements connected to the containment shell experienced large increases (up to 110%) due to structure-to-structure interaction. The average statistics do not explicitly show this fact.

Hence, structure-to-structure interaction has an important effect on response. The next section interprets these increases from a systems viewpoint, i.e. what impact on risk.

3.3 Effect of Structure-to-Structure Interaction on Seismic Risk

A detailed discussion of the impact of structure-to-structure interaction on seismic risk is contained

in Ref. 2 which permits the results to be placed in perspective with other modeling uncertainties. Reference 2 itemizes its impact on initiating event probabilities, radioactive release probabilities per category, core melt frequencies, and dose to the public. A summary is presented here.

The overall effect of structure-to-structure interaction is to increase core melt frequency per year by approximately 20% (3.57 E-6 vs. 2.94 E-6) and to increase the dose to the public by approximately 10% (9.63 vs 8.7 man-rem/year). The basic reason for this increase is the increase in seismic responses of the containment building and piping systems therein. In particular, LOCA initiating event probabilities increase more rapidly with structure-to-structure interaction than without for acceleration levels above level 2. This results since LOCA probabilities are the joint failure probabilities contributed from pipe breaks in the primary coolant system and the associated branch lines inside containment. These systems are most affected by the phenomenon. Accident mitigation systems with piping running from the containment to the AFT complex also are affected. In the systems analysis, accident sequences which are dependent on failure of piping rather than structure failure are most affected by this phenomenon.

Table 3.1 Comparison of Median Responses and Beta Values - Acceleration Range 2 (With Structure-to-Structure Interaction vs. Without Structure-to-Structure Interaction)

(a) Foundation and Structure Response (Peak and Spectral Accelerations)

	Ratio of Medians		Ratio of Beta		No. of Response Points
	Mean	COV	Mean	COV	
Containment building foundation					
NS	.999	.035	.947	.088	4
EW	1.01	.018	1.01	.106	4
Vertical	1.56	.108	.909	.045	4
Top of containment shell					
NS	1.11	-	.775	-	1
EW	1.23	-	1.07	-	1
Vertical	1.64	-	.898	-	1
Internal structure					
NS	1.02	.074	.848	.053	10
EW	1.06	.043	1.03	.086	10
Vertical	1.55	.079	.952	.078	8
AFT complex					
NS	.945	.015	.982	.025	40
EW	.976	.027	.997	.031	20
Vertical	1.09	.069	.993	.037	40

Table 3.1 (Continued)

(b) Piping System Response (Accelerations and Moments)

	Ratio of Medians		Ratio of Betas		No. of Response Points	Supporting Structures
	Mean	COV	Mean	COV		
AFW SG-1A to containment						
Accel.	1.01	-	.974	-	1	2
Moments	1.08	.147	.933	.079	23	
AFW outside containment						
Accel.	1.02	.045	1.03	083	25	4
Moments	1.12	.168	.981	.096	116	
SW to AFW pump						
Accel.	.995	.014	1.04	.060	13	3
Moments	1.01	.033	1.02	.053	132	
RHR pump suction						
Accel.	1.05	.086	1.09	.118	8	5
Moments	1.14	.163	1.01	.049	50	
RHR pump discharge						
Accel.	.964	.016	1.05	.017	9	3
Moments	1.02	.037	1.07	.069	34	
RHR and SI-1						
Accel.	1.01	.008	.948	.015	2	4
Moments	1.10	.158	.975	.049	22	
RHR and SI-2						
Accel.	.978	.034	1.02	.051	21	4
Moments	1.02	.127	.998	.066	69	
Charging pump discharge						
Accel.	.976	.030	.992	.159	18	3
Moments	1.01	.070	.972	.125	107	

Table 3.1 (Continued)

(b) Piping System Response (Accelerations and Moments)

	Ratio of Medians		Ratio of Betas		No. of Response Points	Supporting Structures
	Mean	COV	Mean	COV		
Boron inj. tank to containment						
Accel.	1.05	.022	1.00	.005	2	4
Moments	1.17	.071	1.01	.019	15	
RCL and branch lines						
Accel.	1.11	.043	.976	.049	17	1
Moments	1.27	.172	.909	.115	118	
Pressurizer relief lines						
Accel.	1.09	.046	.921	.048	7	1
Moments	1.20	.154	.929	.075	26	
AFW SG-1B to cont.						
Accel.	1.05	-	.983	-	1	2
Moments	1.14	.101	1.01	.110	27	
AFW SG-1C to cont.						
Accel.	1.17	-	1.12	-	1	2
Moments	1.25	.173	1.20	.136	28	
AFW SG-1D to cont.						
Accel.	1.11	-	1.05	-	1	2
Moments	1.19	.159	1.13	.105	27	
MS lines inside cont.						
Accel.	1.09	.005	.924	.015	2	2
Moments	1.65	.185	1.06	.202	8	
MS lines outside cont.						
Accel.	1.08	.005	1.04	.064	2	4
Moments	1.44	.176	1.05	.043	12	

Table 3.1 (Continued)

(b) Piping System Response (Accelerations and Moments)

	Ratio of Medians		Ratio of Betas		No. of Response Points	Supporting Structures
	Mean	COV	Mean	COV		
Aux. MS outside cont.						
Accel.	1.12	.068	.929	.097	4	4
Moments	1.37	.132	1.41	.204	12	
Aux. MS inside cont.						
Accel.	-	-	-	-	0	2
Moments	1.27	.187	1.15	.210	52	

Supporting Structures

1. Inside containment -- internal structure alone
2. Inside containment -- internal structure and containment shell
3. AFT complex alone
4. AFT complex to containment shell
5. AFT complex to internal structure

4. SOIL-FOUNDATION SEPARATION

4.1 Background

A seismic risk analysis considers not simply one or two levels of earthquake, e.g. OBE and SSE, but the range of possible earthquakes at the site as defined by the seismic hazard curve. It is necessary, then, to consider phenomena which may not be of major consequence in the design process but may play a significant role at high excitation levels. One such phenomena is soil-foundation separation or uplift.

For massive structures with large height to base ratios, large overturning moments are developed during an earthquake. Unless the soil-foundation interface has the capacity to transmit tension, there is a tendency for a portion of the foundation to lift off the supporting soil when sufficient overturning moment is developed. The consequences of uplift are several:

- Reduced effective stiffness of the soil-foundation interface due to the reduced contact area. This affects all response components; however, it is most significant for rocking behavior. This stiffness reduction introduces changes in the frequency response characteristics of the soil-structure system. In addition, a reduction in radiation damping effects is likely.

- In-structure member forces and accelerations are reduced probably due to there being a lower capacity to transmit seismically induced forces across the interface between the soil and foundation.

- Increased high frequency response is predicted due principally to impact upon recontact of the foundation

and soil. This effect may be somewhat over-stated in the literature due to the conservative treatment of gap closure as an elastic impact and due to representing soil material behavior in the region of high stress by equivalent linear properties [7, 8, 9, 10, 11].

- Soil failure may ocur at the toe-end of the foundation due to the increased soil pressures caused by uplift. The consequences of soil failure can be large relative displacements between adjacent buildings and the failure of interconnecting piping and conduit.

It is important to emphasize that the mere fact that soil-foundation separation is predicted during an earthquake is not important; it is the consequences of the phenomenon which dictate its importance.

The basic approach to the analysis of a soil-structure system including soil-foundation separation has been nonlinear time history analysis. At least three different procedures have been used. A nonlinear impedance function approach where the soil impedances are constructed as a function of the contact area has been applied in several instances [7, 8, 9]. A simple discrete element approach where the contact surface between the foundation and the soil is modeled by distributed springs with no tensile capability has been used [10, 11]. A finite element analysis, where gap elements or other kinematic constraints, such as slide-line theory, has also been applied [12, 13]. The cited references contain several quantifications of the effects of uplift and their review aided our treatment in the SSMRP systems analysis.

Three of the four above-mentioned consequences (reduced effective stiffness of the soil-foundation interface, reduced member forces and accelerations, and increased high frequency respons) were considered to be contributors to variability in

response and included in the range of SSI input parameters selected for the response calculations. The fourth consequence (soil failure) was included explicitly, but in an approximate manner, in the system analysis. The approach is described next.

4.2 Approximate Zion containment building uplift analysis

Two approaches were considered for the investigation of the potential for soil-foundation separation and consequent soil failure of the Zion containment building. The first approach was to perform a series of linear analyses using SMACS and the complete SSMRP structure and SSI models for a range of earthquakes. The effect of the nonlinearity introduced by the phenomenon of soil-foundation separation would then be incorporated by the use of a calibration factor based on previously published results, e.g. Refs. 7 and 8, comparing linear and nonlinear responses. The second approach was to simplify the structure and SSI models and to perform a limited number of nonlinear analyses to determine peak soil pressures and maximum uplift displacements. This approach requires simplifying the frequency dependent scattering and impedance matrices, i.e. the SSI model. The former approach was taken and described here.

SMACS analyses were performed using the complete SSMRP structure and SSI models. The methodology and its application to the Zion nuclear power plant are described in detail in Refs. 1 and 2. Selected salient points are mentioned here. Analyses were performed for five of the six discretization intervals of the seismic hazard curve, i.e. for earthquakes with peak free-field accelerations in the ranges of 0.30 to 0.45g, 0.45 to 0.60g, 0.60 to 0.75g, 0.75 to 0.98g, and greater tha 0.98g. The seismic hazard corresponded to that used in the SSMRP Phase I analysis. Within each acceleration range, an ensemble of 30 earthquakes described the seismic input. In the SMACS analyses, variability in SSI and structure characteristics were included.

The output from SMACS to be used in our uplift assessment were force and moment time histories at the bases of the structures (six components each for the internal structure and containment shell), and acceleration time histories of the foundation (3 translations and 3 rotations). These were used in the next step, i.e. determining the resultant forces and moments acting on the soil.

The SMACS output permits one to determine the resultant force and moment time histories acting on the surface of the soil due to the dynamic response of the structures and foundation. To find the net forces and moments, two static loads must also be taken into account -- the dead weight of the building and buoyancy force. Having obtained time histories of net forces and moments, time histories of peak soil pressures were calculated assuming a linear stress distribution on the contact surface. The effect of the side soil was approximately taken into account by reducing the calculated overturning moments by the ratio of the rocking impedances for a surface foundation vs. the embedded foundation. This is an excellent measure of the amount of moment reacted by the side soil. Approximately 20% of the overturning moment was reacted by the side soil. Peak soil pressures were determined for combined horizontal and vertical motions in first the N-S direction and then the E-W direction. For each interval of the seismic hazard curve considered, thirty values of peak toe pressure corresponding to the thirty sets of seismic input were calculated.

Two approaches were pursued to approximately account for the effects of the nonlinearities on the calculated soil pressures. The first approach was to determine a calibration factor to apply to the linearly calculated peak soil pressures. This factor was based on a review of published results comparing peak soil pressures calculated by linear and nonlinear techniques for a range of soil conditions. References 7 and 8

presented results in this form. The second approach was to determine a stress distribution on the soil based upon the linearly calculated forces and moments but assuming no tensile capability of the mat/soil interface. Only those forces acting over the area of the foundation still in conctact with the soil would therefore contribute to a restoring moment. This partially accounts for the nonlinearities, i.e. in the soil stress distribution.

We initially employed this second approach. The dynamic equations of equilibrium took the form of two coupled transcendental equations relating peak soil toe pressure and foundation uplift to the mat/soil contact area. This technique was only partially successful and instabilities arose at the higher excitation levels. Hence, the first approach was relied upon.

Based on a comparison of peak soil pressures calculated by linear and nonlinear techniques, a calibration factor of 2 was used to reduce the soil pressure values calculated by our linear analysis method. Figure 4.1 indicates these scaled peak toe pressure values calculated for the five seismic intervals. For each interval, results corresponding to seismic input in both the N-S and E-W directions are shown. These results were compared with the ultimate soil capacity of 45 KSF calculated for the Zion site [14]. The analytical results indicated a mean toe pressure of 49 KSF for seismic interval six (free-field accelerations greater than 0.98g). This corresponds to a peak horizontal acceleration of the containment building foundation of approximately 0.70g.

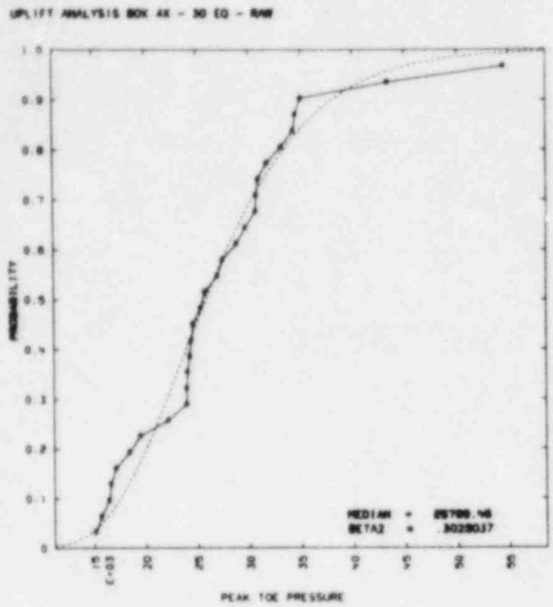

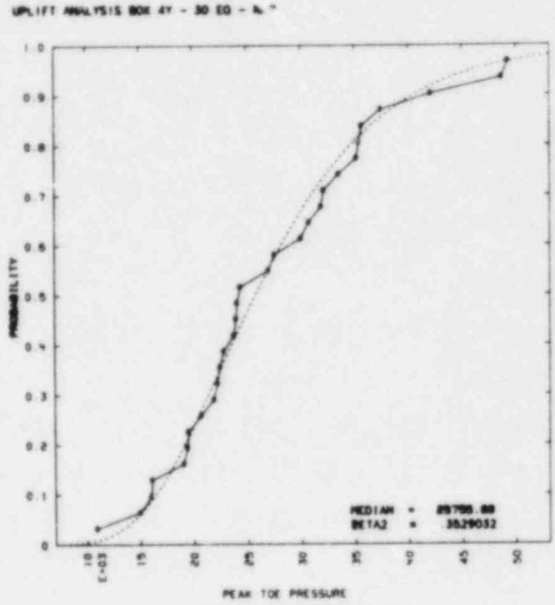

E-W Analysis N-S Analysis

4.1c Input Acceleration Range
0.60 - 0.75g

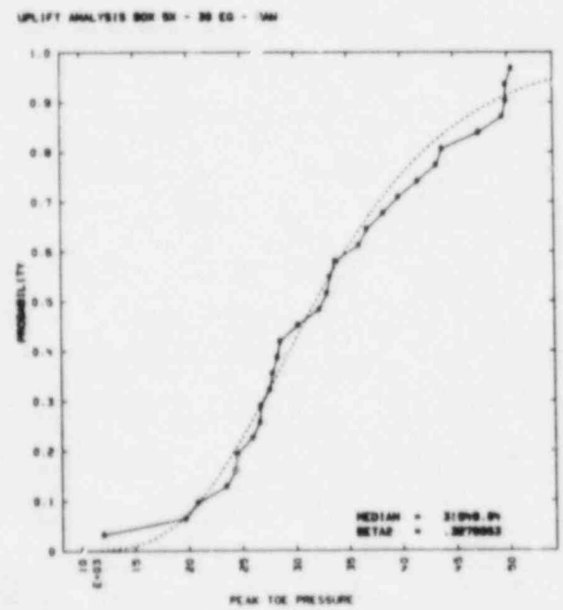

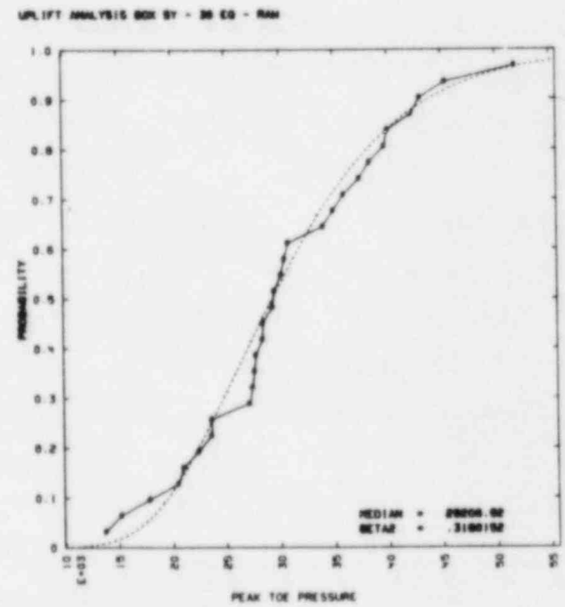

E-W Analysis N-S Analysis

4.1d Input Acceleration Range
0.75 - 0.98g

Fig. 4.1 (continued)

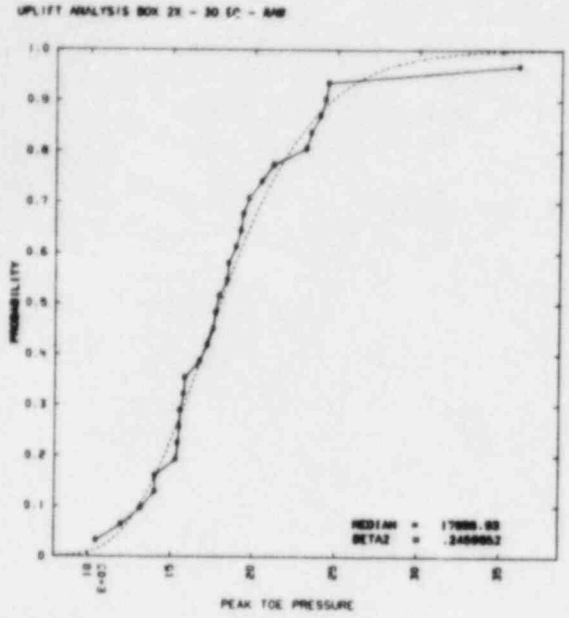

E-W Analysis

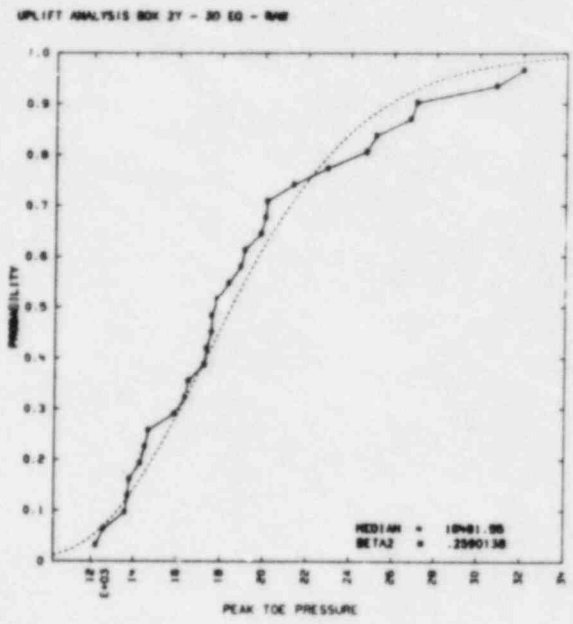

N-S Analysis

4.1a Input Acceleration Range
0.30 - 0.45g

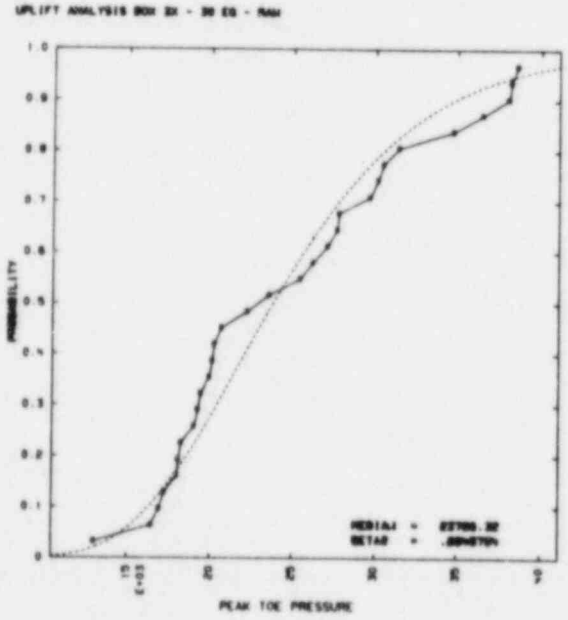

E-W Analysis

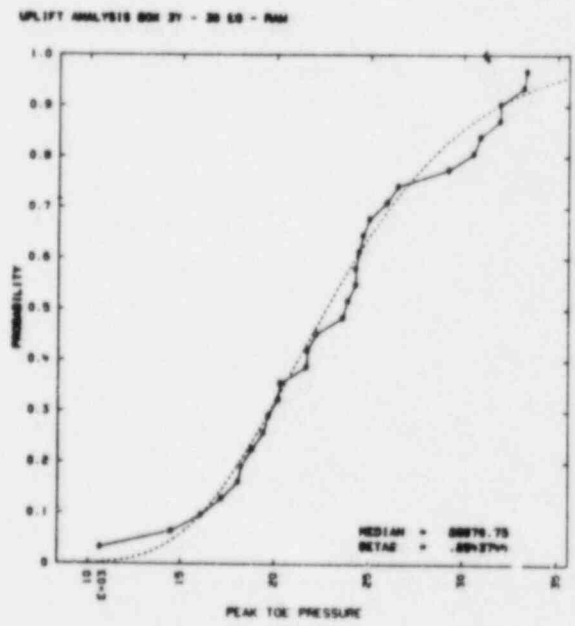

N-S Analysis

4.1b Input Acceleration Range
0.45 - 0.60 g

Fig. 4.1 Median peak toe pressures at the foundation/soil interface corresponding to free-field acceleration ranges of (a) 0.30 to 0.45g (b) 0.45 to 0.60g (c) 0.60 to 0.75g (d) 0.75 to 0.98 g (e) 0.98g.

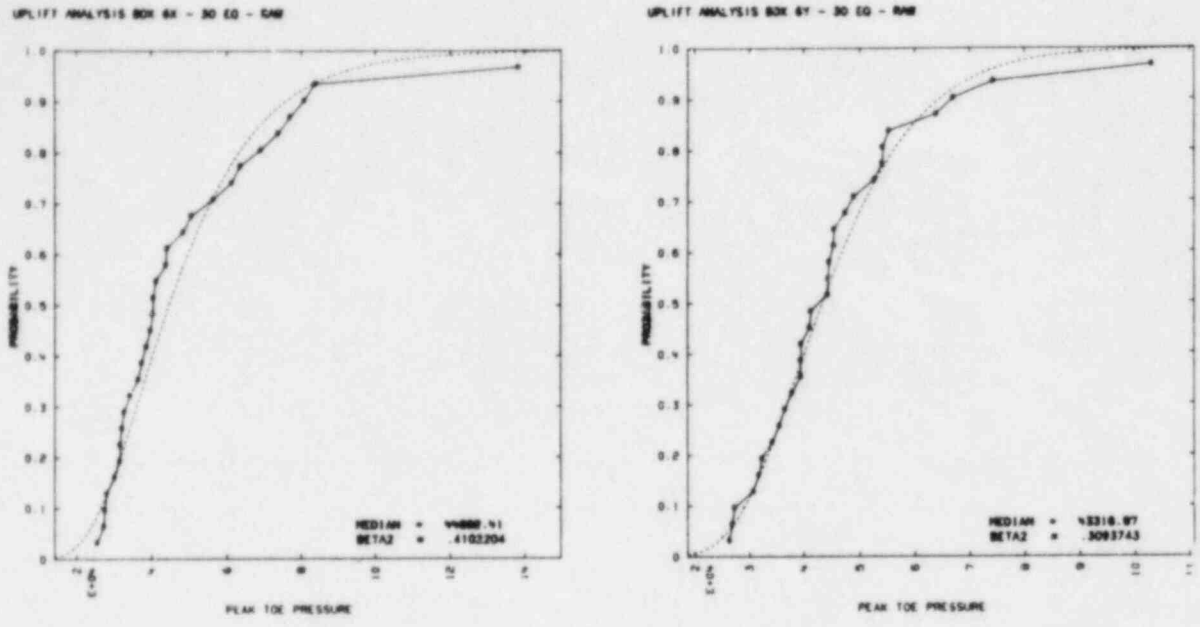

E-W Analysis N-S Analysis

4.1e Input Acceleration Range >0.98g

Fig. 4.1 (continued)

5. CONCLUSIONS AND RECOMMENDATIONS

Three aspects of the SSI analysis of the Zion nuclear power plant were investigated in detail and included in the SSMRP Phase II response calculations where appropriate: flexible foundation modeling, structure-to-structure interaction, and basemat uplift.

Analysis of the Zion AFT complex assuming its foundation to behave flexibly demonstrated the importance of including the stiffening effects of the structure. The AFT complex has a foundation of large plan dimensions -- one for which flexibility would seem important. Indeed, analyzed as a series of plates resting on the soil surface with no structural connections, it behaves flexibly. However, this study demonstrates that when one includes stiffening effects due to the structure, its effective stiffness greatly increases and assuming the foundation to behave rigidly is a good assumption. Hence, for the Zion AFT complex, modeling its foundation rigidly in the SSMRP response calculations was a valid assumption.

Three aspects enter into an evaluation of foundation flexibility -- foundation stiffness itself, structural stiffening of the foundation, and the soil stiffness relative to the effective stiffness of the foundation. This study was performed on a single specific structure and three related site conditions which is an inadequate data base to draw generic conclusions. However, it appears that shear wall structures with mat foundations, typically found at nuclear power plants, provide significant additional stiffness to their foundations which allows their foundations to behave rigidly. To draw generic conclusions requires a systematic evaluation of likely structure and site conditions. It is recommended that such a study be undertaken. Clearly, one situation where flexibility of the foundation may be important is structures with strip footings.

Structure-to-structure interaction was investigated for the Zion nuclear power plant. Two characteristics of the structures and foundations affect the phenomenon -- the relative size of the foundations and the relative mass of the structures. In both cases, the larger affects the smaller. For Zion, vibrations of the AFT complex induced additional motions in the containment building. Structure-to-structure interaction was shown to have a significant effect on selected structure and piping system response; increases of greater than 100% were seen for selected components. The effect of structure-to-structure interaction on seismic risk was also quantified -- an increase in core melt frequency per year of approximately 20% and an increase in dose to the public of approximately 10%. These latter values suggest structure-to-structure interaction has a minimal effect on seismic risk for the Zion nuclear power plant.

Seismic risk analyses must consider the range of earthquakes defined by the seismic hazard curve at the site. In so doing, phenomena, which may not be of major consequence in the design process, must be considered. One such phenomenon is soil-foundation separation or basemat uplift. Uplift, per se, is not critical. The consequences of uplift are, in general, of second order. However, the potential exists for large soil pressures to develop due to redistribution of stress. Peak toe pressures may increase to the point of exceeding the soil bearing capacity causing failure. A consequence of uplift itself and soil failure is increased relative displacements between adjacent structures which then causes failure of interconnecting pipes.

Our treastment of basemat uplift for the Zion unit 1 containment building was based on performing a series of linear analyses with SMACS to estimate peak toe pressures for the range of earthquakes. These linearly calculated peak toe pressures

were modified to approximately account for nonlinear effects. Soil failure was correlated with peak horizontal acceleration of the containment building foundation (median value of 0.70g). The consequences of soil failure were relative displacements of 2 in. or more which caused failure of interconnecting pipes. In the Zion seismic risk analyses [2], this failure mode was shown to be extremely important. In addition, this phenomenon is generic, i.e. one which can be expected to be present at many nuclear power plants. Hence, additional analyses should be performed including explicitly treating its nonlinear aspects. This will provide validation for the Zion case and information for its future treatment.

6. REFERENCES

1. Johnson, J. J., Goudreau, G. L., Bumpus, S. E., Maslenikov, O. R., Seismic Safety Margins Research Program Phase I Final Report -- SMACS - Seismic Methodology Analysis Chain with Statistics (Project VII), Lawrence Livermore National Laboratory, Livermore, CA, UCRL-53021, Vol. 9, NUREG/CR-2015, Vol. 9 (1981).

2. Bohn, M. P., et al., Application of the SSMRP Methodology to the Seismic Risk at the Zion Nuclear Power Plant, Lawrence Livermore National Laboratory, Livermore, CA, UCREL-53483, NUREG/CR-3428 (1983).

3. Johnson, J. J., Maslenikov, O. R., Chen, J. C., Chun, R. C., Seismic Safety Margins Research Program, Phase I Final Report -- Soil Structure Interaction (Project III), Lawrence Livermore National Laboratory, Livermore, CA, UCRL-53021, Vol. 4, NUREG/CR-2015, Vol. 4 (1982).

4. Luco, J. E., Wong, H. L., Personal Communication.

5. Benda, B. J., Johnson, J. J., Lo, T. Y., Seismic Safety Margins Research Program Phase I Final Report -- Major Structure Response (Project IV), Lawrence Livermore National Laboratory, Livermore, CA., UCRL-53021, Vol. 5, NUREG/CR-2015, Vol. 5 (1981).

6. Maslenikov, O. R., Chen, J. C., Johnson, J. J., Uncertainty in Soil-Structure Interaction Analysis Arising from Differences in Analytical Techniques, Lawrence Livermore National Laboratory, Livermore, CA, UCRL-53026, NUREG/CR-2077 (1982).

7. Kennedy, R. P., Short, S. A., Wesley, D. A., Lee, T. H., "Effect of Nonlinear Soil-Structure Interaction Due to Base Slab Uplift on the Seismic Response of a High Temperature Gas Cooled Reactor (HTGR)," Nuclear Engineering and Design, Vol. 38, (1976).

8. Wolf, J. P., Skrikerud, P. E., "Seismic Excitation with Large Overturning Moments: Tensile Capacity, Projecting Base Mat or Lifting - Off?" Nuclear Engineering and Design, Vol. 50 (1978).

9. Wolf, J. P., "Soil-Structure Interaction with Separation of Base Mat (Lifting-Off)," Nuclear Engineering and Design, Vol. 38 (1976).

10. Bervig, D. R., Chen, C., "Stability and Toe Pressure Calculation of a Reactor Building Subject to Seismic Disturbance," Transactions of the Third International Conference on Structural Mechanics in Reactor Technology, London, United Kingdom, K3/7 (1975).

11. Cofer, L. et al., "The Influence of Uplift and Sliding Nonlinearities on Seismic Response of a Small Test Reactor Building," Transactions of the Fifth International Conference on Structural Mechanics in Reactor Technology, Berlin, West Germany (1979).

12. Chun, R. C., Maslenikov, O. R., Goudreau, G. L., Johnson, J. J., "Uncertainty in Soil-Structure Interaction Analysis of a Nuclear Power Plant - A Comparison of Linear and Nonlinear Analysis Methods," Transactions of the Sixth International Conference on Structural Mechanics in Reactor Technology, Paris, France (1981).

13. Isenberg, J., Vaughan, D. K., Sandler, I., "Nonlinear Soil-Structure Interaction," Weidlinger Associates, EPRI No. NP-945 (1978).

14. Dames and Moore, Report of Geological and Seismological Environmental Studies, Proposed Nuclear Power Plant, Zion, Illinois, for the Commonwealth Edison Company, June 1967.

NRC FORM 335 (2-84) NRCM 1102, 3201, 3202

U.S. NUCLEAR REGULATORY COMMISSION

SEE INSTRUCTIONS ON THE REVERSE

BIBLIOGRAPHIC DATA SHEET

1. REPORT NUMBER (Assigned by TIDC, add Vol. No., if any)

NUREG/CR-4018
UCID-20212

2. TITLE AND SUBTITLE

SSI Sensitivity Studies and Model Improvements for the US NRC Seismic Safety Margins Research Program

3. LEAVE BLANK

4. DATE REPORT COMPLETED

MONTH: January YEAR: 1984

5. AUTHOR(S)

James J. Johnson, Oleg K. Maslenikov, Brian J. Benda

6. DATE REPORT ISSUED

MONTH: November YEAR: 1984

7. PERFORMING ORGANIZATION NAME AND MAILING ADDRESS (Include Zip Code)

Lawrence Livermore National Laboratory
Post Office Box 808, L-90
Livermore CA 94550

8. PROJECT/TASK/WORK UNIT NUMBER

9. FIN OR GRANT NUMBER

A0126

10. SPONSORING ORGANIZATION NAME AND MAILING ADDRESS (Include Zip Code)

Division of Engineering Technology
Office of Nuclear Regulatory Research
U.S. Nuclear Regulatory Commission
Washington DC 20555

11a. TYPE OF REPORT

Technical

b. PERIOD COVERED (Inclusive dates)

12. SUPPLEMENTARY NOTES

13. ABSTRACT (200 words or less)

The Seismic Safety Margins Margins Research Program (SSMRP) is a US NRC-funded program conducted by Lawrence Livermore National Laboratory. Its goal is to develop a complete fully coupled analysis procedure for estimating the risk of an earthquake-induced radioactive release from a commercial nuclear power plant. In Phase II of the SSMRP, the methodology was applied to the Zion nuclear power plant. Three topics in the SSI analysis of Zion were investigated and reported here--flexible foundation modeling, structure-to-structure interaction, and basemat uplift. The results of these investigations were incorporated in the SSMRP seismic risk analysis.

14. DOCUMENT ANALYSIS - a. KEYWORDS/DESCRIPTORS

soil-structure interaction
seismic risk analysis

b. IDENTIFIERS/OPEN-ENDED TERMS

15. AVAILABILITY STATEMENT

unlimited

16. SECURITY CLASSIFICATION

(This page) Unclassified

(This report) Unclassified

17. NUMBER OF PAGES

18. PRICE

UNITED STATES
NUCLEAR REGULATORY COMMISSION
WASHINGTON, D.C. 20555

120555078877 1 IAN1RD
US NRC
ADM-DIV OF TIDC
POLICY & PUB MGT BR-PDR NUREG
W-501
WASHINGTON DC 20555